SOLANO PERMITTEES

Green Stormwater Infrastructure

Reasonable Assurance Analysis Modeling Report for PCBs and Mercury

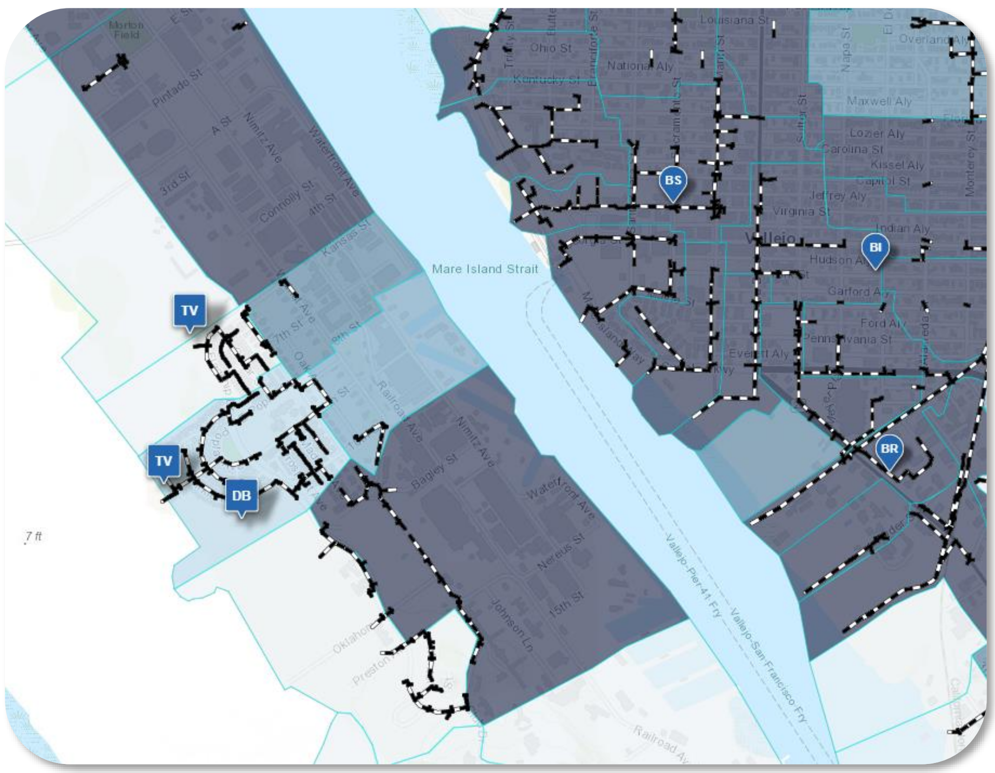

FINAL REPORT

SEPTEMBER, 2020

In compliance with Provision C.11 and C12.c of Order R2-2015

Prepared by:

2NDNATURE

500 Seabright Ave
Santa Cruz, CA 95060
831.426.9119
www.2ndnaturewater.com

Table of Contents

FIGURES

Tables

APPENDICES

Appendix A. swTELR article published in Journal of Environmental Management

Appendix B. swTELR BMP type definitions

Appendix C. Catchment routing and attributes

Appendix D. Decentralized BMPs implemented and planned by Solano Permittees

Acronyms

BASMAA	Bay Area Stormwater Management Agency
BMP	Best Management Practice
C3	Refers to Provision C3 in the MRP
cBMP	Centralized BMP. Also called regional treatment measures
CN	Curve number
CRC	Characteristic runoff concentration
dBMP	Decentralized BMP, also called distributed BMPs
FSSD	Fairfield Suisun Sewer District
GI	Green Infrastructure
GIS	Geographic Information System
GSI	Green Stormwater Infrastructure
HSG	Hydrologic soil. group
LID	Low Impact Development
MRP	Municipal Regional Stormwater Permit
NLDC	National Land Cover Dataset
NPDES	National Pollutant Discharge Elimination System
NRCS	National Resource Conservation Service
RAA	Reasonable Assurance Analysis
RWSM	Regional Watershed Spreadsheet Model
RWQCB	Regional Water Quality Control Board
PCBs	Polychlorinated Biphenyls
SCS	Soil Conservation Service
SFEI	San Francisco Estuary Institute
swTELR	Stormwater Tool to Estimate Load Reductions
TMDL	Total Maximum Daily Load
USDA	United States Department of Agriculture
USEPA	United States Environmental Protection Agency
WLA	Waste load allocation
VFWD	Vallejo Flood and Wastewater District

EXECUTIVE SUMMARY

This report communicates the methods and results of a Reasonable Assurance Analysis (RAA) modeling study, in fulfillment of Municipal Permit (MRP) Provisions C.11and C.12.c. Those provisions require Solano Permittees to quantify the degree to which they expect to meet future Polychlorinated biphenyls (PCBs) and mercury reduction targets by implementation of Green Stormwater Infrastructure (GSI). This study was coordinated with other SF Bay Area Permittees via the Bay Area Stormwater Management Agencies Association (BASMAA) to ensure consistency of methods, rigor, documentation, and logistics within the Bay Area region. The modeling relied strongly on input data from the Solano Permittees and required substantial input and iteration of information with stormwater management staff from the Cities of Fairfield, Suisun, and Vallejo; the Fairfield Suisun Sewer District; and the Vallejo Flood and Wastewater District. This modeling study has been completed in parallel with development of a Green Stormwater Infrastructure Workplan, so that the outputs may inform future GSI implementation. Thus, this report represents the result of a concerted, collaborative effort on the part of the Solano Permittees to determine PCB and mercury reduction progress to date and the most likely trajectory forward given the best information currently available.

The Solano permittees have employed a practical and proven approach for quantifying load reductions that reflects both a need to be efficient with limited resources and a commitment to transparent linkages between planned improvements and expected water quality benefits. This approach is based on outputs from the purpose-built stormwater hydrologic and pollutant loading model Stormwater Tool to Estimate Load Reductions (swTELR) reported in Beck et al. (2017), Conley et al. (2019); and Conley et al. (2020). swTELR is a scalable computational approach to quantify urban catchment-scale stormwater runoff, pollutant loading to receiving waters, and reductions from BMPs. The model provides spatially-explicit accounting of stormwater and pollutant reductions to inform more strategic stormwater management decisions with a parsimonious structure that relies strongly on the input data. This approach also makes the model easier to use and understand, lower cost, and more amenable to both field verification and updating with new information as it becomes available.

Future modeling scenarios were completed for the Solano Permittee MS4 Area that includes the cities of Fairfield, Suisun, and Vallejo for the years 2020, 2030, and 2040 to quantify reductions of stormwater runoff, PCBs and mercury. These scenarios included land use changes associated with new development and redevelopment as well as implementation of decentralized and centralized structural BMPs that infiltrate and treat stormwater runoff. These scenarios do not include source control measures, which will also contribute to TMDL wasteload allocation reductions, as these will be handled in a separate RAA study pending the completion of a regionally adopted accounting method by BASMAA scheduled to be completed in April of 2020.

Baseline modeling (no BMPs) corresponding to the year 2005 showed that PCB loading is predominantly driven by the presence of Old Industrial and Source Area land uses. Since these land uses dominate Vallejo's Mare Island and are prevalent on the Vallejo Waterfront, these areas represent the greatest opportunities within the Solano Permittee MS4 Area for realizing pollutant load reductions and meeting WLA targets in the future (see maps below). Model outputs were highly sensitive to the land use based pollutant runoff concentration layer used by all Bay Area RAA models that includes a PCB concentration range over 1,000x and 10x for mercury. Estimated baseline loads from swTELR were lower than TMDL estimates for the Solano Permittees, especially for mercury, whose baseline estimate from swTELR was below the wasteland allocation target for the Solano Permittees. The divergence between the two estimates is likely due to the strong reliance on population as the method to distribute loads in the TMDL estimates. Strong correspondence between swTELR and the Regional Watershed Spreadsheet Model (RWSM) provides additional confidence in the veracity of swTELR outputs.

Future modeling scenarios showed that the Solano Permittees are expected to meet target GSI reductions for both PCB and mercury in the coming decades. Reductions calculated for the years 2020, 2030, and 2040 surpass the required GSI reductions by several multiples for both PCBs and mercury, primarily due to the conversion of Old Industrial/Source Area land uses to New Urban land use on Mare Island. The GSI reductions represent substantial progress towards WLA targets specified in the TMDL (SFRWQCB, 2006; SFRWQCB, 2008), with the PCB GSI reductions accounting for 72% of reductions required to achieve the Solano Permittee's 2040 PCBs WLA target (100 grams). Mercury reductions represent a 14% reduction from baseline estimates by 2028 which are already below the Solano Permittee WLA target. Large tracts of land have been acquired by private development firms and demolition, grading, and/or construction is already underway throughout Mare Island. If these redevelopment projects proceed as planned over the next two years, load reductions are expected to accelerate towards the modeled 2020 estimates. A spatial prioritization analysis was completed to identify the best parcels and road segment opportunities for additional GSI implementation, that may provide additional benefits, which will be addressed in the GSI Workplan. However, it is anticipated that already planned redevelopment projects will meet the GSI reduction targets and that source control measures will make up most of the remaining required reductions to meet WLA targets.

While the Solano Permittees are on track to achieve the pollutant reduction expectations for GSI implementation, as GSI and source control measures are implemented, new opportunities and challenges will inevitably arise, causing changes to the planned scenarios. It will be critical for Solano permittees to adopt a cost-effective and updateable tracking and accounting system so that iterative quantification of reductions can ensure that progress aligns with estimated projections. Integration of pollutant load reduction accounting with GSI data management and reporting can improve Solano Permittee stormwater program efficiency, and provide interim progress verification for ongoing assurance that pollution reduction expectations are indeed reasonable.

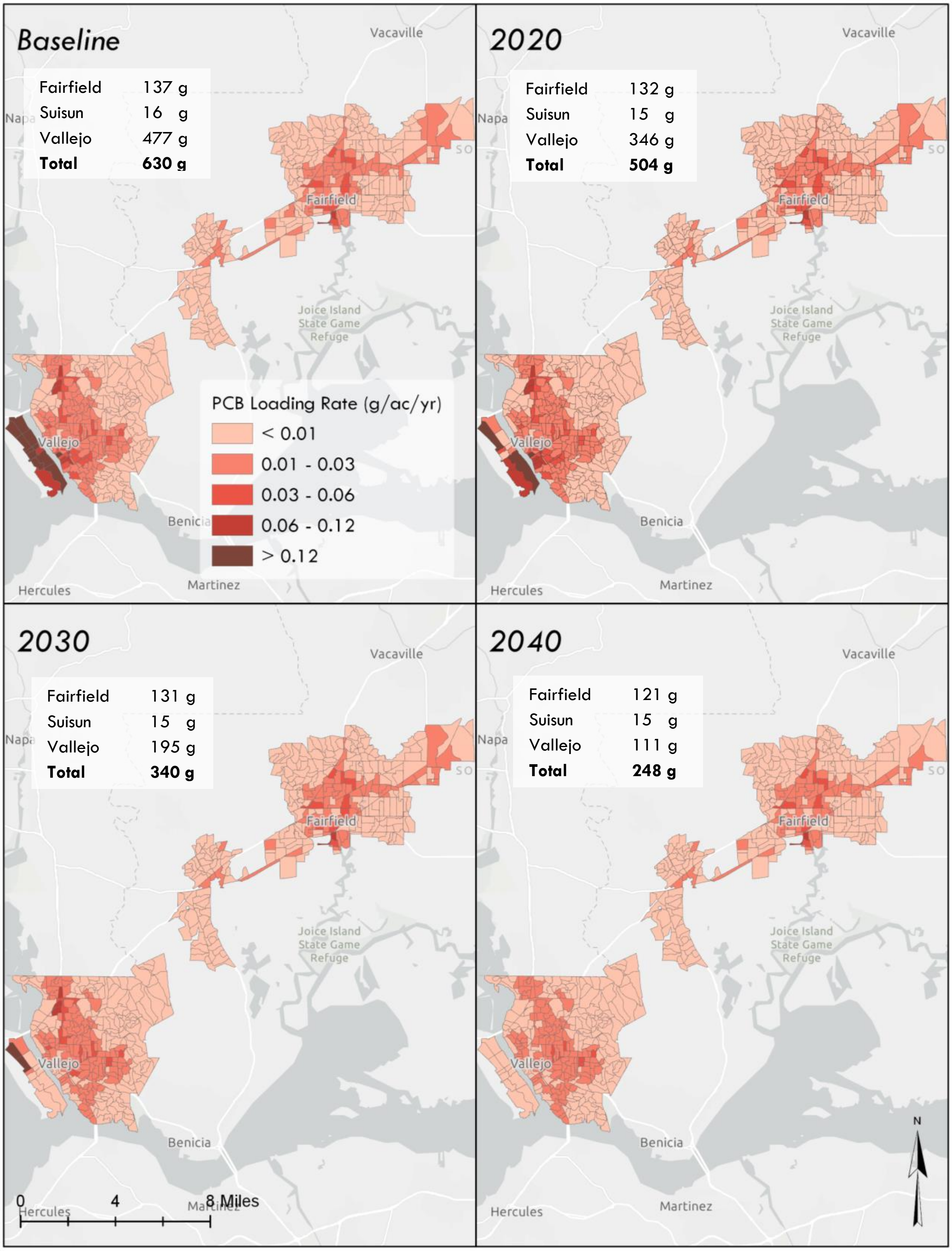

Spatial distribution of annual PCB load estimates for baseline and future scenarios

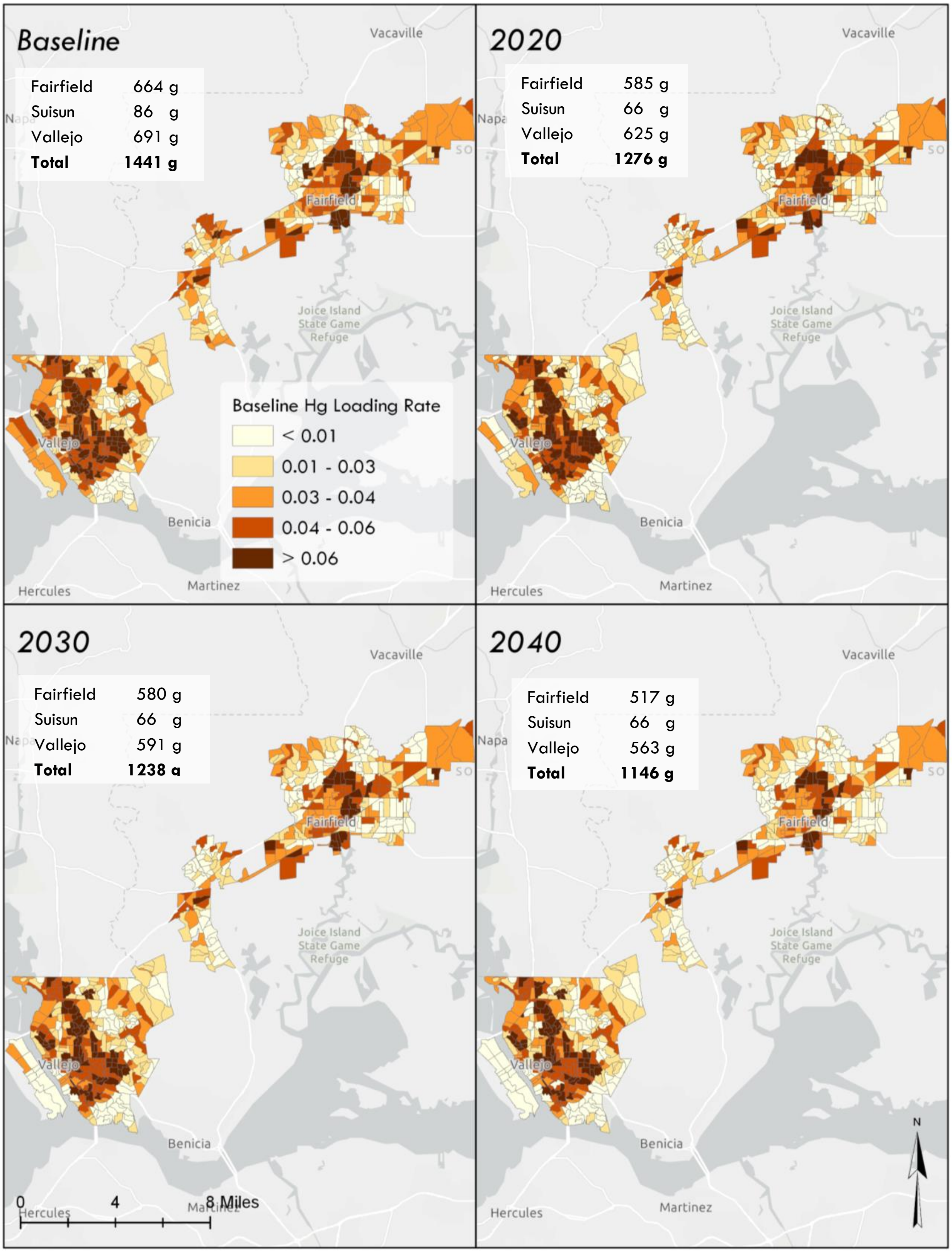

Spatial distribution of annual mercury load estimates for baseline and future scenarios

1 Introduction

1.1 Regulatory Mandate

The Solano Permittees (City of Fairfield, City of Vallejo, and Suisun City) are subject to the requirements of the California Regional Water Quality Control Board for the San Francisco Bay Region's (RWQCB's) Municipal Regional Stormwater Permit (MRP). The MRP was last reissued in November 2015[1], and mandates implementation of a comprehensive program of stormwater control measures and actions designed to limit contributions of urban runoff pollutants to San Francisco Bay. MRP Provision C.11and C.12.c requires the Solano Permittees to prepare a Reasonable Assurance Analysis, to be submitted with its Annual Report to the RWQCB due September 30, 2020.

"Green Infrastructure" (GI), also known as "Green Stormwater Infrastructure" (GSI[2]), refers to the construction and retrofit of storm drainage to reduce runoff volumes, disperse runoff to vegetated areas, harvest and use runoff where feasible, promote infiltration and evapotranspiration, and use bioretention and other natural systems to detain and treat runoff before it reaches receiving waters. Green stormwater infrastructure can be incorporated into construction on new and previously developed parcels, as well as new and rebuilt streets, roads, and other infrastructure within the public right-of-way.

Water quality in San Francisco Bay is impaired by polychlorinated biphenyls (PCBs) and mercury. Sources of these pollutants to the Bay include urban stormwater. By reducing and treating stormwater flows, GSI reduces the quantity of these pollutants entering the Bay and will hasten the Bay's recovery.

Provisions C.11 and C.12 in the MRP require Solano County Permittees to reduce estimated PCBs loading by 8 grams/year and estimated mercury loading by 2 grams/year using green stormwater infrastructure by June 30, 2020. Regionally, all Bay Area Permittees must also project the load reductions achieved via GSI by 2020, 2030, and 2040, showing that collectively, reductions will amount to 3 kg/year PCBs and 10 kg/year mercury by 2040[3]. Of these regional 2040 reduction targets, the Solano Permittees are responsible for reductions of approximately 110 grams/year

[1] Order R2-2015-0049

[2] Although the MRP uses the term green infrastructure (GI), the Solano Permittees prefer to use the term green *stormwater* infrastructure (GSI) for clarity. Henceforward, the term GSI will be used.

[3] Permittees shall "quantitatively demonstrate that PCBs load reductions of at least 3 kg/yr will be realized by 2040 through implementation of green infrastructure projects" (C.12.c.ii.2.d) Percent of Solano Permittee load reduction is 20.8% PCBs and 16.1% mercury from BASMAA RAA Guidance Document (6/30/17).

PCBs and 48 grams/year mercury based on current baseline estimates (Table 1.1) (see Section 4.2.4 Compliance Demonstration for details.

Table 1.1 Future GSI reduction targets for Solano Permittees from modeled baseline loading

	Scenario	GSI Reduction Target (g)*
PCBs	2020	8
	2030	58
	2040	110
Mercury	2020	2
	2028	33
	2040	48

*2020 Reduction targets are fixed values specified in the MRP, 2040 Reduction targets have been rescaled based on new calculated baseline values per RAA Guidance Section 3.5 as a proportion of total estimated reductions (20.8% for PCBs, 16.1% for mercury)

1.2 Scope and Purpose

This RAA provides a demonstration that GSI control measures included in the Solano Permittees' GSI Plan as required by MRP Provisions C.3, C.11, and C.12, will meet the PCBs and mercury Total Maximum Daily Load (TMDL) MRP required green infrastructure reductions for urban stormwater runoff. This RAA quantifies PCB and Mercury reductions, given the type, size, number, location, and time frame of GSI control measures needed to comply with load reduction goals stated in MRP Provisions C.3.j and C.11/C.12.c. This report fulfills the MRP requirement of quantifying reductions achieved via GSI (C.11.c/C.12.c) which will be documented in the 2020 Annual Report for the Solano Permittees.

The vision for this RAA is to map a path towards achieving TMDL wasteload allocation targets (WLA) and also provide a structure for ongoing compliance demonstration. A modeling approach has been developed that is amenable to iteratively verifying runoff and pollutant load reductions as new stormwater BMPs are implemented over time. The outputs provide timely information at spatial scales that can inform implementation decisions. It creates a practical means for quantifying load reductions over time that is also amenable to direct monitoring verification at individual BMPs and urban stormwater drainage scales. This RAA analysis has been performed in conjunction with development of a Green Stormwater Infrastructure Workplan to ensure that load reduction requirements dynamically informed the identification of sites and types of green infrastructure planned in the future.

1.3 Background and Understanding

1.3.1 PCBs and mercury Total Maximum Daily Loads

The MRP pollutant-load reduction requirements are driven by Total Maximum Daily Load (TMDL) requirements adopted by the RWQCB for mercury (Resolution No. R2-2004-0082 and R2-2005-0060) and PCBs (Resolution No. R2-2008-0012). Each TMDL allocates allowable annual loads to San Francisco Bay (a Waste Load Allocation, or WLA) from identified sources, including from urban stormwater. The urban stormwater WLA, in turn, is apportioned among MRP Permitees in proportion to population, based on the naïve assumption that PCB loadings vary in proportion to population[4]. The Solano Permittees constitute approximately 4.7% of the population total for all cities named in the MRP.

The Bay Area-wide WLA for PCBs for urban stormwater is 2 kg/yr by 2030, which is a ninety percent reduction from baseline urban stormwater loads estimated in the TMDL. The overall reduction in all external loads, including urban stormwater, was developed based on multiplying the target final sediment PCB concentration (1 µg/kg) by the estimated annual sediment load discharged from local tributaries. The target final PCB concentration in sediment was developed based on a fish tissue target of 10 nanograms (ng) of PCBs per gram (g) of fish tissue. This target is based on a cancer risk of one case per an exposed population of 100,000 for the 95th percentile San Francisco Bay Area sport and subsistence fisher consumer (32 g fish per day). The fish tissue target (10 ng/g) is translated to the sediment target (1 µg/kg) using a food web model developed by San Francisco Estuary Institute (SFEI).

The mercury TMDL addresses two water quality objectives. The first, established to protect people who consume Bay fish, applies to fish large enough to be consumed by humans. The objective is 0.2 milligrams (mg) of mercury per kilogram (kg) of fish tissue (average wet weight concentration measured in the muscle tissue of fish large enough to be consumed by humans). The second objective, established to protect aquatic organisms and wildlife, applies to small fish (3-5 centimeters in length) commonly consumed by the California least tern, an endangered species. This objective is 0.03 mg mercury per kg fish (average wet weight concentration). To achieve the human health and wildlife fish tissue and bird egg monitoring targets and to attain water quality standards, the Bay-wide suspended sediment mercury concentration target is 0.2 mg mercury per kg dry sediment (0.4 mg/kg or 200 µg/kg). A roughly 50% decrease in sediment, fish tissue, and bird egg mercury concentrations is necessary for the Bay to meet water quality standards. Reductions in sediment mercury concentrations are assumed to result in a proportional reduction in the total amount of

---

[4] Monitoring data demonstrates that this is an oversimplified assumption, because PCB yields per unit land area are higher in some land uses (e.g., "old industrial") compared to others (e.g., "new urban"). The PCBs TMDL and resulting permit provisions allow permittees to provide alternate formulae for allocating load reduction requirements among permittees.

mercury in the system, which will result in the achievement of target fish tissue and bird egg concentrations. These receiving water goals are translated by the TMDL into a roughly 50% mercury load reduction requirement from urban stormwater.

Because the ninety percent reduction for PCBs is more stringent than the fifty percent reduction for mercury, current implementation strategies for Bay Area stormwater programs are based on the assumption that achieving PCB WLAs will result in achieving mercury WLAs. This assumption is intended to be revisited through periodic review of progress on attainment of TMDL goals.

1.3.2 PCBs and mercury sources, transport, and distribution

1.3.2.1 *PCBs sources to urban runoff*

PCBs were manufactured in the United States from 1929 to 1977 and were widely used by many industries because of their low electrical conductivity, high boiling point, chemical stability and flame retardant properties. PCBs were predominantly used in electrical equipment, including transformers and capacitors, but also found in hydraulic fluids, dust control, flame retardants, lubricants, paints, sealants, wood preservatives, inks, dyes and plasticizers (Abbot 1993, Binational Toxics Strategy 1998 and 1999, EIP Associates 1997)[5]. In 1979, the manufacture, import, and distribution of PCBs was banned in the United States. However, PCBs still remain in use in certain closed system devices (e.g. transformers and capacitors), which may still contribute to stormwater loads.

A conceptual model developed by McKee et al. (2006) estimated that erosion of sediments from urban watersheds is the largest source of PCBs to Bay Area. Construction sites, open spaces, and vacant lots can represent areas of legacy PCB accumulation over the past 50 years. The second largest sources identified were building demolition, and continued PCB use in transformers and capacitors. Lesser sources included atmospheric deposition and contaminated industrial areas.

1.3.2.2 *Mercury sources to urban runoff*

Mercury is a naturally-occurring, persistent, bioaccumulative (as methylmercury) metal that can be present in the elemental, inorganic, or organic forms in the environment. It is both a legacy pollutant and has modern sources. Historically, mercury has been used in a variety of products. Primary among the historical industrial uses were battery manufacturing and chlorine-alkali production; along with paints and industrial instruments. It is also used in laboratories for making thermometers, barometers, diffusion pumps, and other instruments, including mercury switches and other electrical apparatuses. Gaseous mercury is used in mercury-vapor lamps (e.g., fluorescent tubes) and advertising signs. Mercury is also the basis of dental amalgams and preparations, and can be a byproduct of burning fossil fuels and refining petroleum. Mercury has not been mined as a principal

[5] Review of Potential Measures to Reduce Urban Runoff Loads of PCBs to San Francisco Bay, by EOA, Inc. for Santa Clara Valley Urban Runoff Pollution Prevention Program, March2004.

mineral product in the U.S. since about 1992. Product substitutions (e.g. LEDs for mercury-containing fluorescent lights) have resulted in substantial reductions in commercial mercury usage in recent decades (McKee et al, 2006).

Erosion from the surface of the urban watershed is also the largest source of mercury to Bay Area urban stormwater (McKee et al., 2006). However, in contrast to PCBs, atmospheric deposition of mercury to urban watersheds provides a substantial source of mercury to SF Bay urban stormwater. Mercury in atmospheric deposition over Bay Area watersheds originates from the release of mercury from global and local sources, both natural (e.g. volcanos, wildfires) and human-caused (e.g. coal combustion).

1.3.2.3 *PCBs and mercury transport*

Conceptual model development by Mangarella et al (2010) defined the principle pathways of PCBs and mercury transport. Wind dispersal, vehicle tracking and road deposits and surface runoff from source areas were defined as the primary transport vectors for sediment-bound pollutant transport throughout the SF Bay Area. Sediments transported into the MS4 accumulate on roadways (including curbs and gutters), storm drain inlets/catch basins, stormwater pipelines, and other structures (e.g., stormwater pump stations).

1.3.2.4 *PCBs and mercury spatial patterns in the SF Bay*

McKee et al. (2015) produced multi-year synthesis of PCBs and mercury data collected by numerous researchers as part of the SF Bay Regional Monitoring Program (RMP) to directly address management questions and identify patterns across the SF Bay Area. Sediment studies in the SF Bay Area and its watersheds have consistently measured higher PCB concentrations in areas of urban development compared to regions of open space or non-urban land uses (McKee et al, 2015, Hunt et al., 1998; Daum et al., 2000; KLI, 2002; Gunther et al., 2001). Maps included in McKee et al. 2015 (p.18) illustrated that PCB concentrations in fish tissues and in sediments are relatively low in watersheds and Bay waters adjacent to Solano County, with levels much lower than other identified areas of concern.

Watersheds that have ongoing disturbances through human development or that have legacy point sources show higher water column concentrations of total mercury than other less impacted watersheds. Elevated mercury concentrations are mostly caused by a combination of mercury stored in source areas and available for transport, and greater sediment (and perhaps organic carbon) loading rates (McKee et al., 2015). Concentrations of mercury in small fish have also been investigated by the RMP (Greenfield and Jahn, 2010). In contrast to PCBs, the small fish mercury data do not strongly indicate specific areas within the SF Bay Area of particular concern.

Sequential rounds of conceptual and mass balance model development have resulted in land-use based estimates of PCB and mercury production throughout the Bay Area (McKee et al. 2006, Mangarella et al. 2006; 2010). These initial efforts were built upon by information extracted from BASMAA integrated monitoring reports, which used a unique land-use grouping that relied primarily on the identification of 'Old' and 'New' urban land uses. They were later used to develop the land use layer for the Regional Watershed Spreadsheet Model (RWSM), designed to estimate relative watershed-scale yields (Lent and McKee, 2011; Lent et al., 2012; McKee et al., 2014; Wu et al. 2016). McKee et al 2015 point out that a primary challenge faced in RWSM development was poor quality of the underlying land use layer and cautions that it may hamper the use of the model to smaller areas or at higher resolution.

Since the early1990's, several locations within the SF Bay nearby to Solano County have been sampled by regional monitoring programs such as the SF Bay Regional Monitoring Program (RMP). The Contaminant Data Display & Download (CD3)[6] system, administered by SFEI, provides access to these data and tools for viewing metadata. Given the nature of the sampling schedules, the mercury and PCBs data available are primarily useful for characterizing historic spatial patterns of pollutant concentrations within receiving waters. These data provide a snapshot of conditions for both PCBs and mercury at specific locations in the Bay, allow probabilistic inference over wider areas, and fulfill the objectives of specific scientific studies.

From 1993-2001 there are 28 recorded sampling sites for PCBs and mercury collected within Grizzly Bay, Suisun Bay, Carquinez Straight, nearly all of which record a single sample for each constituent. There have been 19 samples for both mercury and PCBs in water collected at one site in the Mare Island Straight as part of the RMP. There were 3 samples for PCBs in water collected at a site on Austin Creek in the NW corner of Vallejo in 2017. There are also 9 sediment sampling sites, with 1 sample at each site for both PCBs and mercury distributed throughout Vallejo Waterfront and Mare island collected in 2008. Two sites along Suisun Creek had both mercury and PCBs samples collected once in 2005 as part of the Portable Remote Sensing Image SectroMeter (PRISM) study, and one site within Suisun City had 1 mercury sample collected in 2013 as part of the Surface Waters Ambient Monitoring Program (SWAMP).

1.3.2.5 *PCBs source identification in Solano Permittee MS4s*

Solano Permittees have identified and assessed potential PCB source areas for remediation throughout their cities which have been documented in Pollutants of Concern Implementation Plan (FSURMP, 2014) and Control Measures Implementation Status Report (VSFCD, 2016). There has been very little historic PCB related industrial activity in the Cities of Fairfield and Suisun City, and thus, very few potential remediation sites. Seven potential sites were identified for sediment sampling in Fairfield/Suisun. The largest (by land area) potential source area identified, the Travis

[6] https://cd3.sfei.org/

Air Force Base, was rejected as a potential monitoring site, since it is a federal facility covered under its own NPDES permit.

During MRP 1.0 and MRP 2.0 (2009 – 2018), potential remediation areas were identified throughout the City of Vallejo, as part of the PCBs Source Area Identification Screening Program, in coordination with BASMAA's Monitoring and Pollutant of Concern Committee. Out of a total of 191 Vallejo parcels surveyed, 30 are now categorized as high likelihood source parcels, and were further assessed for sampling suitability (VFSD and City of Vallejo, 2016.

Prior to the MRP 1.0 and MRP 2.0 investigations, the Solano Permittees collaborated with several other Bay Area stormwater management agencies to measure concentrations of PCBs and other pollutants of concern in embedded sediments collected from stormwater conveyances throughout the Bay Area (KLI, 2002) via the Joint Stormwater Agency Project. The primary goal of this study was to characterize the distribution of pollutants in watersheds draining to the Bay. A total of about 150 samples were collected during the fall of 2000 and 2001. More than six of the samples were collected within the Solano Program's jurisdiction in residential/commercial, industrial, open space and mixed land uses. In 2014, Source Area Maps were developed that described PCB distribution throughout Solano County and the entire SF Bay.

The overall findings of source investigations in Solano Permittee jurisdictions show that much of the new urban and older residential areas have low probability of having substantial PCB source areas. The former Mare Island Naval shipyard is considered an old industrial area based on historic land use. Some old waterfront sections of Vallejo are also considered old industrial and may be examined more closely in the future.

1.3.3 Reasonable Assurance Analysis

Given the risk of PCB and mercury delivery to local waterways, Solano Permittees are required to an analysis to provide 'reasonable assurance' that planned GSI implementation actions are expected to result in reductions that meet MRP 2.0 targets and the TMDL. Reasonable assurance can be defined as the demonstration that the implementation of control measures will, in combination with existing or proposed storm drain system infrastructure and management programs, result in sufficient pollutant reductions over time to meet TMDL waste load allocations or other water quality targets specified in a municipal separate storm sewer system (MS4) permit (USEPA, 2017). RAAs can provide MS4 permittees with a feasibility pollutant reduction roadmap to meeting their future waste load allocations and achieve receiving water limitations. If RAAs are conducted in a way that is well aligned with long-term stormwater planning information needs, they can also be used to support tracking, evaluation, and on-going reporting of the actual progress achieved enroute to the defined regulatory milestones.

2 Reasonable Assurance Analysis (RAA)

2.1 Approach Overview

2.1.1 RAA process

This goal of the Reasonable Assurance Analysis (RAA) is to provide evidence of the degree to which the Solano Permittees' planned control measures will reduce PCBs and mercury loading to meet waste load allocation targets specified in the TMDL and required by MRP Provisions C.3, C.11, and C.12. The MRP requires that both the green infrastructure RAA (C.11.c/C.12.c) and the wasteload allocation attainment RAA (C.11.d/C.12.d) be documented in the 2020 Annual Report. RAA involves implementation of a numeric hydrologic and pollutant loading model and comparing the anticipated progress to waste load allocation targets. This analysis includes only the RAA for green infrastructure, as the wasteload allocation attainment RAA will be documented in a separate report. By performing this RAA in parallel to development of the Green Stormwater Infrastructure Workplan, information from the RAA results were iteratively used to inform Plan development. This approach allows the Solano Permittees to efficiently integrate science-based tools with their stormwater planning processes and provide them with the power to iteratively verify outcomes and track progress over time.

The primary hypothesis addressed in this RAA can be stated as:

> The current level of GSI control measure implementation planned will result in PCBs and mercury load reductions that are sufficient to meet the reduction targets for the Solano Permittees specified in the MRP.

The experimental design is defined by a sequence of future scenarios during which the Permittee urban landscape is modified via changes in land use and impervious coverage, and implementation of GSI. If the expected changes are large enough to overwhelm the uncertainty associated with input data and the modeling process, then the primary hypothesis can be validated or rejected with a reasonable level of confidence.

The structure of this RAA draws substantially from the RAA already completed in Los Angeles County (Geosyntec, 2015). This analysis informed development of the RAA Guidance (BASMAA, 2017) that provides a process and structure for RAA in the SF Bay Area, which is reflected in the current analysis.

The RAA process involved compiling spatial data from various sources and information form Solano Permittees on levels of current and planned redevelopment, new development, and GSI implementation as inputs to several modeling scenarios. The basic steps in the RAA process were the following:

1. Define the modeling problem and identify an appropriate model structure and scale
2. Create a geodatabase to define urban catchment characteristics and drainage
3. Estimate baseline loading conditions and current levels of GSI implementation
4. Verify baseline modeling scenario results
5. Develop future modeling scenarios that reflect the level of projected land use changes and GSI implementation.
6. Compare the estimated reductions to GSI reduction targets for each relevant time horizon
7. Use the modeling scenarios to inform a parcel-scale spatial prioritization analysis for GI implantation site identification
8. Integrate additional planned GSI projects to update modeling scenarios

2.1.2 Correspondence with RAA Guidance Document recommendations

This RAA was coordinated with other Bay Area Permittees via the Bay Area Stormwater Management Association (BASMAA). This included participation in BASMAA workgroups, document review, and aligning the methods of analysis with recommendations included in the BASMAA RAA Guidance (BASMAA, 2017). The intent of the BASMAA RAA Guidance is to maintain a degree of consistency in the way that model analyses for PCBs and mercury are performed throughout the throughout the SF Bay region.

The RAA Guidance creates a useful structure in terms of specifying the scope of the analysis, input data sets, recommended modeling approaches, and allocation of control measures to various future scenarios. Modeling natural systems always requires several subjective decisions whose appropriateness depends on the data available to support the model and the information needs required from the outputs and the model structure. The RAA Guidance attempts to standardize several of these decisions. Sparse comment is provided on others, such as spatial resolution, aligning process representation complexity to the data available, or impacts of various sources of modeling uncertainty. For example, calibration and parameter set non-uniqueness has long been widely acknowledged as one of the most important sources of output uncertainty in hydrology (see Beven, 2001, 2006), and more recently in applied stormwater quality modeling (Wijesiri and Liu, 2018).

Modeling methods for pollutant load reduction estimation employed by the Solano Permittees is generally consistent with the RAA Guidance and aligns directly with recommendations whenever appropriate. Computational methods to modelling urban stormwater hydrology and pollutant loading continue to evolve to meet the needs of stormwater programs and regulators. Modeling decisions included in this analysis are grounded in commitment to create planning tools that are practical and useful for both short and long term stormwater decisions, responsive to evolving regulatory requirements, and readily updatable with new information to empower stormwater managers to implement effective and adaptable programs.

2.1.3 Study area

2.1.3.1 *Solano Permittee MS4 Area*

The study area for the RAA analysis includes the Solano Permittee MS4 area, that includes the cities of Fairfield, Suisun, and Vallejo only, and no areas draining to these areas. This excludes a substantial portion of Solano County that surrounds the Solano Permittee cities (Figure 2.1) As such, the runoff and pollutant load modeling is discrete to these MS4 areas, regardless of upstream flow generation, which typically moves through cities via streams and rivers classified as receiving waters. Since there are no long-term streamflow gauging stations downstream from the cities of Vallejo, Fairfield, and Suisun, the Permittee setting precludes calibration to observed flows. This precludes the need to incorporate additional drainage areas upstream of the Solano Permittee MS4 area in the modeling.

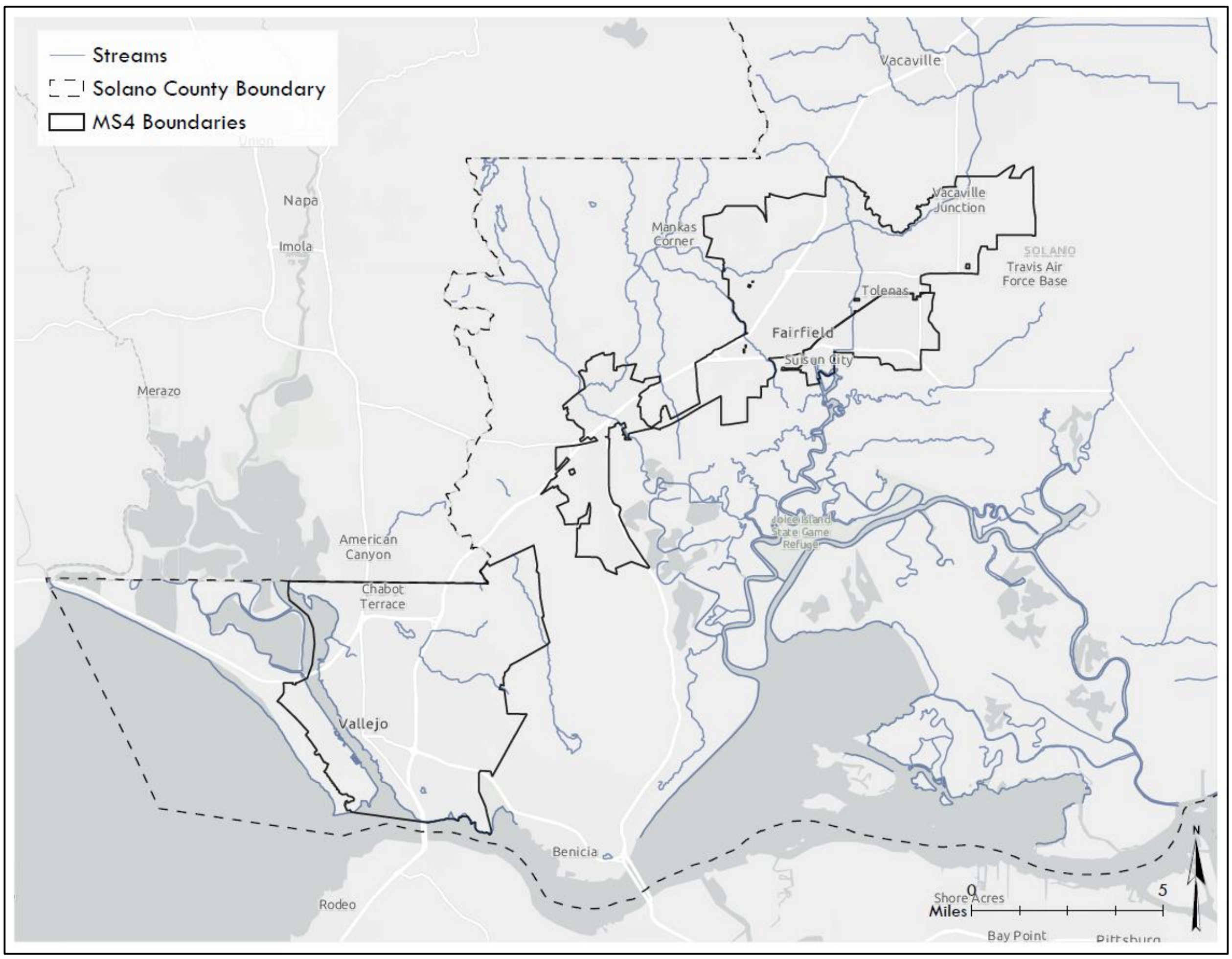

Figure 2.1. Solano Permittee MS4 Area

2.1.3.2 *Municipal Geographies*

The City of Fairfield is located along the Interstate-80 corridor between the major metropolitan areas of San Francisco and Sacramento. Fairfield is surrounded by undeveloped grazing and grasslands, hills to the north, and wetlands to the south beyond Suisun City. Fairfield is the county seat for Solano County and consists of three main areas: Central Fairfield, Cordelia, and the Travis Air Force Base.

The City of Suisun City is in the northern San Francisco Bay Area just south of the City of Fairfield. The Suisun Marsh and additional waterways lie along the southern extent of the city. The area surrounding the city includes hills and mountains. Suisun City has a downtown historic waterfront area that is its distinguishing characteristic.

The City of Vallejo is in the northern San Francisco Bay Area between San Pablo Bay and the Carquinez Strait. The city is surrounded by waterways, wetlands, rolling hills, and open space areas. Vallejo served as the California state capital in the state's infancy, before the state seat was permanently established in Sacramento. Additionally, Mare Island was the first Naval shipyard on the West Coast. Due to the historic context of the city, Vallejo has many historic buildings. Vallejo is in a desirable development location with because of transportation links via road, rail and water. The waterfront area, Mare Island, and downtown are focal points of community development.

2.1.3.3 *Climate and Physical Geography*

Solano County is the easternmost county of the North Bay has a mild coastal Mediterranean climate, with average temperatures increasing by about 10°F from the cooler coast to hotter inland cities. The coastal city of Vallejo is influenced by its position on the northeastern shore of San Pablo Bay, but less sheltered from heatwaves than areas directly on or nearer the Pacific Ocean/Golden Gate such as San Francisco and Oakland. Nearly all the precipitation is delivered between October and May, with an average annual precipitation totals of 21 inches for Vallejo and 24.9 inches for Fairfield/Suisun.

Runoff from the City of Vallejo primarily drains to the Napa River, the Mare Island Straight, and the Carquinez straight, all of which flow to San Pablo Bay. Other receiving waters for urban runoff include American Canyon Creek, Blue Rock Springs Creek, Lake Chabot, Lake Dalwigk, Rindler Creed, Southampton Bay, Sulphur Springs Creek, and White Slough. Fairfield and Suisun both drain to a complex series to tidal marshes and Sloughs that ultimately flow to Grizzly Bay and Suisun Bay. Runoff from Northern Fairfield and Suisun flows creeks and branches of the Suisun Slough, while Southern Fairfield flows primarily to Cordelia Slough. Receiving waters include Alonzo Creek, American Canyon Creek, Dan Wilson Creek, Freeborn Creek, Green Valley Creek, Jameson Creek, Laurel Creek, Ledgewood Creek, McCoy Creek, Soda Springs Creek, and Union Creek.

2.1.4 Conceptual Understanding of Pollutant Load Reduction Mechanisms

The computational model used in this RAA analysis follows from our conceptual understanding of urban drainage hydrology and redevelopment that includes pollutant fate and transport through the stormwater system. To represent these processes, a sequential accounting of runoff and pollutant load reductions is followed:

1. New development and redevelopment alter impervious cover, which affects runoff generation
2. Land use changes alter pollutant characteristic runoff concentrations
3. Source controls reduce pollutants available for transport
4. Rainfall is converted to runoff based on site-specific factors and mobilizes pollutants
5. Areas treated by non-structural LID measures produce less runoff, reducing on-site pollutant mobilization.
6. Decentralized BMPs infiltrate runoff near its source, reducing storm flows via infiltration and retention of pollutants.
7. Excess runoff leaves sites, moving downstream to centralized BMPs where runoff and pollutants are further reduced via infiltration, particle capture, filtration, and/or biogeochemical cycling.
8. Runoff and pollutants not infiltrated or treated by centralized BMPs flow downstream to other catchments or receiving waters.

In this model, water movement follows urban catchments delineations (approximately 100 acres) which define the hydrography of the urban landscape and serves as the primary unit of analysis for routing and connectivity to receiving waters. Urban drainages are aggregations urban catchments that represent the smallest non-arbitrary hydrographic divisions of the MS4.

While this RAA focuses only on GSI implementation, the computational model can easily be extended for the WLA RAA to include source control measure reductions in a subsequent modeling study. By separating the GSI RAA from the WLA RAA, care must be taken not to double count reductions since several source control and GSI components interact with each other. Inconsistencies would probably only become apparent when source control implementation can be defined in specific locations and modeling is performed in a spatially explicit manner as in swTELR. The modeling sequence defined above ensures a consistent accounting of reductions so that results are logically coherent.

2.1.5 Green Stormwater Infrastructure Definition

Green stormwater infrastructure are pollution control measures broadly defined in the MRP (as green infrastructure') (p.147) as:

> *"Infrastructure that uses vegetation, soils, and natural processes to manage water and create healthier urban environments. At the scale of a city or county, green infrastructure refers to the patchwork of natural areas that provides habitat, flood protection, cleaner air, and cleaner*

> *water. At the scale of a neighborhood or site, green infrastructure refers to stormwater management systems that mimic nature by soaking up and storing water."*

This corresponds roughly with the definition provided by the EPA, which overlaps substantially with a traditional definition of Low Impact Development (LID). One difference between the two is that LID usually includes the provision that runoff is managed as close to its source as possible. The definition used in the MRP covers most structural BMPs whether they are small decentralized/distributed BMPs that receive sub-parcel scale drainage or larger centralized/regional BMPs which typically receive neighborhood-scale stormwater drainage.

2.2 Model Selection Rationale

2.2.1 Key modeling considerations and trade-offs

Since all environmental models are simplifications of much more complex systems, an important initial step is to identify the compromises that will be required. These choices are often driven by resource availability and the purpose of the model. The most salient question is: *What do we need to use the model to do?* The answer to this question can dictate much of what gets left in and what gets left out of the model, and there are costs on both sides of that proposition. The problem is often framed as a trade-off between the degree of model complexity and the data required to support that complexity to obtain outputs with a reasonable degree of certainty. Figure 2.2 shows the problem as framed by EPA in their *Guidance on the Development, Evaluation, and Application of Environmental Models* (EPA, 2009). As structural complexity increases, the framework uncertainty decreases, since more of the system detail is represented. However, complex structures require higher order parameterizations, which rely on more data to specify and verify the model, so the additional complexity tends to produce greater uncertainty associated with the underlying data. A key modeling task is to identify the best balance these two sources of uncertainty for the specific modeling purpose.

Figure 2.2 conveys the concept that if we select a relatively simple model (e.g, computing peak flows using the rational method instead of continuous simulation), then we are left wondering if over-simplification leads to false conclusions. If we adopt a more complex model (e.g, continuous simulation at fine-scale spatial resolution), we are challenged with gathering enough real world monitoring data to supply all needed model inputs, or left wondering whether assumptions about model inputs leads to false conclusions. Thus, we seek to achieve just the level of model complexity needed to reach the point of minimum overall uncertainty resulting from the combination of model framework uncertainty and data uncertainty.

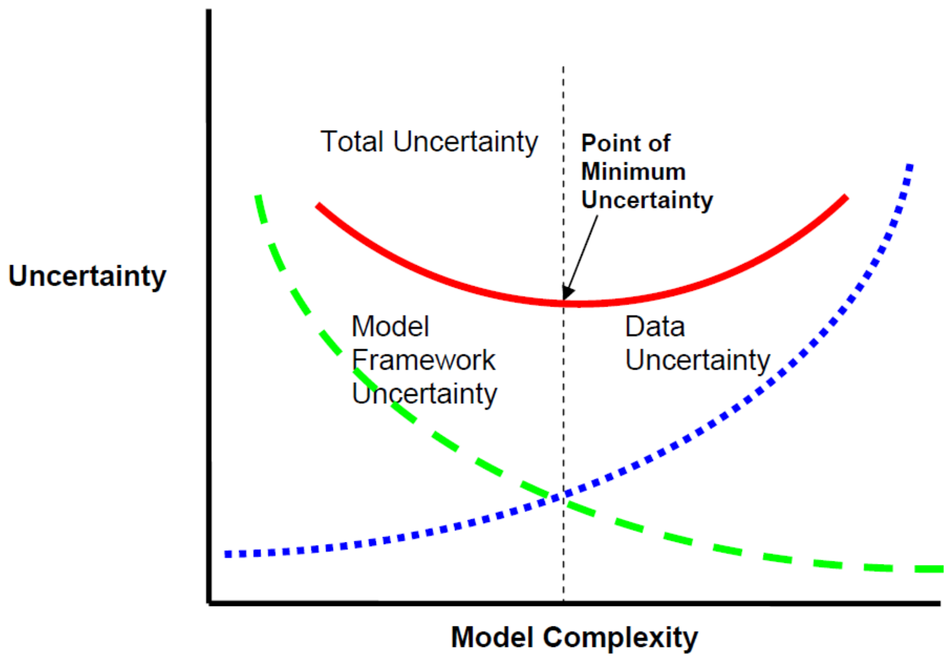

Figure 2.2. Relationship between model framework uncertainty and data uncertainty, and their combined effect on total model uncertainty (Adapted from Hanna, 1988, as presented in EPA, 2009, p.13).

In relatively complex model alternatives, there are numerous free parameters that usually require calibration, but there may be only a few input variables that contribute significantly to the outputs (Li et al. 2014). Over-parameterization, which is exceedingly common, results in a high degree of uncertainty in the model outputs due to subjective decisions required during the calibration process (Beven 1989, Beven 2001). Moreover, parameter values can vary substantially over time and space (Hossain and Imteaz 2016). Even where good hydrological data are available, they are probably only sufficient to support reliable calibration of models of very limited complexity (Jakeman and Hornberger 1993, Gaume et al. 1998). The inability to discern water quality changes over time or spatial patterns in hydrologic models is often due to poorly defined model parameters and resulting output uncertainty (Freni et al., 2011; Beven 2001, Nandakumar and Mein 1997). If the model cannot resolve the effects of management actions outside of predictive uncertainty, it is not a useful tool for estimating the water quality benefits of stormwater BMP implementation, and therefore less value to inform stormwater management decisions.

2.2.2 Aligning model specifications with management information needs

The intended use of model results should ultimately guide model selection and the necessary degree of model complexity (Leavesley et al. 2002). The least complex model that reliably meets the application at the relevant scale is often the best alternative (Chandler 1994, Rauch et al. 2002, Dotto et al. 2012). The goal of this RAA is to quantify pollutant load reductions over time associated with implantation of GSI. For stormwater planning, model selection often boils down to choice between a greater degree of granularity across space or detail of process representation in time. Attempting to do both is computationally expensive, resource intensive, and provides more detail than required. While detailed process representation used in continuous simulation models may improve performance over short time steps, it comes at the expense of greater structural complexity (Snowling and Kramer 2001), without necessarily increasing the usefulness of outputs (Lindenschmidt 2006).

Since stormwater impact mitigation problems invariably have an important spatial component and are typically less concerned with short-term outcomes, modeling approaches that employ parsimonious process-representation in favor of greater spatial granularity make intuitive sense. While continuous simulation models provide a better way to understand dynamics of runoff generation and timing, simpler computational approaches provide a more practical alternative for stormwater managers due to lower costs and fewer data requirements. Indeed, it was recognized long ago by the earliest developers of continuous simulation stormwater models that they would be too detailed for many users and that there is a need for a wide range of procedures for assessment of stormwater pollution control costs and priorities (Heaney et al. 1976). This is especially true when resources are limited and one primary use of the outputs is to track changes over time (e.g. Schueler 1987, Chandler 1993;1994). Simpler approaches may even provide comparable performance to more complex ones (e.g., Kokkonen and Jakeman 2001, Perrin et al. 2001, Bormann and Diekkruger 2003, Reed et al. 2004; Petrucci and Bonhomme 2014), particularly when high time resolution outputs are not required.

2.2.3 RAA modeling approach

A pragmatic approach to model development was taken that eliminates elements that do not serve the purpose of ongoing stormwater load reduction quantification. The intent was to increase model transparency, usability, and updatability, to lower costs, and limit data uncertainty. Most available stormwater modeling tools are either intended exclusively for expert users (Atchison et al. 2012), or do not provide an efficient method for modeling multiple catchments or generating spatial outputs (e.g., Rossman 2013, Tetra Tech 2011).

This RAA uses the Stormwater Tool to Estimate Load Reductions (swTELR) (Beck et al 2017), a purpose-built model with an economical structure, that provides spatially explicit outputs designed to track stormwater BMP implementation over time. Identifying the best trade-offs between complexity and data requirements were a primary driver of the model structural design. These factors were considered within the context of data and resources that are likely available to stormwater managers in the long term. A computationally efficient approach can run via the web and may be used for ongoing quantification of pollutant load reductions and iterative verification of results by non-modeling experts. In this way, it can provide a dynamic alternative for ongoing planning and compliance decades after this RAA has been completed.

2.3 The swTELR Model

In this section we present the primary concepts and calculations used in the swTELR to perform this RAA. Additional documentation is available in Appendix A, contain sensitivity analyses, results of validation experiments, discussion of model limitations.

2.3.1 Model structure overview

swTELR is designed to have lower data input requirements than existing alternatives. Hydrologic computations combine a set of metrics that describe a 35-year rainfall distribution with well-tested algorithms from the National Resources Conservation District (NRCS Curve Number) for rainfall-runoff transformation and routing to generate average annual runoff estimates. Key inputs include spatially distributed rainfall, hydrography, soil types, land use, and impervious cover, along with BMP data. Pollutant generation is modelled via land-use based characteristic runoff concentrations (CRCs) to represent the generation, fate and transport of urban-derived pollutants. In effect, swTELR includes two parameters (CN and CRC), both of which are specified by the spatial data. The Curve Number method for runoff generation has been widely used in several watershed and stormwater models including the current iteration of EPA's Stormwater Management Model (SWMM 5).

A spatially explicit mass balance accounting method is used to quantify the runoff and pollutant reductions achieved with control measures. A hydrograph separation approach is used to quantify the water quality benefits of centralized, large-scale structural BMPs, and a simpler approach is used for small decentralized BMPs that omits accounting for flow timing. Validation experiments have shown that runoff estimation aligns closely with high-resolution monitoring data as well as results generated from more complex, well-accepted continuous simulation models (Beck et al., 2017), providing confidence that the swTELR computational approach is technically well-suited to inform stormwater planning applications.

2.3.2 Spatial and temporal scales of representation

Stormwater models vary widely in terms of how urban catchments are delineated and how landscape characteristics are discretized. swTELR employs a semi-distributed approach where runoff, loading and decentralized BMP reduction calculations happen on 30-meter grid scale (Figure 2.3), and hydrologic routing is performed at the urban catchment scale (approximately100 ac). Accounting of reductions from BMPs are spatially explicit so that the site-specific runoff generation and pollutant loading characteristics specific to the BMP drainage are preserved. Explicit of flows across grid cells features is not represented as it would be in fully distributed models (e.g. Bicknell et al. 1997, Lee et al. 2012), rather this is handled at the catchment scale.

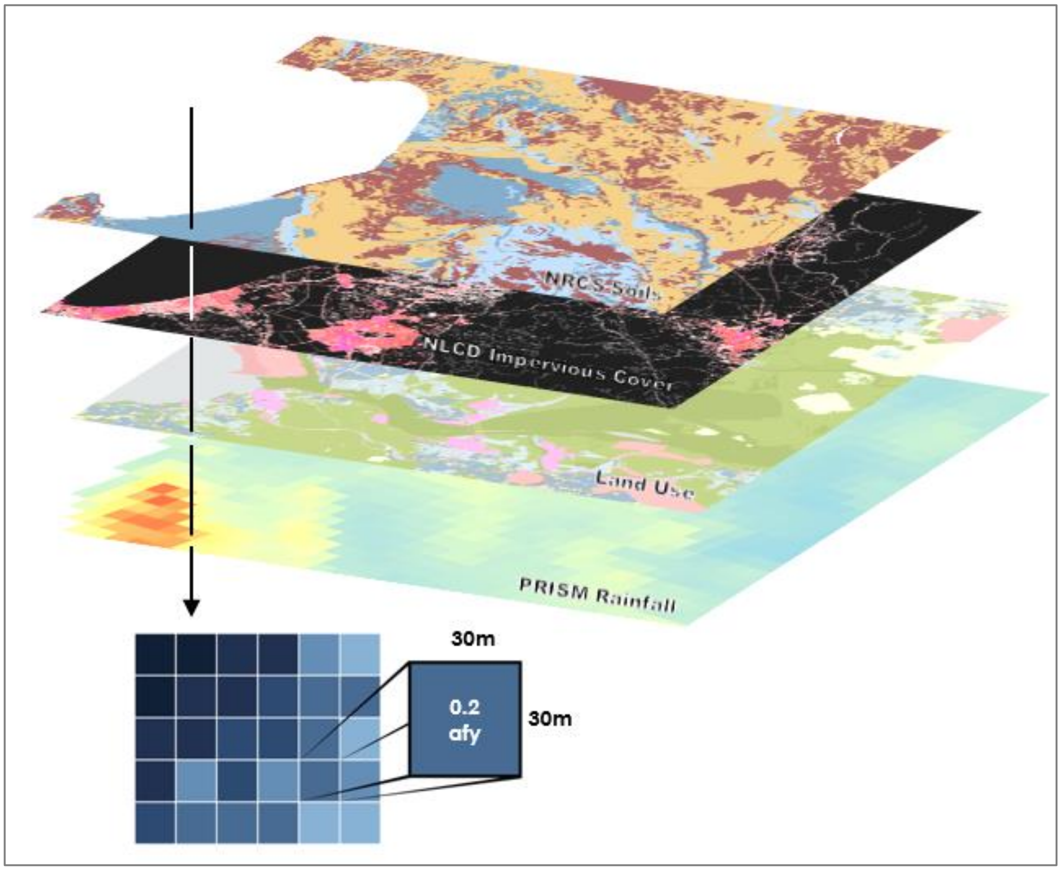

Figure 2.3. Graphical representation of raster calculations performed in swTELR to generate gridded runoff estimates.

Typically, stormwater runoff is modeled using 1 of 2 approaches: a single storm event methodology or a multi-year, high-resolution (daily or sub-daily) continuous simulation. Event-based approaches are programmatically simple but were originally designed to simulate runoff for a single storm event size (USDA 1986). Continuous simulations are generally better able to capture the dynamic range of rainfall-runoff responses by accounting for antecedent catchment moisture conditions (Harbor 1994, Bicknell 1997, Rossman 2008). swTELR employs a hybrid event-based approach that combines a set of events drawn from a long-term regional precipitation distribution to provide average annual runoff estimates. In effect, swTELR brackets the range of rainfall and runoff responses with a probabilistic approach, rather than a sequential, time-explicit approach (described in section 2.3.3).

This swTELR approach allows substantially simplified computation compared to continuous simulation, allowing substantially more spatially granular outputs that indicate precisely locations within the urban landscape that hold the greatest opportunities for runoff and pollutant load reductions. In addition, this approach avoids the model outputs being tied to a short time period, which may not capture a long-term representation of the range of event magnitudes. Given the lifespan of stormwater infrastructure is typically several decades, and the simulations included in this RAA will span 20 years, using a multi-decadal period to characterize rainfall seems prudent. In short, we believe that a probabilistic treatment of rainfall provides the best compromise for generating outputs that most closely align with the purpose of RAA.

2.3.2.1 *Precipitation data*

Raster-based rainfall estimates are from the PRISM Climate Group[7] at Oregon State University are used for runoff generation in swTELR, typically covering a 35-year time span. These data provide spatially distributed precipitation at 800m resolution and are processed in swTELR to provide a probabilistic description of rainfall. The extracted raster-based precipitation estimates from PRISM have been independently validated using Western Regional Climate Center (WRCC) rain gauges for 15 cities located on the California Coast.

2.3.2.2 *Soils*

The USDA Natural Resource Conservation Service (NRCS) defines four hydrologic soil groups (HSGs): A, B, C, and D. A has the largest infiltration potential and is associated with the least amount of runoff whereas HSG D has the lowest infiltration potential and is associated with the most amount of runoff. The NRCS HSGs are based on soil composition and textural properties and align with NRCS curve number values for pervious surfaces. The classification of soils is determined by the soil layer with the lowest saturated hydraulic conductivity and the depth to any layer that is impermeable or depth to a water table (if present). HSGs reflect infiltration in the subsurface at depths of up to 2 feet or greater. Bay Area soils predominantly belong to groups C and D, making infiltration slower than more permeable soils in many locations. swTELR uses spatial soils data from two sources, the NRCS SSURGO database, which offers higher resolution, and the STATSGO2 database, which provides greater coverage in some areas.

2.3.2.3 *Impervious cover*

A key input for runoff generation in swTELR is satellite-derived impervious cover derived from the Landsat satellite series (https://viewer.nationalmap.gov/launch/) and available from the USGS at 30-meter resolution. Impervious cover dramatically reduces runoff infiltration to soils and thus transforms incident rainfall to runoff at substantially higher proportions than undeveloped lands. Use of satellite imagery to estimate impervious cover has several important benefits to estimate urban runoff. Satellite impervious coverage data is widely available, regularly updated, and can be easily accessed by any municipality. The use of satellite imagery rather than on-the-ground mapping of impervious cover incorporates the urban tree canopy to estimate overall impervious area. Extensive research has documented the reductions that urban trees provide to the rainfall-runoff transformation in urban drainages (Dwyer et al., 1992; Roy et al., 2012). The 30m resolution

[7] http://prism.oregonstate.edu/

of the Landsat data align with the other swTELR spatial inputs, making the data compilation and processing efficient.

2.3.2.4 *Catchment connectivity*

Catchment connectivity is a critical element of generating reliable estimates of average annual runoff and loading derived from an urban catchment and delivered to a receiving water. Catchment connectivity is defined as the proportion of stormwater discharging from a catchment discharge point that reaches the receiving water and is not diverted in some way. All catchment runoff and loading estimates reported from swTELR are adjusted based on the relative hydrologic connectivity of each catchment to the receiving water. MS4 mapping guidance (2NDNATURE, 2018) includes a systematic process for a user to determine the relative hydrologic connectivity of a catchment to receiving waters based on the distance, substrate and visual characteristics of the flow path that physically connect the discharge point of a specific catchment to the receiving water. Working inland from the receiving waters, all catchments that drain into another catchment inherit the same connectivity as the downstream catchment, unless there is evidence suggests that some surface volume loss occurs between the two catchments. Catchment delineation and connectivity is typically completed in coordination with city stormwater staff.

2.3.2.5 *Stormwater BMPs*

Stormwater TELR was developed to easily incorporate both structural and non-structural stormwater BMPs of various types, sizes, and applications. Stormwater BMP locations, types, and specifications are documented and typically communicated to 2NDNATURE via spreadsheets or uploaded to the swTELR web interface. An iterative process is performed to verify BMP attributes and recommend field verification where necessary. BMPs are stored within an asset management system that includes tracking, field protocols, and mobile apps for performance verification that are integrated to the stormwater model.

2.3.3 Precipitation data processing

Precipitation inputs are designed to bracket the seasonal and inter-annual variability demonstrated by historic data, defined using the PRISM dataset published by Oregon State University. We used the historic distribution of 24-hr rainfall depths (24-hr event frequencies) and the average annual number of days with measured rainfall to drive runoff generation. The 35-year (1981-2016) precipitation cumulative distribution function for each precipitation region was broken into a set of percentile values. This approach provides a way to bracket the likely event magnitudes in each region, incorporates extreme events in a manner proportional to their likelihood of occurrence, and serves to standardize the inputs from one modeling scenario to another using a small number of representative metrics.

Stormwater TELR calculates various 24-hr precipitation depths and the average annual number of days with measurable precipitation to represent the overall distribution and accurately estimate total average annual depths. We calculated, d, the average number of rain days per water year when daily rainfall exceeds 0.01 inches (0.25 cm) and, P(x), various 24-hr event frequency estimates, where P is the 24-hr rainfall depth for the xth percentile event. On a water year basis, we selected 24-hr event rainfall frequencies and applied the trapezoid rule to estimate the integral of the 24-hr event cumulative distribution function to obtain a long-term average 24-hr runoff volume for days when it rains. We approximated the integral using the following equation for non-uniform intervals of x:

$$\int_0^{100} P(x)\,dx \approx$$

$$\frac{1}{2}\sum_{k=1}^{N}(x_{k+1} - x_k) * (P(x_{k+1}) + P(x_k)) \qquad (2.1)$$

where x is a number between 0 and 100, and k is number in the sequence of total, N, percentile events used to estimate the integral. To obtain a long-term average annual runoff volume, P365, we multiplied the 24-hr average by the number of rain days per year, d:

$$P_{365} = d * \int P(x)dx \qquad (2.2)$$

The average annual 24-hr rainfall for days when it rains is calculated using a set of 4 percentile events that correspond with common post-construction permit requirements and structural BMP design criteria (85th and 95th percentile storm events), which also include the median and the lower quartile. Figure 2.4 shows the historic 24-hr event frequency distribution for a typical precipitation distribution and a graphical representation of how the trapezoid rule is used to estimate the long-term average 24-hr rain events. This approach has been compared with several other approaches to characterizing the long-term precipitation distributions (Beck et al. 2017).

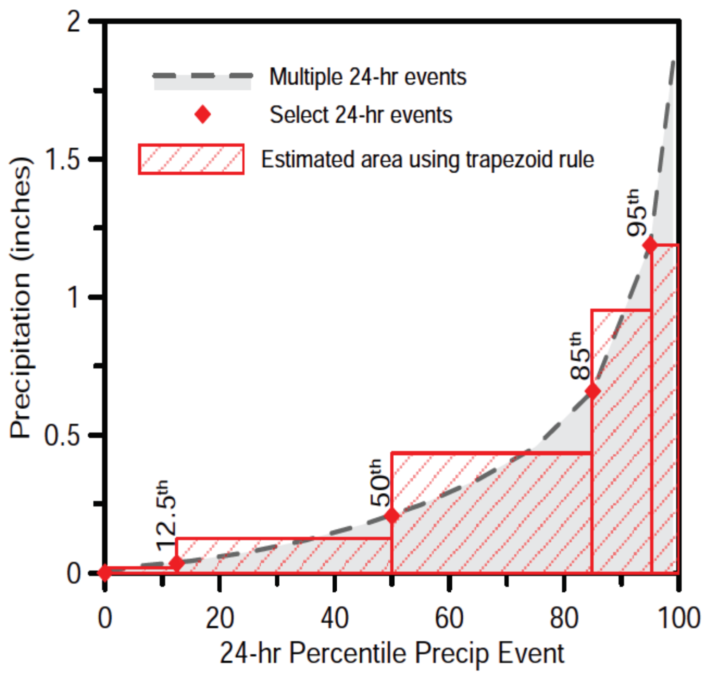

Figure 2.4. Illustration of the trapezoid method used to sum the area below the curve of the precipitation cumulative distribution function.

2.3.4 Rainfall-runoff transformation

For a given storm magnitude and duration, the runoff generation module defines the fraction of flow that infiltrates over pervious surfaces and the fraction of overland runoff that is eventually discharged to the receiving waters. Stormwater TELR relies on the Soil Conservation Service (SCS) curve number (CN) method and the approach detailed in Technical Release 55 (TR-55) to estimate runoff from small urban catchments (USDA 1986). The SCS runoff equation is:

$$Q = \frac{(P - I_a)^2}{(P - I_a) + S} \quad (2.3)$$

where Q is the runoff depth, P is the 24-hr rainfall depth, S is the potential maximum retention after runoff begins, and I_a is the initial abstraction depth. The initial abstraction incorporates all losses before runoff begins, including water retained in surface depressions, water intercepted by vegetation, evaporation, and infiltration. Runoff does not begin until the initial abstraction has been met. I_a is variable across the landscape but is highly correlated to the curve number. The initial abstraction is 20% of the storage,

$$I_a = 0.2S \quad (2.4)$$

and

$$S = \frac{1000}{CN} - 10 \qquad (2.5)$$

More recent data suggest that 0.20*S might be too high and that 0.05*S is more appropriate (Woodward et al. 2003, Lim et al. 2006, Shi et al. 2009) especially for hydrologic soil groups C and D (Jiang 2001). If 5%, rather than 20%, is used, S must also be modified. The relationship between $S_{0.05}$ and $S_{0.20}$ obtained from model fitting results is (Lim et al. 2006, Hawkins et al. 2002)

$$S_{0.05} = 1.33 * S_{0.20}{}^{1.15} \qquad (2.6)$$

We used the adjusted initial abstraction ratio (equation 6) and by substituting equation 4, modified for 5% of storage, into equation 3, we obtain

$$Q = \frac{(P - 0.05S_{0.05})^2}{P + 0.95S_{0.05}} \qquad (2.7)$$

Curve numbers range from 30 to 98 and lower numbers indicate low potential runoff whereas higher numbers indicate increasing runoff potential. The major factors that determine SCS curve numbers are the soil type, the land use (specifically, the percent impervious of the land use), the hydrologic condition and soil infiltration capability. To simply account for variations in soil permeability and infiltration, the NRCS has classified soils into 4 hydrologic soil groups (HSGs). A curve number for a given land use with impervious area can be estimated by the following (USDA 1986):

$$CN_c = CN_p + \frac{P_{imp}}{100}(98 - CN_p) \qquad (2.8)$$

where CN_c is the runoff curve number for the entire land use, CN_p is the pervious runoff curve number and P_{imp} is the percent imperviousness. The pervious curve numbers used are those defined for open space in poor condition (grass cover < 50%) (USDA, 1986), since urban soils are often disturbed or compacted, and are listed in Table 2.1.

Table 2.1. Urban pervious curve numbers used in swTELR (USDA, 1986)

Soil Type	A	B	C	D
Curve Number	68	79	86	89

The model generates discrete runoff outputs which mirror the 24-hr event percentile precipitation inputs. Using equations 1 and 2, we replaced the rainfall *P(x)* with runoff *R(x)*, where *R* is the runoff calculated by the approach described above for a set of 24-hr rainfall events. Similar to the calculation described for the rainfall, the trapezoid rule is applied to the x^{th} percentile event which are summed to approximate the area under the probability distribution function and obtain the average annual runoff.

Antecedent runoff conditions are a critical component to accurately determining runoff and the SCS curve numbers originally incorporated average antecedent runoff conditions (USDA 1986). The ability of continuous models to represent varying catchment moisture condition is a distinct advantage over event-based models. Recent studies have shown the importance of adjusting CNs based on antecedent runoff conditions (Bhaduri et al. 2000, Michel et al. 2005). Because swTELR was developed to estimate long-term average annual runoff conditions, we do not adjust the CNs and assume average antecedent runoff conditions for all simulations.

2.3.5 Pollutant loading

Urban pollutant modeling approaches commonly estimate pollutant loading at the land use spatial scale and use a variety of approaches to determine the associated land use characteristic pollutant concentrations. Algorithms to represent pollutant build-up and wash-off over time are common in continuous simulation models (Freni et al., 2009; 2011; Mannina and Viviani, 2010; Hossain and Imteaz, 2016), which has been shown to improve pollutant modeling performance in some cases (Wang et al., 2011). However, optimal parameters for these calculations are difficult to identify with precision or validate with sampling (Freni et al., 2009). While Monte Carlo sampling of the parameter space can improve parameter identifiability (Strecker et al., 1990; Wagener and Kollat 2007; Freni et al., 2011), high degrees of uncertainty in model outputs remain (Petrucci and Bonhomme, 2014). Further, other researchers have found that pollutant accumulation and generation on event time scales is extremely difficult to predict and that similar seasonal or annual results could be obtained using constant concentrations (Sage et al., 2015).

Since pollutant loads are strongly dependent upon runoff volumes at longer time scales, attempting to capture the short-term variability in pollutant concentrations is less important for swTELR's application. Using static runoff concentrations for different land-uses was identified as the best approach. Stormwater TELR calculates pollutant loads as the product the stormwater volume and a pollutant concentration. This approach ignores the event-specific dynamics that depend on rainfall duration and intensity that have been linked to variations in pollutant concentrations throughout an event. However, at the average annual scale, these effects are substantially less important on catchment loads than the catchment inputs and runoff volumes for explaining pollutant loads (Lee and Bang, 2000; Brezonik and Statelmann, 2002).

Annual pollutant loading (L) is calculated for each grid cell, (Lg) as the product of the average annual land use runoff Qa, and the land use specific characteristic pollutant runoff concentration [p] (mg/L) for that grid cell, with proper unit conversions.

$$L_g = Q_a * [p]_{LU} \quad (2.9)$$

Annual catchment pollutant load (L) is the sum of the grid cells within that catchment,

$$L_c = L_{g1} + L_{g2} \ldots + L_{gi} \quad (2.10)$$

where i is the total number of grid cells in the catchment. Pollutant load estimates can be compared within and across municipalities by normalizing by the catchment size, A, to obtain an average annual loading rate, *{La}*,

$$\{L_a\} = L_c/A \quad (2.11)$$

2.3.6 Pollutant association with sediments

Urban pollutant load reductions calculated in swTELR for PCBs and mercury correspond to BMP reduction efficiencies associated with sediment removal, often measured as total suspended solids (TSS) or Suspended Sediment Concentration (SSC) reductions. Like many other uban pollutants, PCBs and mercury are both strongly hydrophobic and have a tendency to adsorb to particulates. Pollutants such as metals are often bound to particulate matter in runoff (Loganathan et al., 2013; Chen and Chang, 2014; Herngren et al., 2005; Sartor et al., 1972; Kayhanian et al., 2012). Strong correlations have been observed between particulates measures and total organic carbon, nutrients, heavy metals, oil and grease (Kayhanian et al., 2012; Nasrabadi et al., 2016) polycyclic aromatic hydrocarbons (PAHs) (Rugner et al., 2013), and Bacteria (Stein et al., 2007).

We expect sediment reduction in BMPs to be a useful proxy for most conservative constituents such as PCBs and mercury. PCBs are mostly found in a particulate phase, are associated with coarse-grained particles, and behave like sediment particles. Previous studies in heavily urbanized watersheds have found more than 75% to 100% of the total PCB load was associated with the particulate phase (Ko and Baker, 2004; Bressy et al. 2012). In the SF Bay Area, Gilbreath et al (2012) also noted a strong association of high turbidity levels and elevated PCB concentrations.

Yee and Mckee (2010) found that 55% of PCB particles in stormwater settled out within 30 minutes, and concluded that PCB behaved very much like a sediment particle, and that effective settling of moderate to larger sediment particles was capable of achieving a minimum 50% PCB removal. A European study found that urban tree pits and their associated bacteria have the capability to degrade PCBs in the soil (Leigh et al, 2006). This finding suggests that practices such as bioretention which have aerobic media conditions may also promote the growth of PCB-reducing bacteria.

Monitoring studies have shown that mercury levels in storm flow are strongly correlated with turbidity (Gilbreath et al, 2012), suspended particulate matter and particulate organic matter

(Mason et al, 1999). David et al (2009) reported a strong correlation between mercury concentrations and suspended sediment in urban and agricultural rivers in California. Settling column experiments by Yee and Mckee (2010) using stormwater runoff and sediment samples from urban watersheds in the San Francisco Bay area found that 10 to 30% of mercury entrained in stormwater settled out within 20 minutes, and 90% of mercury re-suspended from creek sediments settled out within 10 minutes. Based on these experiments, Yee and McKee concluded that mercury behaved very much like a sediment particle, and that any urban BMP that promoted settling of fine sediment particles or captured fine-grained street solids should be effective at reducing mercury loads in urban watersheds.

2.3.7 Decentralized BMPs

Decentralized BMPs types either reduce volume, treat pollutants, or do both (Table 2.2). Runoff volume reductions are achieved via infiltration and net exfiltration and these reductions in volume as a result of BMP interactions could be measured. Pollutant concentration reductions can be measured due to retention, filtration or capture that prevents some fraction of the particulate load delivered to structural BMP from exiting. Detailed descriptions of decentralized BMP types represented in swTELR are listed in Appendix D.

Table 2.2. Decentralized BMP types represented in swTELR

BMP Type	Runoff reduction	Pollutant concentration reduction
Biofiltration		✓
Bioretention	✓	✓
Bioswale	✓	✓
Filtration Device		✓
Infiltration Feature	✓	
Pervious Pavement	✓	
Sediment Trap		✓
Settling Basin		✓

Runoff and pollutant load reductions from decentralized BMPs are calculated as the difference of model outputs. Baseline flows and loads are first calculated, then decentralized BMPs are added, and the model is re-run as a future scenario. The flow and load reductions are calculated as the difference between baseline and future scenario model outputs. In practice, future scenarios include both decentralized and centralized BMPs.

2.3.7.1 *Decentralized BMP runoff reductions*

Decentralized BMP runoff reductions are calculated based on their design storm specifications and impervious drainage areas. All runoff generated up to the design storm depth is either infiltrated or treated and flows generated above the design capacity are bypassed and routed downstream. For example, if a BMP is designed to the 85th percentile rainfall event, all runoff generated from events up to and including the 85th percentile event will be infiltrated or treated. Reduced flows from decentralized BMPs that are intended to infiltrate stormwater (see table 2.2) are calculated for each 30-meter grid cell proportional to the impervious drainage area treated for each BMP, per Equation 2.12

$$QR_g = \int_0^{85} Q_g(x)\,dx \approx \quad (2.12)$$

where QR_g is the treated runoff volume (ac-ft) for the 85th percentile design storm from a single grid cell. In this instance, events larger than the 85th percentile storm would remain untreated. The total runoff volume treated by decentralized BMPs is the sum of each cell within a decentralized BMPs drainage area,

$$QR_d = QR_{g1} + QR_{g2} \ldots + QR_{gi} \quad (2.13)$$

Based on Equation 2.13, the volume reduction realized from decentralized BMPs has a commensurate pollutant load reduction even without any reduction in pollutant concentration. In this example, the grid cell pollutant load is reduced solely due to the reduction of stormwater runoff volumes,

$$PR_g = QR_g * [p]_{LU} \quad (2.14)$$

where PR_g is the pollutant load that includes the respective runoff volume reduction (QR_g) multiplied by the is the characteristic runoff concentration ($[p]_{LU}$, mg/L) for the land use associated with that grid cell. Pollutant load reductions (PR_d) for each catchment after treatment by decentralized BMPs is the sum of all grid cells within that catchment.

$$PR_d = PR_{g1} + PR_{g2} \ldots + PR_{gi} \quad (2.15)$$

2.3.7.2 *Decentralized BMP pollutant concentration reductions*

As already discussed (section 2.3.6), swTELR provides decentralized BMP pollutant concentration reductions commensurate with expected BMP sediment reductions. This approach mirrors that taken in the Chesapeake Bay to simplify reduction accounting for the range of urban BMP types using curves that reflect sediment removal since it closely corresponds closely with removal of particulate bound urban pollutants of concern (see Scheuler and Youngk, 2015).

To estimate pollutant concentration benefits from decentralized BMPs, we assume decentralized BMPs that capture pollutants are 80% effective at reducing pollutant concentrations up to the 85th percentile 24-hr storm event at benchmark or optimal condition (CASQA, 2003; Water Environment Federation, 1998). For example, a grid cell treated by decentralized BMPs that reduces pollutant concentrations has a treated pollutant concentration, $[p]Tr_g$ (mg/L) calculated as:

$$[p]Tr_g = [p]_g * (1 - 0.8) \tag{2.16}$$

where $[p]_g$ (mg/L) is the original grid cell land use CRC. The pollutant load reduction (PR_g) from a grid cell draining to a decentralized BMPs that only reduces pollutant concentrations is,

$$PR_g = QTr_g * [p]Tr_g \tag{2.17}$$

If a grid cell is treated by a decentralized BMP that reduces both runoff volumes and pollutant loads (e.g., bioretention), then there is an indirect and direct pollutant load reduction as a result of infiltration and pollutant retention. Following equations 2.13, the load reduction from a grid cell with both a volume and pollutant concentration reducing BMP is

$$PR_g = QR_g * [p] + (Q_g - QR_g) * [p]Tr_g \tag{2.18}$$

where QR_g is the flow reduction from the grid cell as a result of infiltration, as calculated by equation 2.12. While flows above the design level are not infiltrated by the decentralized BMP, particles are still captured via particle settling and interaction with vegetation and flows are slowed by pooling. The total catchment pollutant load after reductions from decentralized BMPs is the sum of grid cells treated by decentralized BMPs within their respective drainages.

$$PR_d = PR_{g1} + PR_{g2} \ldots + PR_{gi} \tag{2.19}$$

2.3.8 Centralized BMPs

Large scale centralized structural BMPs (e.g., treatment vaults, infiltration basins, dry basins) typically treat stormwater runoff from mixed land use catchments and have treatment capacities on the order of an acre-foot or more (approximately 1,200 m^3). Stormwater can exit a centralized BMP in 1 of 3 ways: loss through infiltration, discharge via treatment aperture, or via bypass where no treatment or detention has occurred. Some models also include evaporative losses, but given proper functioning, structural BMPs should have drawdown times on the order of hours and we assume this term is negligible. The relative components of volume loss depend on the BMP type and design specifics. For example, an infiltration BMP has only infiltrated and bypassed volumes, while a treatment vault has only treated and bypassed volumes. Figure 2.5 provides schematics of centralized BMPs represented in swTELR, from which swTELR assumes volume loss via 3 potential critical pathways: infiltration, treated outflow, and bypass. BMP types represented in swTELR are listed in Table 2.3 with their relevant pollutant and runoff reductions.

Table 2.3. Centralized BMP types represented in swTELR

BMP Type	Runoff reduction	Pollutant concentration reduction
Bed Filter		✓
Detention Basin		✓
Dry Basin	✓	✓
Infiltration Basin	✓	
Media Filter		✓
Treatment Vault		✓
Wet Basin		✓
Retention Basin	✓	✓

Calculation of runoff flow and pollutant load reductions from centralized BMPs are calculated as the difference of model outuputs. Baseline flows and loads are first calculated, then centralized BMPs are added, and the model is re-run as a future scenario. The flow and load reductions are calculated as the difference between baseline and future scenario model outputs. In practice, future scenarios include both decentralized and centralized BMPs.

2.3.8.1 *Centralized BMP runoff reductions*

Stormwater TELR derives each volume loss term from the outflow hydrograph using a hydrograph separation approach to estimate the fraction of volume infiltrated, treated, and bypassed flow based on 4 key user inputs: treatment capacity, basin footprint, and, if applicable, the infiltration rate and drawdown time (Table 2.4). Infiltrated volumes are net volume reduction as a result of BMP interaction. Stormwater discharges through a treatment aperture are termed treated volumes and assumed to have experienced pollutant retention via particle settling, filtration or biogeochemical process. Bypass volumes are those where no treatment has occurred due to unacceptable residence times within the BMPs. Other volume loss terms, such as evapotranspiration, are assumed insignificant on an average annual basis and ignored. The volume routing pathways by BMP type are graphically summarized in Figure 2.5.

Table 2.4. Centralized BMP types and attributes

BMP Type	Treatment Capacity	Footprint	Infiltration Rate	Treatment Rate	Drawdown Time	Wet Pool Capacity
Bed Filter	✓	✓		✓		
Detention Basin	✓	✓			✓	
Dry Basin	✓	✓	✓		✓	
Infiltration Basin	✓	✓	✓			
Media Filter	✓	✓		✓		
Treatment Vault	✓	✓		✓		
Wet Basin	✓	✓			✓	✓
Retention Basin	✓	✓	✓		✓	

The corresponding volumes are calculated using graphical methods (Figure 2.6). Separation of the infiltration volume is determined by drawing a flat line across the hydrograph at the infiltration flow rate, calculated as the product of the infiltration rate and the basin footprint with proper unit conversion). Separation of the treated volume is defined by drawing a flat line across the hydrograph at the treatment flow rate, estimated as quotient of the treatment capacity and the drawdown time with proper unit conversion. Both the infiltration volume and the treated volume are calculated as the area of the outflow hydrograph under the respective flow rates down to a zero flow rate. If the sum of the infiltrated and treated volumes is less than the total outflow volume, then the remaining volume is allocated to bypass. If the sum of the infiltrated and treated volumes is greater than the total outflow volume, then the treatment volume is reduced to accommodate the difference and the volumetric balance between inflow and outflow is retained.

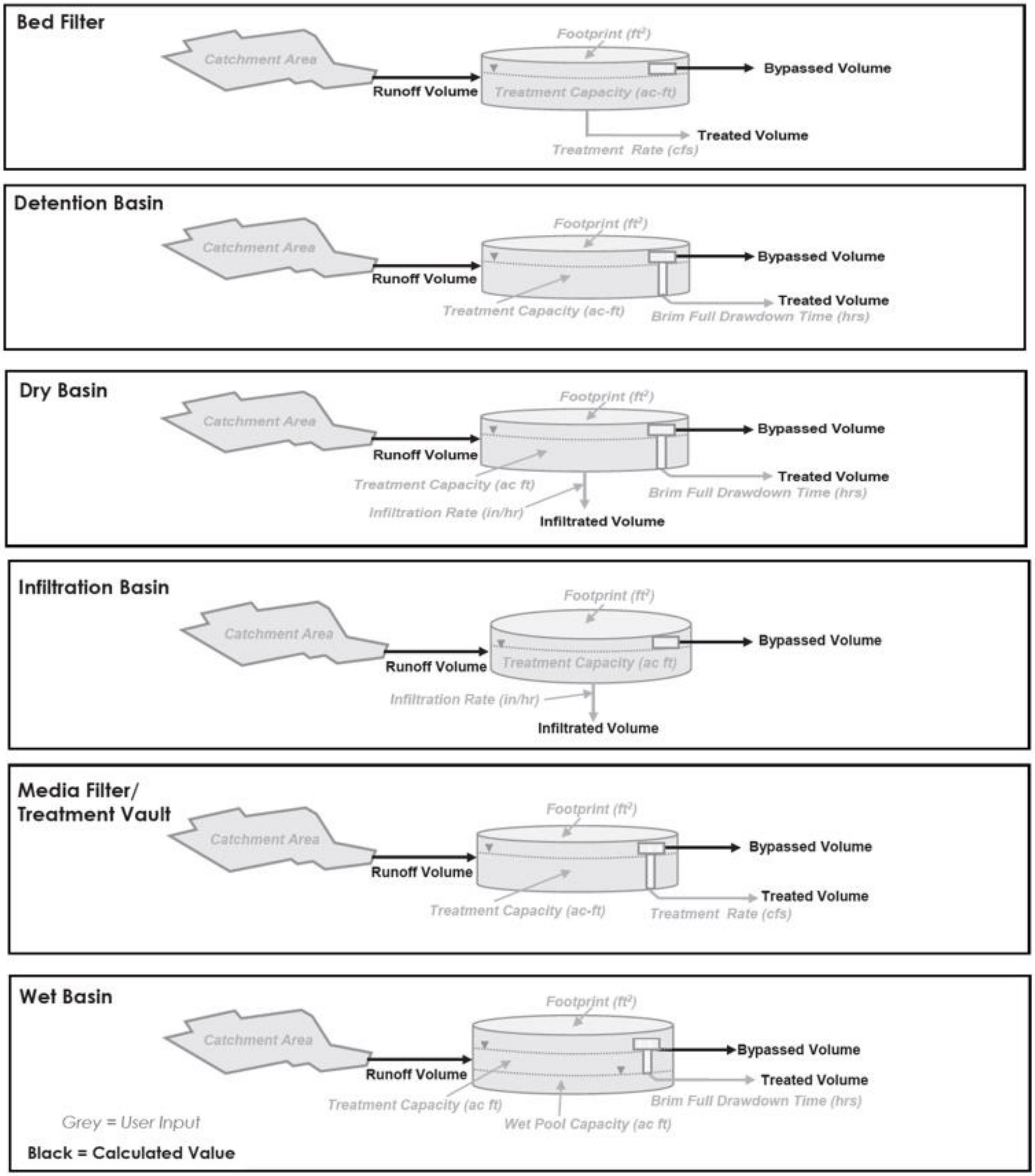

Figure 2.5. Centralized BMP types, inputs and calculated values as implemented in swTELR.

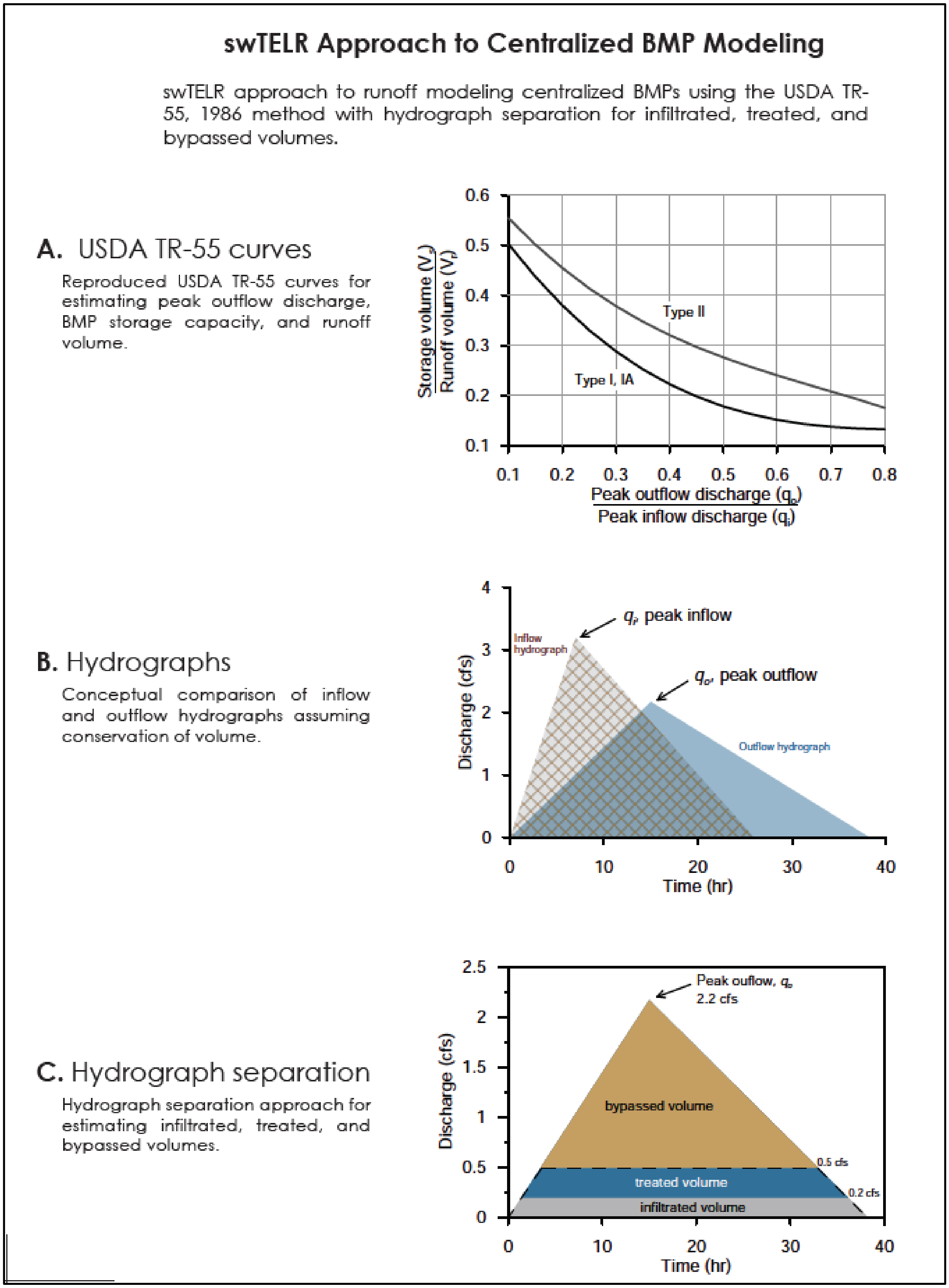

Figure 2.6. Centralized BMP flow partitioning

Average 24-hr and 365-day stormwater runoff volumes from large scale centralized BMPs are modeled using the same approach to estimate baseline runoff from selected 24-hr precipitation events (12.5, 50, 85, 95) that describe the precipitation distribution. The TR-55 (USDA, 1986) approach to estimate peak outflow and the hydrograph separation approach to estimate infiltrated, treated, and bypassed volumes is conducted for each 24-hr percentile precipitation event. Average 24-hr infiltrated, treated, and bypassed volumes for days when it rains are estimated using the trapezoid rule. Average 365-day infiltrated, treated, and bypassed volumes from catchments with large-scale centralized BMPs is estimated by the product between volume and the average number of days per year with measurable rain. When the infiltrated, treated, and bypassed volumes (Q_{infil}, Q_{CEC}, and Q_{BY}, respectively) are properly allocated, the total inflow is equal to the total outflow, Q_{OUT}

$$Q_{OUT} = Q_{infil} + Q_{CEC} + Q_{BY} \quad (2.20)$$

2.3.8.2 *Centralized BMP pollutant concentration reductions*

The pollutant load after interaction with a centralized BMP is the sum of the bypassed and treated loads. Each of these components is the product of the pollutant concentration and associated volume. The concentration of the water infiltrated and bypassed is equal to the incoming concentration of runoff prior to treatment by the centralized BMP. A characteristic effluent concentration (CEC) is assigned to the treated volumes (Table 2.5), $[p]_{CEC}$ (mg/L) that are dependent on the BMP type to calculate *reduced* pollutant loads (PT_r) associated with volumes treated (not infiltrated) by centralized BMPs (Q_{cec}) according to equation 2.21:

$$PTr_c = Q_{CEC} * [p]_{CEC} \quad (2.21)$$

The total outgoing pollutant load from a centralized BMP (PT_c) is the sum of the load from the treated load (PTr_c) and the bypassed load (PBy_c)

$$PT_c = PTr_c + PBy_c \quad (2.22)$$

Where the bypassed volumes are calculated as the product of the bypassed volume Q_{BY} and the inflow pollutant concentration for the centralized BMP drainage $[p]_C$

$$PBy_c = Q_{BY} * [p]_C \quad (2.23)$$

Based on strong evidence for association of PCBs and mercury with particulates (see section 2.3.6), we assumed different centralized BMP types to have proportional pollutant reduction efficiency to that of sediments. Therefore, PCB and mercury reductions (PR_C) are calculated as the product of the pollutant load delivered to the centralized BMP (PTr_d) for pollutants (PCB/Hg) and the percent TSS load reduction.

$$PR_{c\ PCB/Hg} = PTr_{d\ PCB/Hg} * \ (PTr_{d\ TSS} - PTr_{c\ TSS})/PTr_{d\ TSS} \qquad (2.24)$$

Using TSS as a proxy for particulate pollutant reductions has the advantage of substantially greater BMP performance data availability compared to similar data specifically associated with mercury or PCBs. Assignment of sediment CEC values to BMPs included a substantial data compilation effort that included data directly compiled and/or analyzed by 2NDNATURE (2NDNATURE, 2006a; 2006b; 2007; 2008; 2NDNATURE and nhc, 2012a; 2013; 2014; LRWQCB and NDEP, 2007), or obtained from the National Stormwater Quality Database[8]. BMP type definitions in the NSQD are loosely defined and therefore likely include substantial variation within the same specified BMP type. To support this analysis, we also reviewed results documented in available NSQD annual data analysis reports (Geosyntec Consultants and Wright Water Engineers, 2012; 2013; 2014), as well as select marketing and design literature available online for a variety of proprietary centralized structural BMPs.

TABLE 2.5 Characteristic sediments effluent concentration (CEC) values for centralized BMP types

BMP Type	CEC TSS (mg/L)
Wet Basin	5
Dry Basin	6
Infiltration Basin	92
Treatment Vault	20
Media Filter	6
Bed Filter	3
Detention Basin	40
Retention Basin	5

The use of CEC values is preferred over percent load reduction estimates that are commonly used in structural BMP models for two key reasons. First, the use of percent reduction requires a consistent reduction across the range of event magnitudes, including very large events which often provide substantial bypassed flow (Strecker *et al.*, 2001). Secondly, since most devices have an upper limit on performance, when pollutant concentrations are very low, the percent load reduction method tends to overestimate benefits. These observations are based on specific BMP types, within a limited range of conditions, and the difference between these two methods may be less pronounced given a wider range of facility types and pollutant concentrations.

---

[8] http://www.bmpdatabase.org/nsqd.html

2.3.9 Runoff routing

2.3.9.1 *Routing to centralized BMPs*

swTELR models centralized BMPs using the USDA TR-55 (1986) methodology for estimating peak inflow and peak outflow. Calculations for infiltrated, treated, and bypassed stormwater runoff volumes are completed for each prescribed 24-hr percentile storm event. Estimating of peak inflow discharge requires reasonable representation of the time of concentration, the time it takes from water to flow from the most remote part of the watershed to the watershed outlet. There are several different ways to estimate time of concentration (USDA 1986 and 2010). We selected a relatively simple formula (equation 15-4b; USDA 2010) that could be easily implemented for a variety of urban catchments and required minimal additional inputs by the user. Time of concentration is estimated by the NRCS lag method as

$$T_c = \frac{l^{0.8} * (S+1)^{0.7}}{1140 * Y^{0.5}} \tag{2.25}$$

where T_c is time of concentration (hr) for average natural watershed conditions, l is the flow length (ft), Y is the average watershed slope (%), and S is the maximum potential retention from equation 5. Because the lag equation was developed for rural areas, it can overestimate the time of concentration for urban areas which have higher proportion of impervious area and channelized flow that allow water to through the catchment at a faster rate than under natural conditions. The following equation was applied to adjust the T_c calculated by the NRCS lag method (FHWA HEC-19, 1984)

$$T_c' = T_c * CF * IF \tag{2.26}$$

where T_c' is the adjusted time of concentration, T_c is the time of concentration in hours from Eq. 9, CF is the channel improvement factor, and IF is the impervious area factor, both of which are estimated from the impervious area of the catchment.

Next, unit peak discharge, q_u, is computed based on T_c and SCS rainfall distribution type

$$\log(q_u) = C_0 + C_1 \log(T_c) + C_2[\log(T_c)]^2 \tag{2.27}$$

where C_0, C_1, and C_2 are the coefficients from Table F-I (USDA 1986) based on the SCS rainfall distribution type. Rainfall distribution Type I pertains to all examples presented herein. Peak inflow discharge, q_i is estimated as

$$q_i = q_u A Q F_p \tag{2.28}$$

where *A* is drainage area, Q is runoff depth, and F_p is a ponding factor. Finally, estimation of the peak outflow discharge is

$$\frac{V_s}{V_r} = C_0 + C_1\frac{q_o}{q_i} + C_2(\frac{q_o}{q_i})^2 + C_3(\frac{q_o}{q_i})^3 \quad (2.29)$$

where V_S/V_r is the ratio of storage volume to runoff volume of the BMP, q_o/q_i is the ratio of peak outflow to peak inflow, and C_0, C_1, C_2, and C_3 are the coefficients from Table F-2 (USDA 1986) based on the SCS rainfall distribution type. Figure 3A shows the relationship between the storage-runoff volume ratio and the outflow-inflow discharge ratio. Figure 3B shows the shape of the inflow and outflow hydrographs where peak flows are estimated from equations 11 and 12, respectively. The inflow and outflow duration is estimated from peak flow (q_i or q_o) and Q, using graphical methods and assuming conservation of volume.

Note that because swTELR models a range of 24-hr storm events, it is likely that the storage to runoff volume ratio is outside the range ($0.14 < V_s/V_r < 0.5$) presented in Figure 2.6A for a given 24-hr storm event. In the cases where V_S/V_r is outside the range, the low or high endmember of the range is applied. For example, if the measured V_S/V_r is 0.08, swTELR assumes a V_S/V_r of 0.14. If the measured V_S/V_r is 0.56, swTELR assumes a V_S/V_r of 0.50.

2.3.9.2 *Routing between catchments*

Runoff is routed between catchments so that runoff and pollutant load reductions cumulate as flows move downslope towards centralized BMPs or receiving waters. Volumes and pollutant loads delivered to centralized BMPs include reductions achieved by other structural and non-structural BMPs within its contributing drainage. This sequential accounting ensures runoff and pollutant reduction benefits are not double counted. The runoff volume and pollutant concentration introduced at the inlet of each centralized BMP is computed based on the contributing drainage characteristics and level of BMP implementation upstream within the centralized BMP drainage. Travel lengths and slopes to a centralized BMP are calculated based on the configuration of catchments or sub-catchments and different routing configurations will result in different flow timing (see Figure 2.7).

The total runoff for a series of catchments within the same drainage (QTr_{series}) is defined by the summation off the current catchment runoff (QTr) and runoff contributions from a series of upstream catchments that contribute to the downstream centralized BMP. Contributions from upstream catchments without a centralized BMP are defined as the total catchment runoff (QTr) and those with a centralized BMP are defined as sum of the treated (Q_{CEC}) and bypassed (Q_{BY}) volumes as Q_{UBMP}.

$$Q_{UBMP} = Qu_{BY} + Qu_{CEC} \quad (2.30)$$

Variables used for calculating peak inflow discharge (qi) and time of concentration (Tc) for a centralized BMP with contributions from upstream catchments are defined based the combined attributes of the catchment series. Slope for a series of catchments is calculated as the average of the contributing catchments. The contributing area is summed for all contributing catchments without centralized BMPs and with centralized BMPs such that the total area contributions are accounted for downstream. Pollutant concentrations for downstream catchments are calculated as the average concentration of the current catchment and contributing catchments. Catchments can be subdivided for routing portions to more than one centralized BMP, and these subcatchments can also receive water from upstream catchments, as in Configuration 1 in figure 2.7.

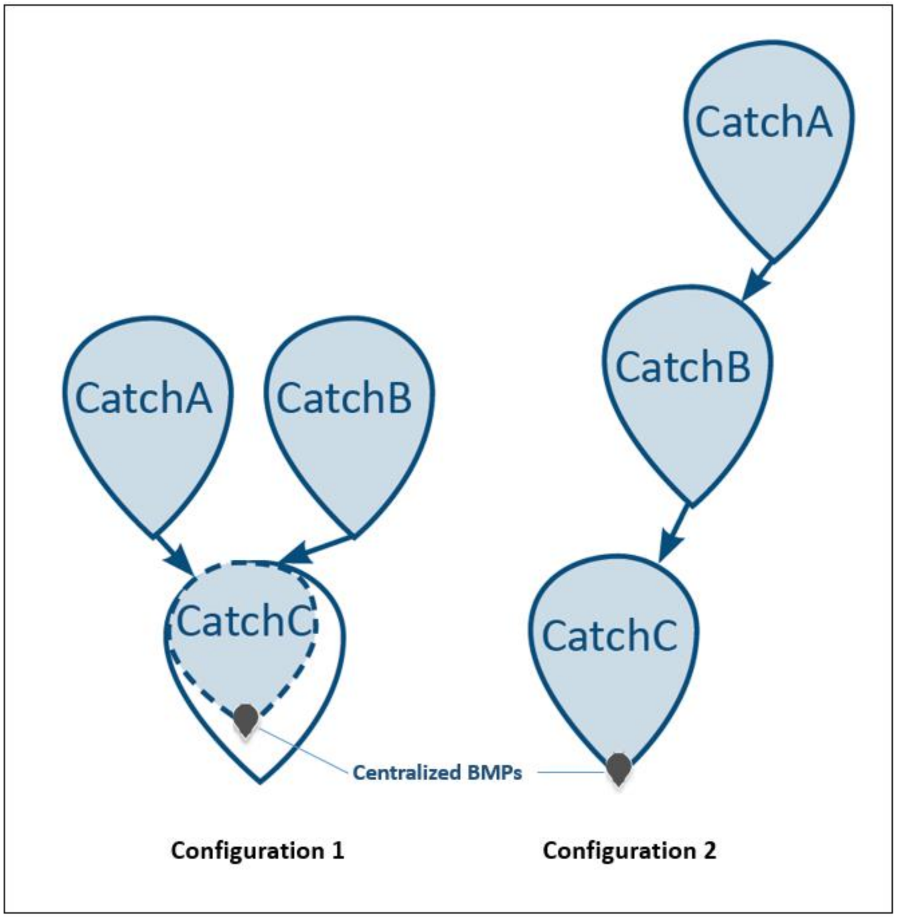

Figure 2.7. Two example catchment routing configurations.

2.3.9.3 *Runoff and pollutant load reductions reporting*

Within a catchment series, centralized BMPs receiving water from upstream catchments provide runoff reductions or pollutant treatment benefits to those upstream catchments. These reductions are allocated to upstream catchments based on their proportional contribution to the downstream centralized BMP after reductions from structural and non-structural BMPS within the catchment. Each catchment is run through the full calculations twice: once to calculate its initial within-catchment reductions and then a second time to account for the catchment series contributions. The initial flow out of a series of the catchments ($QTrI$) is the sum of the initial flows from the current ($QTrI_{current}$) and upstream catchments ($QTrI_{current}$):

$$QTrI_{series} = QTrI_{current} + QTrI_{UC1} .... ..QTrI_{UCi} \quad (2.31)$$

Runoff reductions from a centralized BMP receiving contributions from upstream catchments Q_{cr} are defined as the difference between the initial runoff ($QTrI_{series}$) and the total runoff from the catchment series after reductions from that centralized BMP (QTr_{series}).

$$Q_{cr} = QTrI_{series} - QTr_{series} \quad (2.32)$$

Reductions are distributed upstream to catchments based on their proportional contribution, so that for individual catchments (i), the reduction applied to them is defined by

$$Q_{cr}D_i = Q_{cr} * QTrI_i/QTrI_{series} \quad (2.33)$$

On the second run through the runoff calculations after calculating the initial contributions, the model iterates downstream so that all BMP reductions are cumulated as runoff moves downstream. The same reporting scheme is used in pollutant load reductions reporting so that the pollutant load from a series of the catchments is the sum of the initial load from the current catchment ($PI_{current}$) and all upstream catchments PI_{uc} as:

$$PI_{series} = PI_{current} + PI_{UC1} .... PI_{UCi} \quad (2.34)$$

The difference between the initial pollutant load and the final load after the final centralized BMP reductions is

$$Pr = PI_{series} - P_{series} \quad (2.35)$$

Like runoff reductions, pollutant load reductions are assigned upstream to individual catchments (i) proportional to their initial loading contributions.

$$PD_i = Pcr * P_i/PI_{series} \quad (2.36)$$

3 Modeling Scenarios

Baseline and future Solano Permittee landscape scenarios were completed to fulfill the RAA modeling compliance requirements using a combination of functions automated within the swTELR model and manual GIS processing to implement each future scenario. In this section, the modeling scenario components are described, and there is some overlap with section 2.3 that is retained for clarity.

Time periods modeled include the baseline period (approximately 2005), and future scenarios estimated for the years 2020, 2028/2030, and 2040. Each of these scenarios was modeled in sequence so that land use and BMP implementation changes that occurred in the preceding scenario were preserved in each subsequent scenario. The modeling scenarios include only those stormwater treatment components that are considered part the Green Stormwater Infrastructure (GSI) Scenarios per the BASMAA RAA Guidance Document (BASMAA, 2017). These scenarios therefore do not include source control measures, such as street sweeping or source property abatements[9].

3.1 3.1 Baseline Modeling

3.1.1 Scenario Inputs

3.1.1.1 *Precipitation input data*

Daily raster rainfall data from PRISM were used form the years 1981-2016 using the procedure described in Section 2.3, so that so that the precipitation distribution bracketed the range of likely rainfall conditions across the Solano Permittee MS4 Area. Raster-based rainfall estimates from the PRISM Climate Group[10] at Oregon State University were used to describe the distribution of 24-hour event depths were used to drive runoff generation. 2NDNATURE created a raster data processing program using the R statistical programming language[11] to acquire the appropriate historical raster layers for Solano County between 1981-2016 and perform a series of raster data processing steps. After the 35-year sequence was acquired (12,775 raster layers), a time series of precipitation values was created for each 800 m^2 pixel and the swTELR required percentile rainfall values (12.5, 50, 85, 95) and average days of rain were extracted for each pixel for the entire time series. The 85th percentile precipitation values are shown for the Solano Permittee area in

[9] Since source control measure accounting methods are still under development via a current BASMAA study. Source control actions will be included in the wasteload allocation (WLA) modeling scenarios, which will be communicated in a separate report.

[10] http://prism.oregonstate.edu/

[11] https://www.r-project.org/about.html

Figure 3.1. The 800m PRISM spatial precipitation data were resampled to align with the 30m US Landsat grid used by swTELR.

While the time extent used differs from the range recommended in the RAA Guidance of 2000-2009 (BASMAA, 2017), the greater temporal coverage provides a more representative description of the 24-hour rainfall distributions.

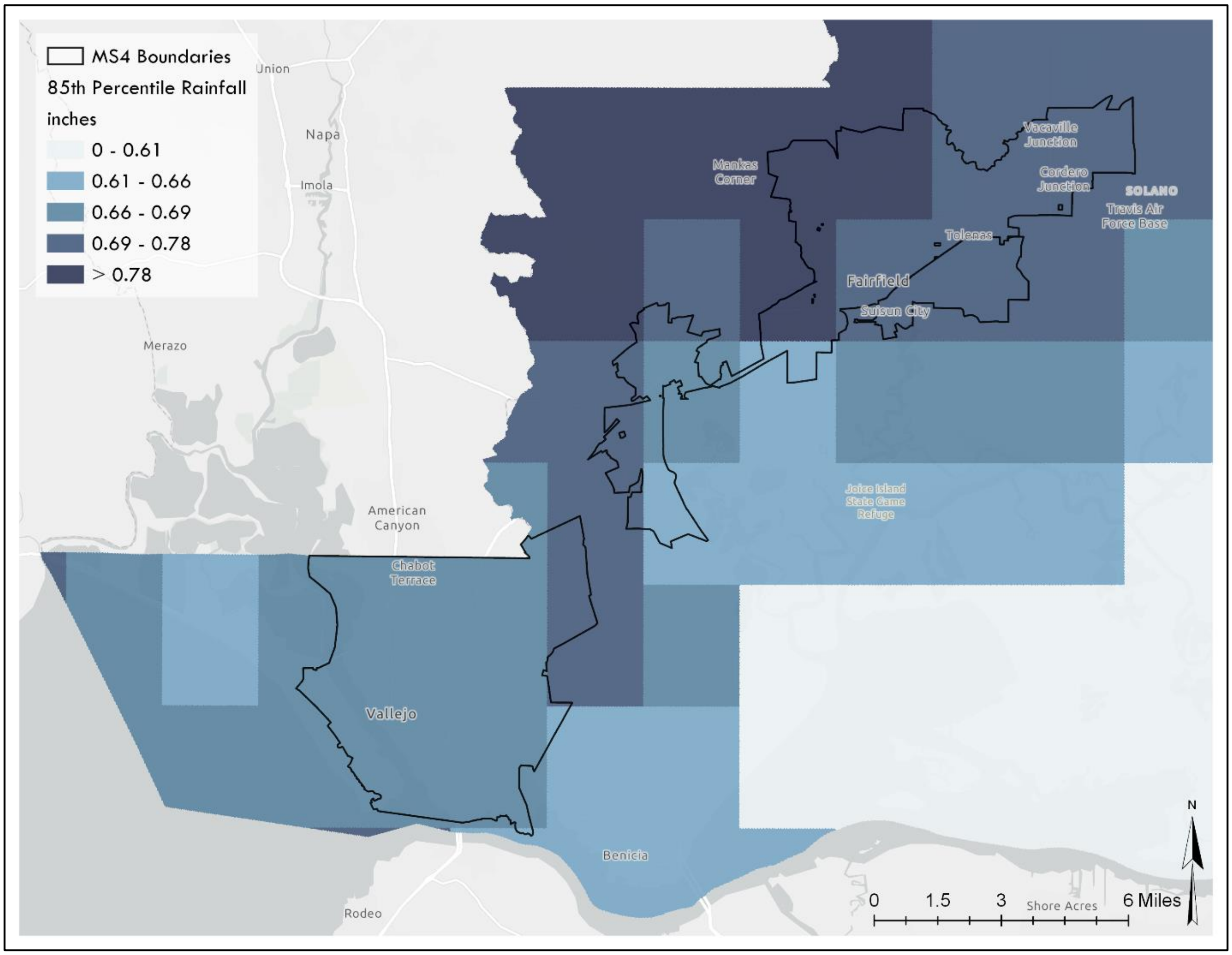

Figure 3.1. Example rainfall data used in swTELR.

3.1.1.2 *Soils*

Soils data from NRCS was used to specify soil types throughout Solano County MS4 boundaries. These data were used in their rasterized form, discretized to 30m pixels, down loaded from the NRCS website (Figure 3.2). The data were clipped to the Solano Permittee MS4 boundary and individual catchment boundaries for use swTELR. The NRCS SSURGO database was used as the primary data source, and the STATSGO2 database (which provides coarser resolution), was used to fill in spatial gaps in coverage that occurred in the SSURFO data.

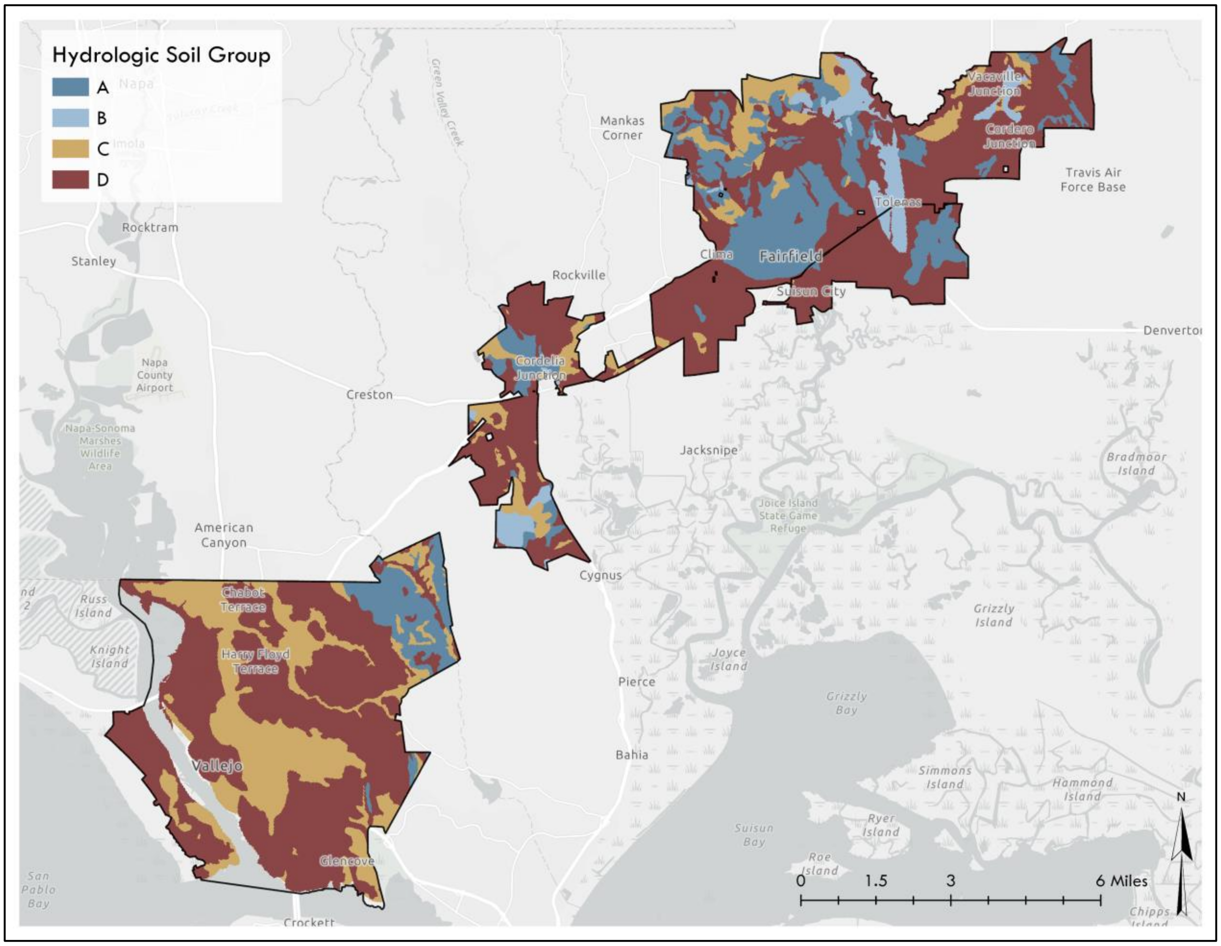

Figure 3.2. Soils data used in swTELR

3.1.1.3 *Impervious cover*

Impervious cover was specified using data from the National Land Cover Dataset[12] that represents the year 2006, provided at 30-meter grid cell resolution, which matches the spatial scale of modeling in swTELR. These data were clipped to the Solano Permittee MS4 boundaries and individual catchment boundaries for use in swTELR (Figure 3.3)

[12] https://www.mrlc.gov/data?f%5B0%5D=category%3Aurban%20imperviousness

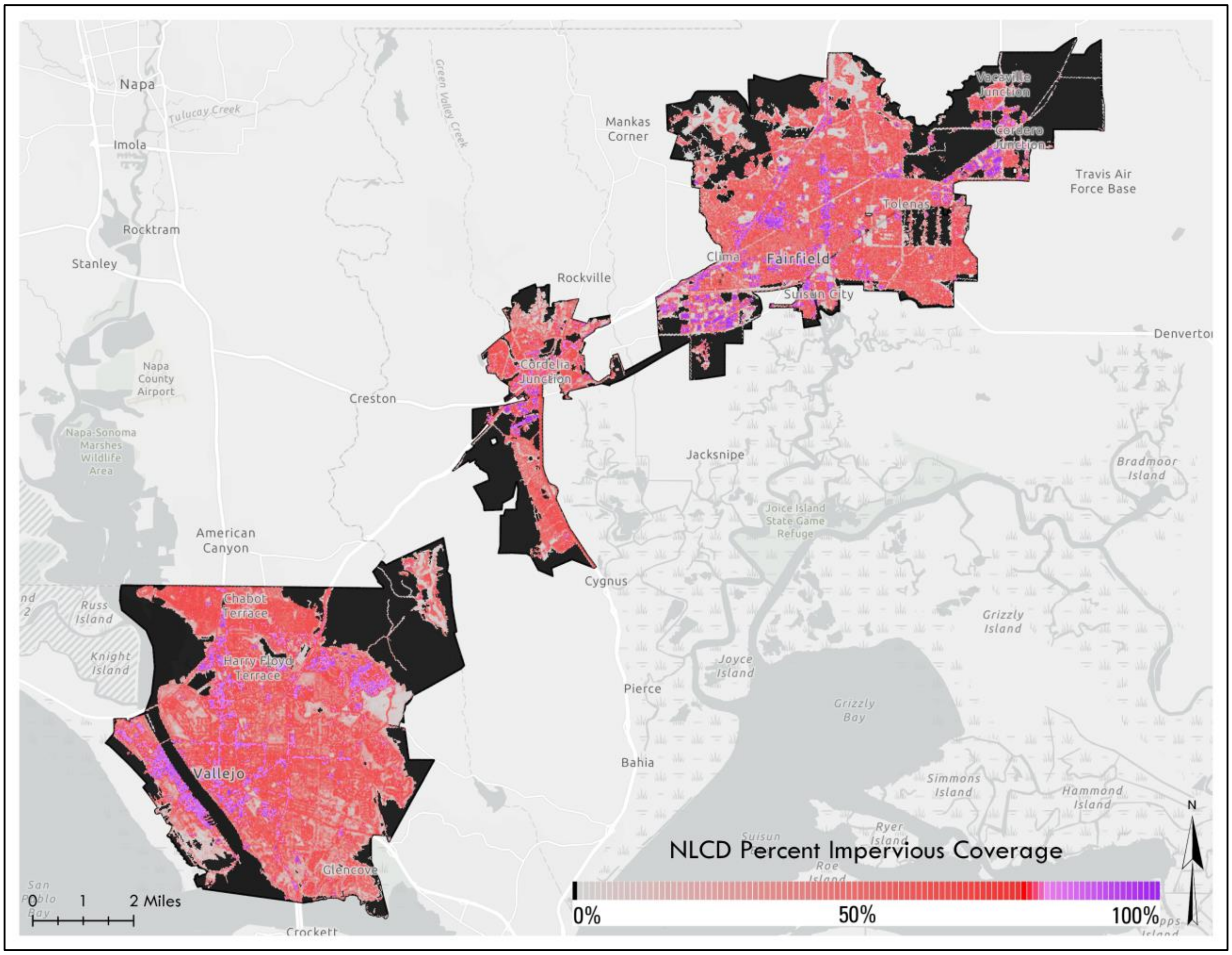

Figure 3.3. Impervious cover data used in swTELR.

3.1.1.4 *Land use*

Land-use data were developed by San Francisco Estuary Institute (SFEI) to specify characteristic PCBs and Mercury runoff concentrations for each land use developed for the Regional Watershed Spreadsheet Model (RWSM)[13]. The land-used runoff concentrations used are those contained in the current version of the RWSM, which differ slightly from those reported by SFEI in the last RWSM progress report (Wu et al, 2016). Land use designations used in RWSM are reflect categories relevant the specific pollutants of concern, PCBs and mercury, and are listed in Table 3.1. Figure 3.4 shows the distribution of difference land use types throughout the Solano MS4 Permittee Area.

[13] https://www.sfei.org/projects/regional-watershed-spreadsheet-model

Table. 3.1 Land-use based pollutant concentrations from RWSM used in swTELR. Note that these concentrations are slightly different than those reported in Wu et al. (2016).

	Land Use	Concentration (ng/L)
PCBs (ng/L)	Ag/Open/New Urban	0.2
	Old Industrial + Source Areas	204
	Old Residential	4
	Old Commercial + Old Transportation	40
Hg (ng/L)	Ag/Open	80
	Old Industrial + Source Areas	40
	New Urban	3
	Old Urban	63

This SFEI land use layer does not appear to account for historic mining activities as a mercury source area within Solano County. For example, Saint John mine that was identified in the Mercury Mines Inventory and Prioritization Report (SWRCB, 2009). This site has tailing piles and mine waste with risk of erosion into Rindler Creek. The mine is within the Vallejo MS4 boundary, located in the northeast corner, but appears to be classified as Agriculture (Figure 3.4). As a practical matter, this classification seems perfectly appropriate, since Agriculture is the highest mercury concentration specified in the dataset.

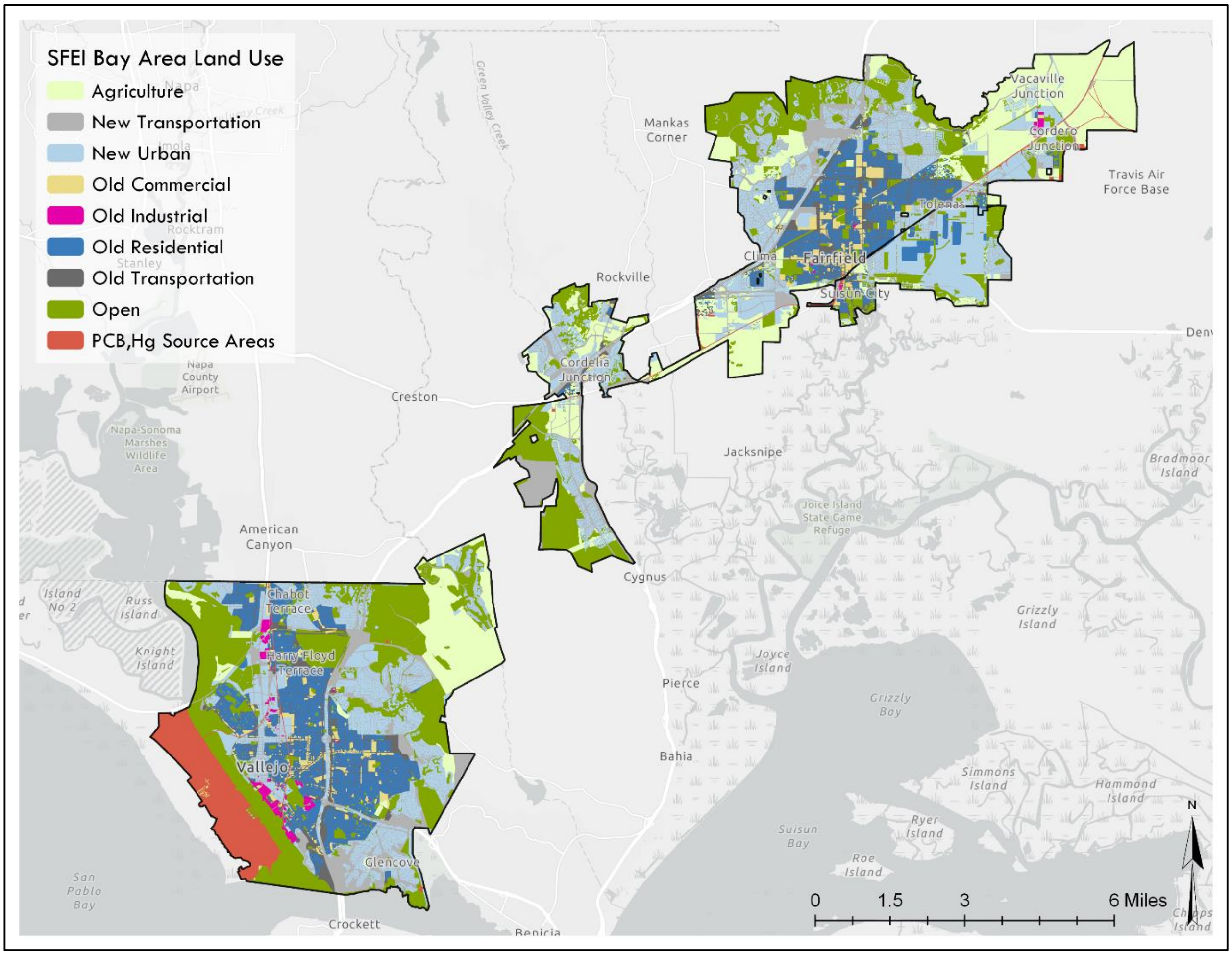

Figure 3.4. Land use map from RWSM used in swTELR.

Although some BMPs may have been implemented before 2005, baseline condition modeling assumed no existing GSI and or land-use changes that occurred after the year 2005. As such, the baseline condition model outputs essentially represent the unmitigated runoff and pollutant loading from Solano Permittees as of 2005. Existing BMPs, land-use, and impervious cover changes identified since 2005 are included in all of the future modeling scenarios.

3.1.1.5 *Drainage and routing*

The delineation of the Solano Permittee MS4 areas into urban catchments was an iterative process with verification by Solano Permittee city staff. Catchments are approximately 100 acres in size and define routing to either a discrete (single point) or distributed outlet (multiple point). Catchment boundaries and routing to receiving waters are defined by surface elevation, surface barriers, stromdrain infrastructure, and connectivity to receiving waters (Appendix C). Figure 3.5 provides an example of a catchment delineation in Fairfield based on the stormdrain network showing routing to receiving water outfalls. Beginning with catchments that had already been delineated by the City of Vallejo, City of Fairfield, and City of Suisun, catchment boundaries were refined, and verified by city staff. The full catchment delineation process used for swTELR is documented in a *Catchment Delineation and Mapping Guidance* (2NDNATURE, 2018). This process involves using the municipal stormdrain infrastructure spatial data in concert with a 10-meter spatial resolution Digital Elevation Model (DEM)[14] to define drainage boundaries. Catchments are nested inside stormwater drainages that all flow to a common receiving water. The final catchment and stormwater drainages delineated for Fairfield/Suisun and Vallejo are shown in Figures 3.6 and 3.7 respectively.

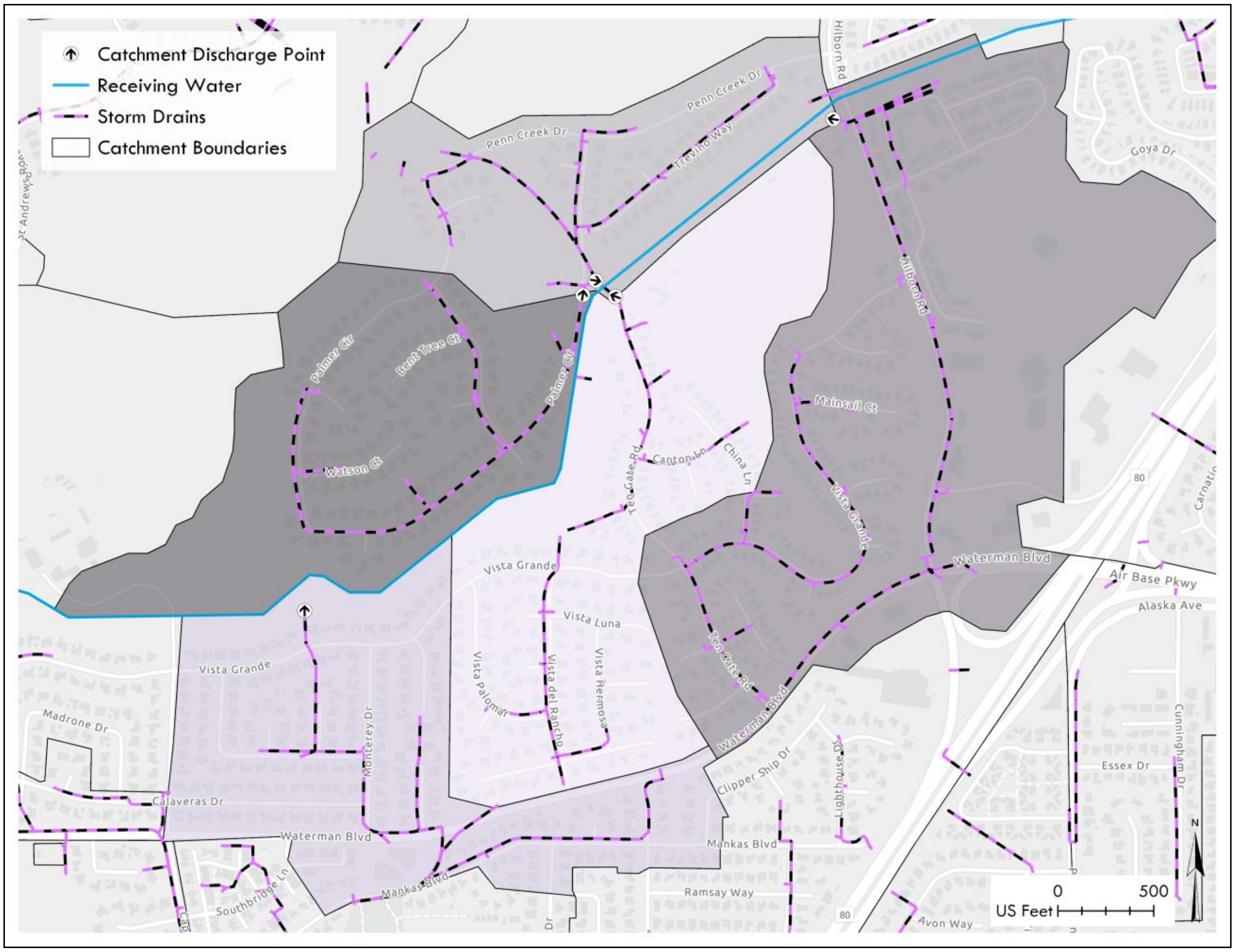

Figure 3.5. Example of catchments delineated via the stormdrain network in Fairfield.

14 https://catalog.data.gov/dataset/usgs-national-elevation-dataset-ned

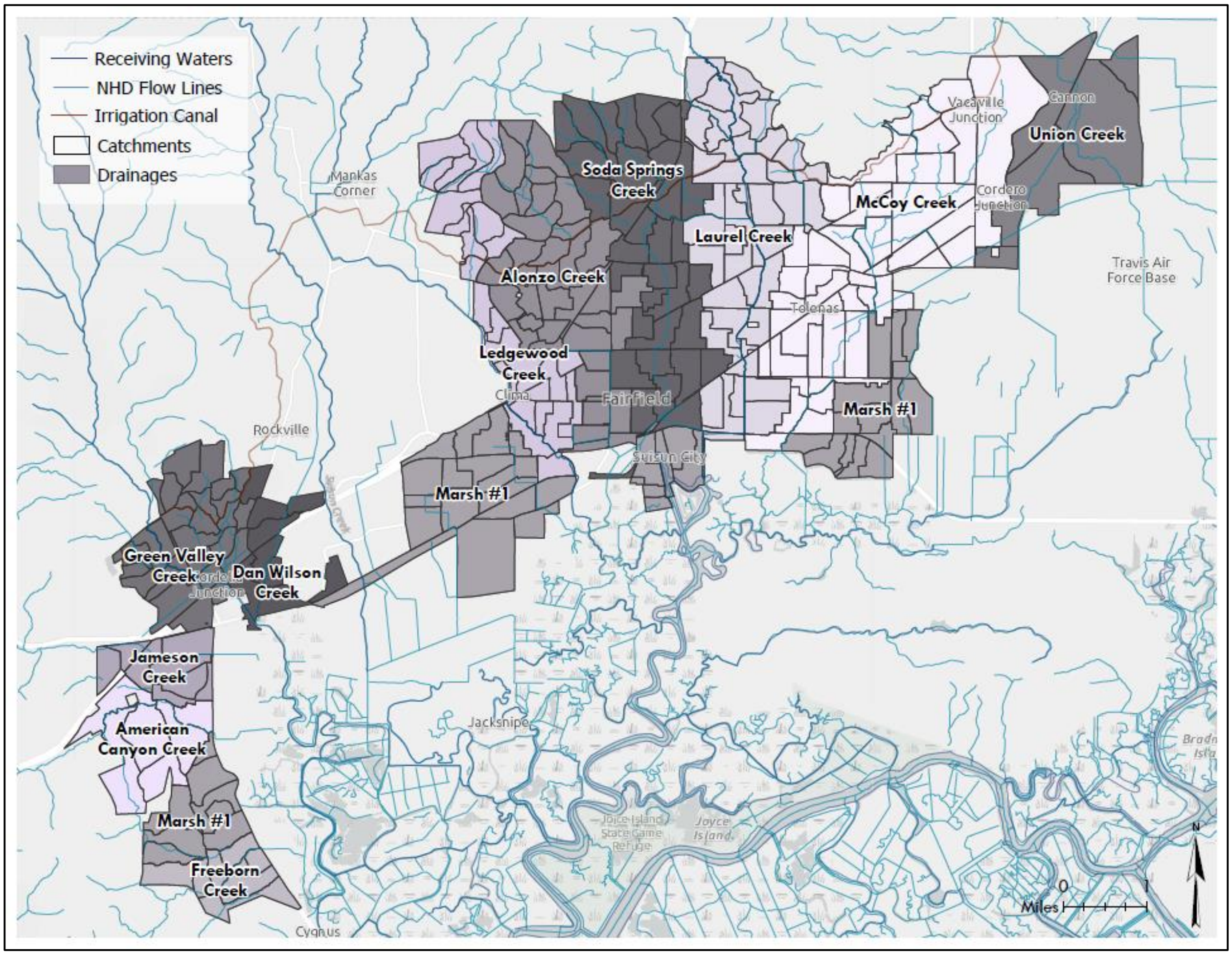

Figure 3.6. Fairfield-Suisun catchments, drainages, and receiving waters.

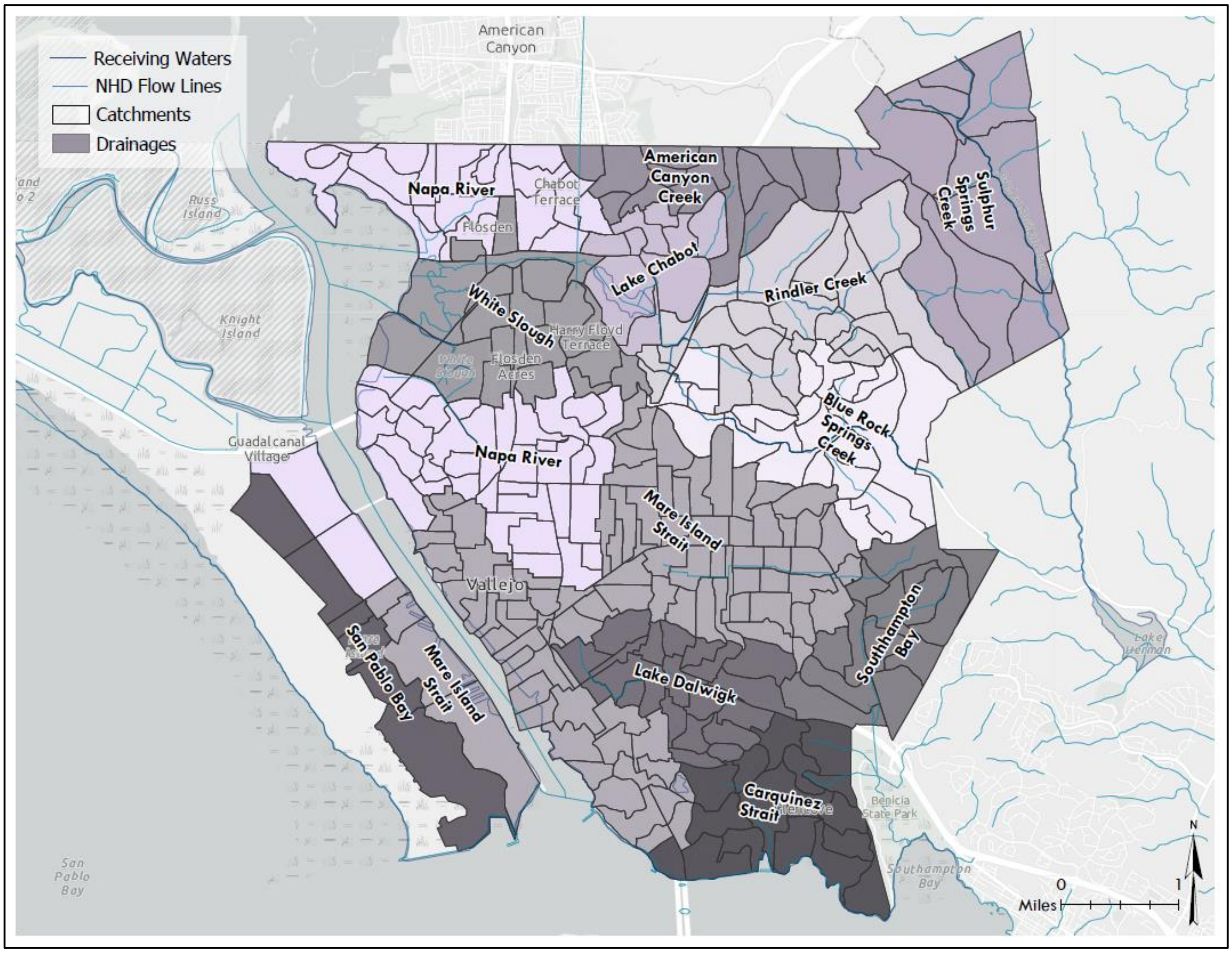

Figure 3.7. Vallejo catchments, drainages, and receiving waters

3.1.2 Model calibration

There are no long-term flow datasets available for watersheds that include the cities of Fairfield, Suisun or Vallejo. So, while the RAA Guidance from BASMAA (BASMAA, 2017) specifies that baseline model runoff estimates should employ a hydrologic calibration procedure, this is not possible for the Solano Permittee MS4 Area. Similarly, there are no concentration data for PCBs and mercury available that are amenable calibration of an urban stormwater model. The historic concentration data available have been described in detail in section in Section 1.3.2.4, and are primarily targeted to short-term study objectives, probabilistic inference over space, and characterizing spatial patterns within the receiving waters of the Bay. As such, measurements are sparse and do not capture the unique response of the urbanized areas, such as monitoring data at the outfalls of the urban drainages would. This means that the estimates from swTELR must rely wholly on the input data without adjustment of numeric quantities to tune the fit of the model to observations, which provides both advantages and shortcomings.

Contrary to the idea that uncertainty associated with model parameterization can be avoided with a careful or sophisticated calibration procedure, the process of fitting parameter values during calibration invariably injects substantial uncertainty to model outputs. This issue has been widely recognized and documented in the hydrologic literature for more than two decades (see Beven, 2001 p. 217). While lack of data with which to compare estimates clearly presents a challenge for direct verification of accuracy, it also avoids the inherent addition of uncertainty that is incurred any time model outputs depend strongly on model calibration. This is particularly true when a model is over-parameterized to a degree that is not supported by the data available, which is exceedingly commonplace (Beven, 2005). Since calibration often involves either complex optimization algorithms and/or several subjective decisions on the part of the modeler, avoiding it adds transparency to the modeling process, since relationships between model inputs and outputs are much more straightforward.

3.1.3 Baseline comparison with the Regional Watershed Spreadsheet Model (RWSM)

In place of a validation experiment via comparison with measured flow values, swTELR results were compared to outputs from the Regional Watershed Spreadsheet Model (RWSM), developed by SFEI. The RWSM is an empirical model developed to estimate average annual regional and sub-regional scale pollutant loads for the San Francisco Bay Area. Since the RWSM is an empirical model, the outputs depend strongly on an extensive dataset of flow and pollutant concentrations collected over more than a decade by regional monitoring programs. The RWSM is the most suitable tool available to extend existing measurements to estimate sub-regional scale pollutant loading in areas of the San Francisco Bay area that lack measurements. swTELR used the same land use layer employed by RWSM to specify PCBs and Mercury characteristic runoff concentrations for each land. Correspondence between swTELR and RWSM was performed using outputs provided on the SFEI RWSM website[15] by clipping raster-based RWSM runoff and pollutant load estimates from the full dataset using the MS4 boundary for each city in Solano County.

3.1.3 Key baseline modeling assumptions and limitations

The baseline modeling employs several assumptions for the purposes of either practicality or data limitations, which include:

- A spatially explicit, probabilistic approach can adequately bracket the range of rainfall-runoff responses via an uncalibrated model.
- PCBs and mercury concentrations are responsive to land use type and the concentrations used are representative of the actual values.

[15] https://www.sfei.org/projects/regional-watershed-spreadsheet-model#sthash.3ZhPRNxw.dpbs

- Uncertainties associated with the input data and model structure are not greater in magnitude than spatially varying factors that drive runoff generation and pollutant loading

These assumptions are primarily based on previously reported studies and were not tested as part of this study. Rather, they served as a practical point of departure for the work reported herein. A true validation of these assumptions and swTELR outputs require monitoring data at the urban drainage scale, which is not commonly available. However, since control measure implementation will proceed over a period of decades, this type of validation should be considered to both inform decision making, test RAA model assumptions, and provide additional information to shore up their limitations. Since swTELR operates at a granular spatial scale, the outputs are amendable to understanding the distinct runoff and pollutant loading response from urbanized drainages and changes that result from GSI implementation over time.

3.2 Model Scenarios for Compliance Demonstration

Baseline and future modeling scenarios were run for the Solano Permittee MS4 Area to demonstrate expected progress towards compliance for meeting GSI pollutant reductions. For each scenario, the rainfall input data and other spatial data that describe urban catchment characteristics remained unchanged, while other factors were altered according to documentation of expected changes (e.g. land use, BMP implementation). New development, redevelopment, and BMP implementation timing and locations were verified by Solano Permittees via a web-mapping application[16]. Three future scenarios were modelled, with a slightly different milestone schedule required for PCBs and mercury (Table 3.2).

The MRP requires that both the GSI RAA (C.11.c/C.12.c) and the WLA RAA (C.11.d/C.12.d) be documented in the 2020 Annual Report. The scenarios reported herein include only reductions associated with GSI. Source control actions will be handled as part of the wasteload attainment (WLA) RAA analysis to be completed in 2020. Modeling scenarios for the GSI and WLA RAA's overlap substantially, with GI comprising a subset of the WLA reductions. Per the BASMAA RAA Guidance (BASMAA, 2017), pollutant load reduction measures included in the GSI RAA include GSI BMP implementation along with land use changes that accompany redevelopment. Reductions included in the WLA RAA analysis are the sum of reductions that result from GSI, land use changes, and source controls such as street sweeping and demolition controls. GSI treatment BMPs include both decentralized BMPs that are often included as part of Low Impact Development (LID) and treat stormwater on site at the parcel scale, as well as centralized BMPs, which route stormwater from several parcels to a regional treatment structure. Source controls will only be included in the 2028/2030 modeling analysis per the BASMAA RAA Guidance Document (BASMAA, 2017).

Table 3.2. RAA model scenarios

	Green Stormwater Infrastructure RAA	Waste load Allocation Attainment RAA
2020	GSI + land use changes	GSI + land use changes
2028/2030	GSI + land use changes	GSI + land use changes + source control
2040	GSI + land use changes	GSI + land use changes

Modeling GSI and WLA scenarios separately requires that GSI and source control reductions can be treated independently, even though there are overlapping components. This presents some conflicts with the most logical reduction sequencing that corresponds with our conceptual understanding of the urban stormwater system, in which source control reductions occur before other types of reductions that require transport of pollutants away from their source and subsequent treatment. The BASMAA source control accounting approach will not be finalized until January 2020. Any such pollutant reduction sequencing issues or assumptions will be documented in WLA RAA modeling report in 2020.

3.3 Redevelopment and new development land use changes

3.3.1 Planned and projected land use changes

Completed and projected land use changes were drawn from several different sources and compiled into a geodatabase to support the future modeling scenarios. Development and redevelopment projects were identified from city general plans, specific redevelopment area planning documents, examination of current and historical aerial imagery, and interpreted outputs from the UrbanSim[17] urban planning model. With the exception of the UrbanSim outputs, land use change data were not available in GIS formats and were translated from PDF documents and manually digitized in GIS. While the UrbanSim outputs provide a regionally standardized way to estimate redevelopment rates, using them in isolation would require ignoring the vast majority of documentation of parcels that are already planned for redevelopment

All land use changes employed in the future scenario modeling simulations are mapped in Figure 3.8 symbolized by the scenario year, and whether the changes will be redevelopment or new development. The GIS database created contains the specific information source used to determine land use change and associated time of conversion for each parcel.

[17] http://www.urbansim.com/urbansim

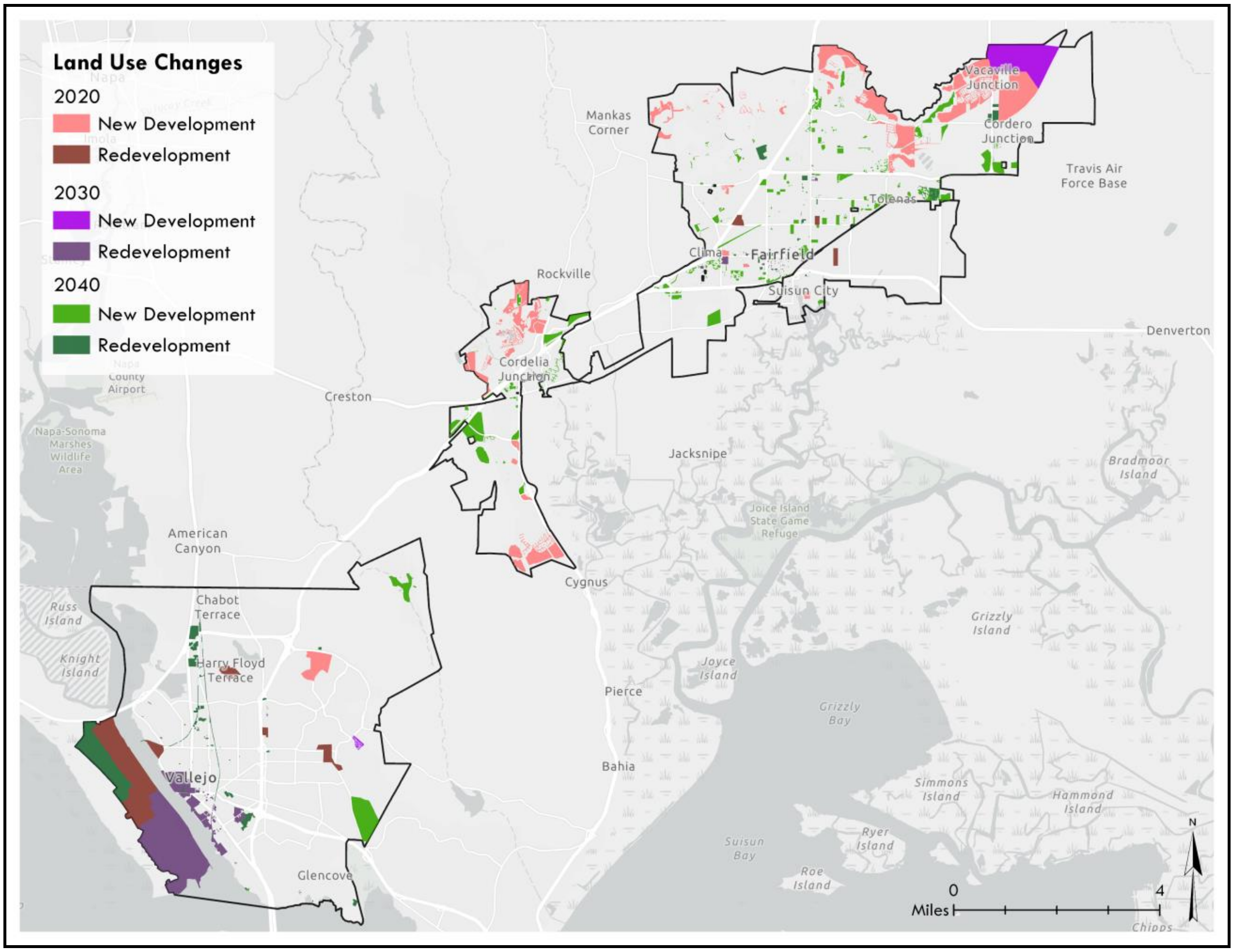

Figure 3.8. Land use changes used in future scenarios.

3.3.2 Land use corrections

Best available satellite time series imagery from Google Earth was used to identify and correct inaccuracies in the SFEI 2005 land use layer (SFEI, 2005). These changes include improper classification of open space that had been developed by 2005 or misclassification of old urban areas that had been redeveloped. Figure 3.9 shows an example of one of the areas within the City of Vallejo that was classified as Open land use and changed to New Urban land use, which was typical of these instances. Other issues identified in the land use layer were related to areas incorrectly classified as Old Transportation land uses (also previously recognized by McKee et al. 2014, p. 90). Examination of historical satellite imagery via Google Earth showed that several of these areas had been redeveloped are recently as 2004, and were therefore changed from 'Old Transportation' to New Urban land use in the 2020 and all subsequent model scenarios.

Figure 3.9. Example of a correction made in a Fairfield neighborhood to the land use layer used as input to the pollutant loading model.

3.3.3 Projected land use changes from UrbanSim

The UrbanSim model was used to project parcel-level land use changes for future scenarios. UrbanSim is an open source simulation system created by Paul Waddell and University of California, supported by grants from National Science Foundation designed to support urban planning. Spatial outputs reflect changes in residential housing units were used to infer redevelopment land use change over time. The Bay Area's application of UrbanSim was developed specifically to support the development of Plan Bay Area, the Bay Area's Sustainable Communities planning effort. The methods and results of the Bay Area UrbanSim model have been approved by both MTC and Association of Bay Area Governments (ABAG) Committees for use in transportation projections and the regional Plan Bay Area development process.

The general workflow to extract new development and redevelopment parcels from the UrbanSim model mirrored that employed by the Contra Costa County Clean Water Program RAA analysis:

1. Intersect the parcel dataset with Solano County MS4 areas
2. Export UrbanSim model runs for the years 2010 through 2040 that includes fields that quantify total job spaces, total residential units, and year built.
3. Use an if-then statement to flag parcel differences for these metrics between 2010 and 2040 and query the year built output to determine which parcels are estimated to change during each scenario timeframe (2010-2020, 2020-2030, 2030-2040)

It was assumed that new development and redevelopment of multifamily residential and commercial/industrial parcels will incorporate GSI in accordance with MRP Provisions C.3.b., C.3.c., and C.3.d. Because of high land values, it is expected that more than 50% of the existing impervious area in each parcel will be replaced if a parcel is developed, and therefore the entire parcel will be subject to Provision C.3 requirements (that is, will be retrofit with Green Stormwater Infrastructure), consistent with the "50% rule" requirements of MRP Provision C.3.b. Land Use changes predicted via the UrbanSim[18] model were incorporated into swTELR for each scenario year according to the output time period.

3.3.4 Planned land use changes

Allocation of planned land use changes to each scenario was based on documented development plans or verification of new development initiation or completion via use of best available satellite imagery up to land use conditions as of 2018. For example, the Callahan Property Company's development in the City of Vallejo Northern Waterfront (52 acres) at Mariners Cove was allocated to the 2020 scenario as development plans have been approved by the City of Vallejo along with a schedule of parcel development[19] and satellite imagery indicates site grading has begun. The Central Waterfront area was instead allocated to the 2030 scenario (see Figure 3.8). Likewise, the 157-acre area located on the northern portion of Mare Island currently owned and under redevelopment by the Nimitz Group was allocated to the 2020 scenario. The 250 acres that Nimitz Group recently acquired from the Lennar Corporation, which is still in the scoping stages, were included as redevelopment areas in the 2030 scenario. The residential developments that have already been completed by Lennar Corporation, such as Farragut Village (completed 2007), or are in progress Coral Sea Circle, Kirkland Isle II were also allocated to the 2020 scenario. The remaining area on Mare Island still owned by Lennar Corporation (approximately 350 acres) is slated for redevelopment, but with no specific plans identified, it was allocated to the 2030 scenario. The remaining areas identified in City of Vallejo General Plans for land use change that

[18] http://www.urbansim.com/urbansim

[19] http://www.ci.vallejo.ca.us/city_hall/departments___divisions/city_manager/economic_development_division/waterfront_project

did not have any specific redevelopment planning documentation available were allocated to the 2040 scenario (Figure 3.8).

All GSI implementation within redevelopment and new development projects was assumed to be bioretention features, which are decentralized BMP types that reduce both stormwater volumes and pollutant concentrations. The sizing of planned bioretention features align with the MRP section C.3.d requirement to reduce and treat the contributing stormwater volume generated up to the 85th percentile 24-hour rainfall depth (SWRCB, 2015).

Relative to the baseline simulation scenarios, areas of new development identified typically produce additional runoff resulting from increased impervious coverage. While these increases will be mitigated with GSI implementation, conversion from Open Space land use to New Urban still usually results in net increases of runoff and pollutant loading. For these scenarios, the impervious coverage layer was changed manually in the GIS so that areas which typically had zero impervious coverage values before new development (e.g. Open Spaces land use) would reflect the typical impervious coverage of the New Urban land use. Exceptions to this rule were in areas that the impervious coverage layer accurately reflected the land use changes that had occurred since 2005, which is when the land use layer was created.

3.3.4.1 *Key land use change assumptions and limitations*

The reliability of the modelling results relies heavily on the following land use data assumptions:

- Past and future land use changes have been adequately captured via automatically classified land-use maps, planning documents, and inspection of historical satellite imagery
- UrbanSim model outputs reasonably reflect the rates and locations of land use change anticipated in the future.
- Land use changes result in reductions of characteristic pollutant runoff concentrations as defined by the PCB and mercury land use layer (SFEI, 2005).

The assumption that land use changes will result in the specified pollutant concentration changes is a substantial source of uncertainty in this analysis. It includes the implicit assumption that all remediation actions and new development standards prescribed in the MRP are closely followed and in perpetuity. While this assumption relies on the best sampling data available to date, which has already been discussed, these data are limited, especially in Solano County.

Comparison of the SFEI 2005 land use data layer to available imagery indicated misclassification of several areas. It is unlikely all errors were identified and corrected. Manual inspection of historical satellite imagery is tedious and only useful for identifying new development or areas that were incorrectly classified as open space. Historical redevelopment is not obvious and would have required a much more detailed study of the area and available data that was beyond the scope of this effort. The options for spatially explicit land-use change estimates are few, and UrbanSim at least provides a more detailed option than applying a uniform rate across each city. However, using model outputs to drive another model holds the substantial disadvantage of compounding uncertainty through different model layers.

3.4 Reductions from Green Stormwater Infrastructure (GSI)

3.4.1 Parcel/Green Street LID

Planned and completed LID projects were mostly green streets within the City of Vallejo that were identified via capital improvement projects and are listed in Table 3.3. Since these projects did not have defined locations or types of structural BMPs yet specified, bioretention feature application for the entire drainage areas was again assumed to the 85th percentile 24-hr design storm as specified in MRP C.3 requirements. Each project area was defined by its outline that was delivered to 2NDNATURE via the City of Vallejo as a GIS shapefile.

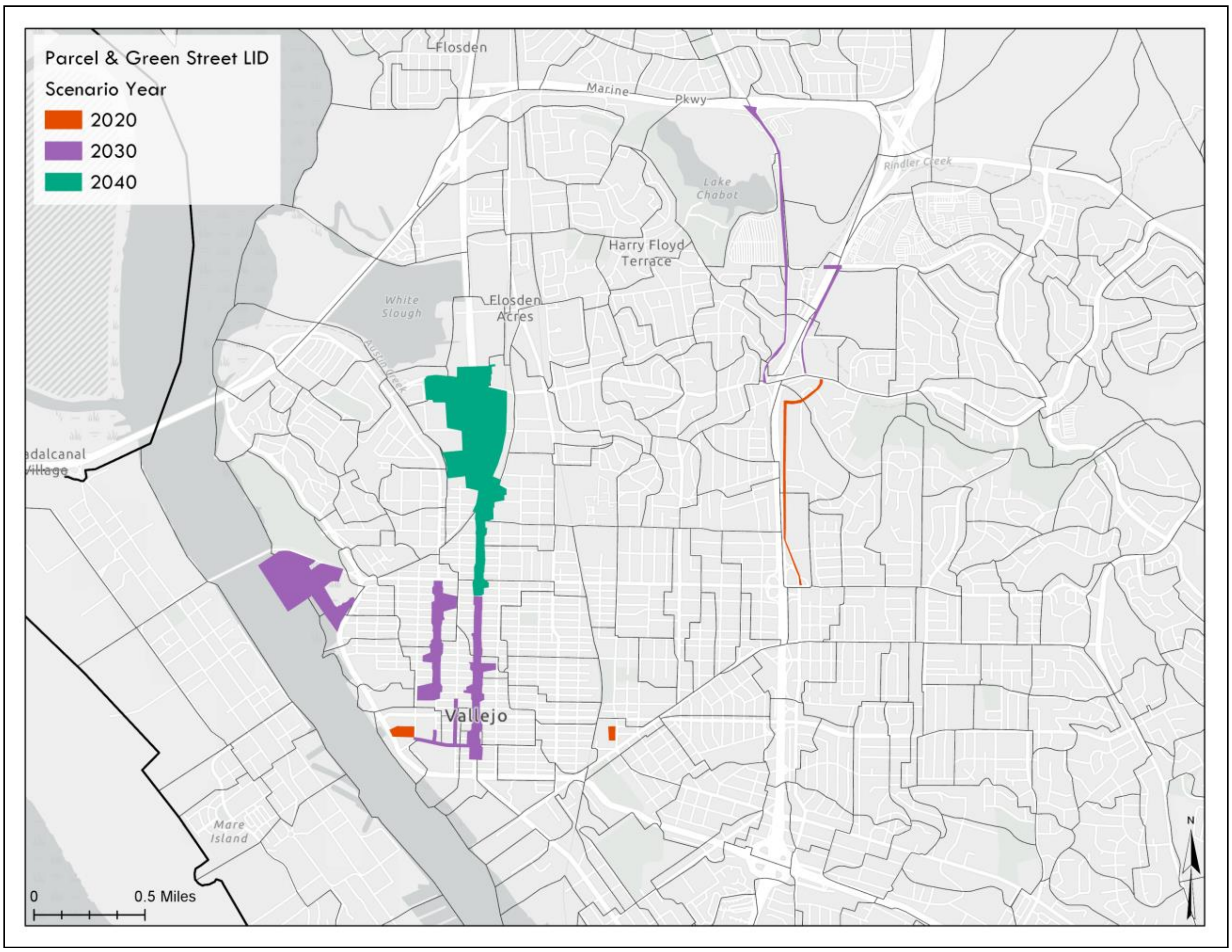

Figure 3.10. Future parcel and Green Street LID projects identified in Vallejo.

Table. 3.3. Future LID projects planned in Vallejo.

City	BMP ID	Status	Scenario	Area (ac)	Catchments	Primary Receiving Water
Vallejo	Sonoma Boulevard Streetscape Phase 5 & 6	Planned	2040	105.94	AC12, CA14, AC15, AC20, AC35, AC37, AC38, AC39, AC41, AC52, AC53	Napa River
Vallejo	Sonoma Boulevard Streetscape Phase 4	Planned	2030	9.69	AC12, DT5	Mare Island Strait
Vallejo	Benicia Road Bridge Replacement Project	Planned	2030	0.87	CP11, CP12	Southhampton Bay
Vallejo	Sonoma Boulevard Streetscape Phase 1-3	Planned	2030	12.53	DT1, DT2, DT5, SA59, DT2, DT5	Mare Island Strait
Vallejo	Marina Sea Wall	Planned	2020	44.58	DT10, DT11, MI22	Napa River
Vallejo	Sacramento Street Streetscape Phase 1	Planned	2030	8.32	DT12	Mare Island Strait
Vallejo	Sacramento Street Streetscape Phase 2	Planned	2030	3.89	DT12, DT 5	Mare Island Strait
Vallejo	Downtown Streetscape Phase 4	Planned	2030	1.61	DT3, DT4	Mare Island Strait
Vallejo	Downtown Streetscape Phase 5 & 6	Planned	2030	1.44	DT3, DT4, DT2	Mare Island Strait
Vallejo	Downtown Streetscape Phase 7, 8 & 9	Planned	2030	2.07	DT3, DT5	Mare Island Strait
Vallejo	Vallejo Station Phase B	Planned	2020	3.04	DT4	Mare Island Strait
Vallejo	Sacramento Street Streetscape Phase 3	Planned	2030	9.06	DT5	Mare Island Strait
Vallejo	Admiral Callaghan Widening	Planned	2020	2.85	LC10, LC11, LC13, LC15A, LC8	Blue Rock Springs Creek
Vallejo	Fairgrounds Drive Improvements	Planned	2030	9.05	LC10, LC11, LC27, LC37A, LC8, LC9, SA44, LC37B	Lake Chabot
Vallejo	Turner Parkway Overcrossing	Planned	2030	0.83	LC11, LC15A	Rindler Creek
Vallejo	Admiral Callaghan Middle Lane	Planned	2020	6.29	LC6, SA39, SA 40	Mare Island Strait
Vallejo	Public Safety Building Rehab and Design	Planned	2020	1.16	SA52	Mare Island Strait

3.4.2 Decentralized BMP implementation

Existing and planned decentralized BMP implementation was modeled in swTELR in a spatially explicit manner, with raster-based calculations for runoff and pollutant load reductions performed at the 30-meter pixel scale for each of the future scenarios (2020, 2030, 2040). Existing GSI BMP specifications were documented by Solano Permittee city staff and provided to 2NDNATURE via spreadsheets and uploaded to the 2Nform spatial platform. The city staff confirmed the locations and attributes of each BMP and GSI project via a web-based mapping interface[20] prior to finalizing the dataset.

For each modeling scenario, GSI benefits are accounted for *after* land use changes are applied. This sequencing of pollutant reduction accounting is important to avoid double counting of benefits, since where redevelopment occurs, pollutant loads delivered to GSI will be lower due to the transformation of Old Industrial to New Urban land uses within the contributing drainages. In areas were new development occurs, the land use changes typically result in additional runoff available for infiltration by BMPs due to increased impervious coverage. All structural BMP types modelled reduce either runoff through infiltration or pollutant concentration through particle capture and filtration, and several GSI types do both. The pollutant reduction processes represented depend on the BMP type as detailed in Table 2.3.

For most existing and several planned BMPs, exact locations and BMP types were available from Solano Permittees, so that benefits were calculated according to the type and location of each BMP and included in the 2020 scenario (and carried over into all subsequent scenarios). In this way, the modeling outputs preserved the uniqueness of each location in terms of runoff production and pollutant loading from each of their specified drainage areas which were explicitly accounted for in the calculations. The locations of all existing or planned decentralized BMPs are shown in Figure 3.11 and each BMP is listed in Appendix D with their relevant attributes.

20 http://2ndnature.maps.arcgis.com/apps/webappviewer/index.html?id=839c43995b64448cb0da6b4d38c5a6b6

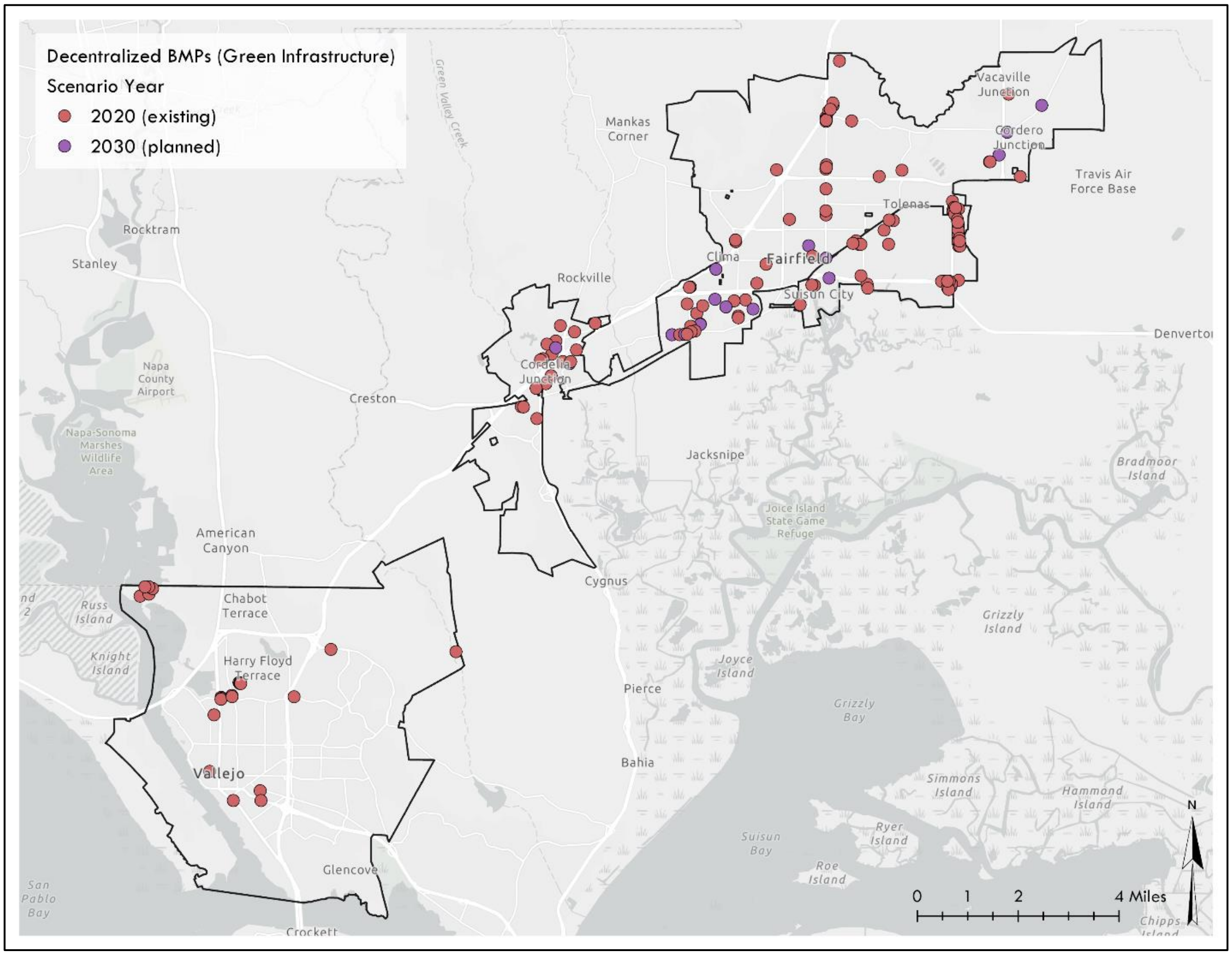

Figure 3.11. Existing and Planned Decentralized BMPs implemented throughout the Solano Permittee MS4 Area.

Current and future reductions from decentralized BMPs were modeled assuming that they were built according to MRP, section C.3d requirements, so that volume-based designs would infiltrate runoff generated by rainfall up to the 85th percentile 24-hour rainfall depth. Since swTELR generates runoff for a several percentile slices of the rainfall distribution, raster outputs of runoff were generated for each percentile rainfall depth. For decentralized BMPs, reductions were calculated as the runoff generated after land use changes minus the volume generated up to the 85th percentile rainfall event for each of the grid cells that comprised the respective BMP drainage area. For calculating pollutant load reductions, the remaining volume was multiplied by either the untreated land-use concentration or a reduced concentration, depending on whether the BMP type provides pollutant treatment in addition to runoff reductions. Since these BMPs generally receive runoff infiltration and treatment close to the site where it was generated, delivery to the BMP is assumed to be instantaneous.

3.4.3 Decentralized BMP performance efficiency

Since the decentralized BMP calculations were performed on raster datasets with coverage throughout the Solano Permittee MS4 area, we can examine the potential for pollutant reductions by sampling grid cells and calculating runoff and pollutant reduction for different BMP types. Figure 3.12 shows the range of location specific potential reductions for BMPs that perform runoff infiltration or treatment and those that do both (e.g. bioretention features). Again, all decentralized BMPs were assumed to be sized and performing in perpetuity to capture runoff generated from the 85th percentile 24-hour storm depths per MRP section C.3.d. Since there is different runoff and loading potential throughout the Permittee MS4 area, there is a range of potential runoff capture and associated BMP load reduction. Given that both PCBs and mercury are hydrophobic and have a strong tendency to adsorb to particulates, we assume similar pollutant reduction capture efficiency for both pollutants. Note that the shape of the curves in the right panels of Figure 3.12 reflect the non-linearity between rainfall and runoff production. Runoff infiltration generally provides somewhat greater benefit than runoff treatment at this design level, and BMPs that do both infiltration and treatment provide substantially greater benefits within a narrower performance range (Figure 3.12).

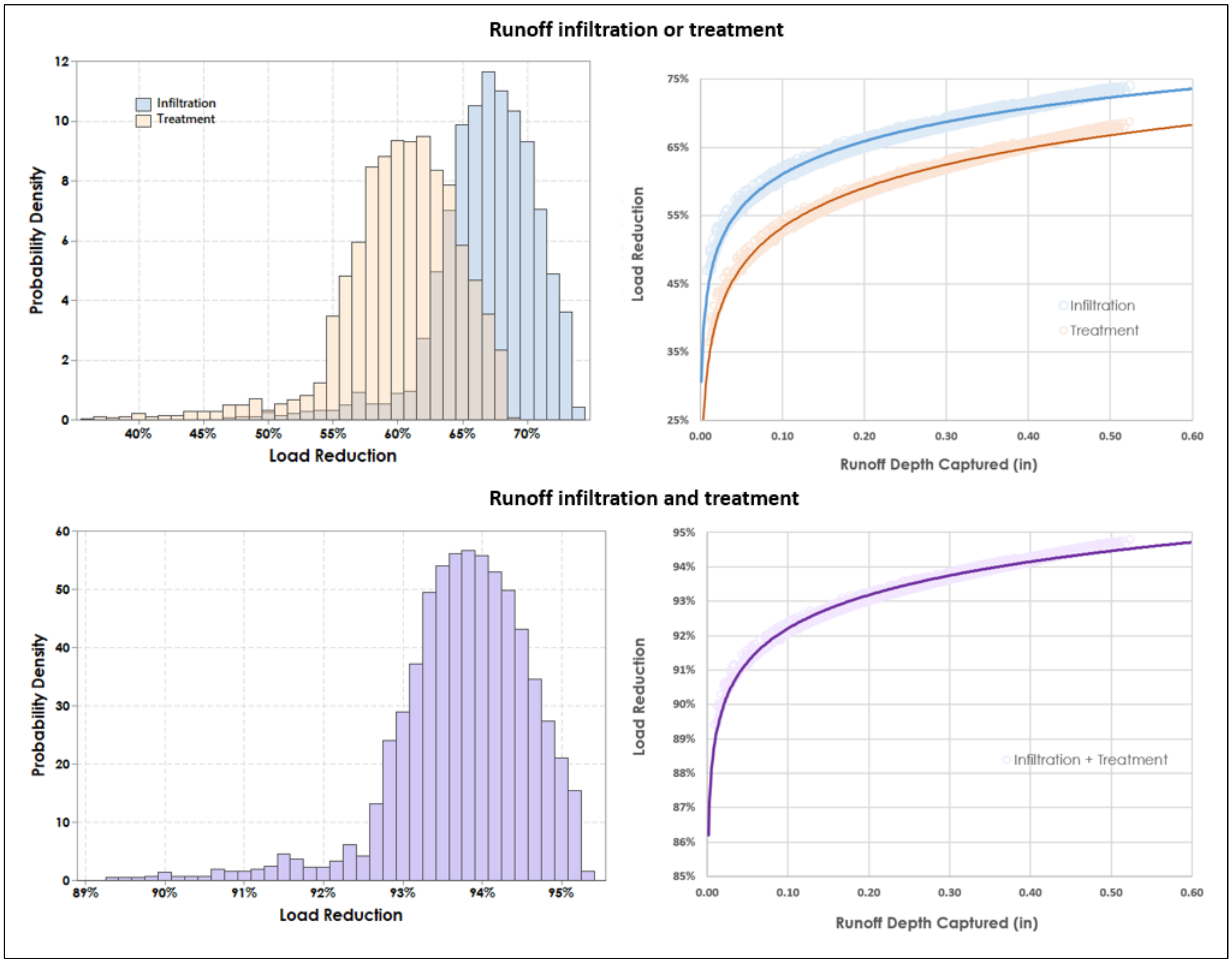

Figure 3.12. BMP performance efficiency. Histograms in panels on the left show load reduction distributions and curves in panels on the right show load reductions per runoff depth captured. Depth capture shown in the range of flows generated by the 85th percentile rainfall event.

The performance curves shown in Figure 3.12 are specific to Solano County, since they incorporate annual rainfall distribution characteristics and site-specific runoff and pollutant generation. As such, they are quasi-empirical in nature. These curves are very similar to those calculated from observed data for the purpose of standardizing load reduction accounting throughout the Chesapeake Bay to support TMDL compliance (Scheuler and Youngk, 2015). Given the sheer number of decentralized BMPs that will need to be accounted for in the SF Bay Area, ongoing accounting of their benefits will likely require a similarly simple accounting system as they have implemented in the Chesapeake Bay Region. For example, there are more than 6,000 BMPs currently catalogued in Prince George County, MD (population 900,000) alone that require ongoing pollutant reduction benefit quantification. Within the decade, the SF Bay Area will likely have tens of thousands of structural BMPs catalogued that require a practical method for accounting for reductions and ongoing verification of performance.

3.4.4 Centralized BMPs

Runoff and pollutant load reduction performance from existing and planned centralized BMPs (also called regional treatment projects) employed the methods described in Section 2.3 to determine routing, timing, and partitioning of infiltrated, treated and bypassed flows for calculating reductions for future scenarios. A primary difference from decentralized BMPs is that with centralized BMPs, stormwater is typically transported a substantial distance away from where runoff was initially generated, so that runoff timing is important for estimating centralized BMP reductions.

Centralized BMP and drainage specifications were documented by city staff and transferred to 2NDNATURE, where they were uploaded to a web-based mapping platform for verification by city staff before inclusion in the modeling scenarios. Centralized BMPs included in the modeling scenarios are listed in Table 3.4 and shown on Figure 3.13. The predominance of dry basins as a centralized BMP in Fairfield vs treatment vaults as the predominant choice for centralized BMPs in Vallejo reflects the difference in soil types: Fairfield has a much greater amount of Type A and B soils (higher infiltration rates) compared to Vallejo (see Figure 3.2).

The hydrologic and pollutant loading to each centralized BMP is calculated based on the land use changes and decentralized BMP reductions within each centralized BMP contributing drainage areas. The performance of each centralized BMP is estimated based on the computational approach outlined in Section 2. While there may be additional centralized BMPs installed with future new development, inclusion in this RAA analysis required that cities had documentation of locations, types, and capacity of future BMPs. Centralized BMPs, both planned and already installed, are listed by Solano Permittee city in Table 3.4 along with location, drainage association, and corresponding modeling scenario.

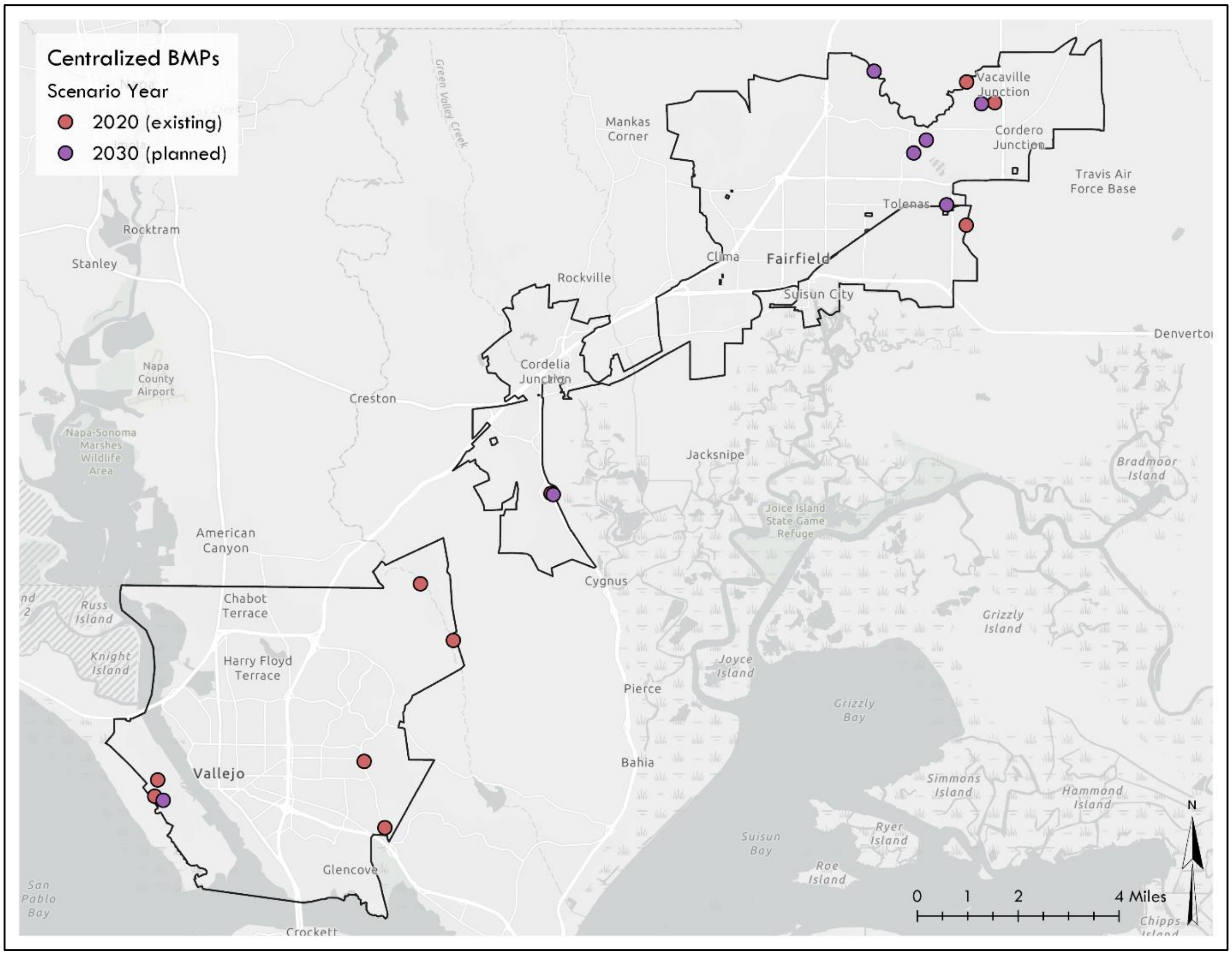

Figure 3.13. Centralized BMPs used in future modeling scenarios.

Table 3.4. Centralized BMPs and attributes.

City	BMP ID	Status	Scenario	BMP Type	Drainage Area (ac)	Receiving Water	Catchment	Latitude	Longitude
Fairfield	Gold Hill Village 1	Installed	2020	Dry Basin	11	Marsh 1	MAR-2	38.18047928	-122.1342695
Fairfield	Gold Ridge-so. of Putah So. Canal	Installed	2020	Dry Basin	124	McCoy Creek	COY-26	38.2928207	-121.9726825
Fairfield	Gold Ridge-no. of Putah So. Canal	Installed	2020	Dry Basin	120	McCoy Creek	COY-30	38.29886642	-121.9829339
Fairfield	Paradise 360	Planned	2030	Dry Basin	9.7	Laurel Creek	LAU-12	38.30187014	-122.0165929
Fairfield	Gold Hill Village 2	Planned	2030	Dry Basin	11	Marsh 1	MAR-2	38.18016302	-122.1334273
Fairfield	Ivy Wreath/Strawberry Fields	Planned	2030	Dry Basin	13.8	McCoy Creek	COY-10	38.26349435	-121.9902188
Fairfield	Villages at Fairfield- Village 2	Planned	2030	Dry Basin	42	McCoy Creek	COY-19	38.27843273	-122.0021546
Fairfield	Discovery @ Gold Ridge	Planned	2030	Dry Basin	15	McCoy Creek	COY-24	38.29252809	-121.9774729
Fairfield	Villages at Fairfield- Village 1	Planned	2030	Dry Basin	76	McCoy Creek	COY-6	38.28212579	-121.9975519
Fairfield	2900 Cordelia	Installed	2020	Bioretention	38.085	Marsh 1	MAR-11	38.22804606	-122.0847827
Fairfield	Gateway 80, Buildings A & B	Planned	2030	Bioretention	35.93	Marsh 1	MAR-11	38.2280516	-122.0856715
Suisun	PR Detention Basin	Installed	2020	Dry Basin	64.7	Marsh #1	MAR-47	38.257646	-121.982987
Vallejo	SA10062T	Installed	2020	Treatment Vault	108	Mare Island Strait	SA10	38.10333666	-122.2021727
Vallejo	2183GT318	Installed	2020	Treatment Vault	35	San Pablo Bay	SP3B	38.0978149	-122.277309
Vallejo	2184GT027	Installed	2020	Treatment Vault	40	San Pablo Bay	SP4	38.09313091	-122.2783658
Vallejo	SV1401T	Installed	2020	Treatment Vault	108	Sulphur Springs Creek	SV1B	38.1381688	-122.1697917
Vallejo	SV1203T	Installed	2020	Treatment Vault	135	Sulphur Springs Creek	SV1C	38.15438193	-122.181801
Vallejo	Lennar Mare Island B3	Planned	2030	Dry Basin	37	San Pablo Bay	SP4	38.09204167	-122.275241
Vallejo	BeniciaRd_Basin	Installed	2020	Dry Basin	600	Southhampton Bay	CP12	38.08431517	-122.1944904

3.4.5 Key GSI modeling assumptions

Calculation of GSI reductions depended upon several assumptions:

- All redevelopment since the 2005 baseline year and future redevelopment complies with MRP C3 requirements to capture and/or treat runoff up to the 85^{th} percentile 24-hr rainfall event.
- Bioretention features or comparable decentralized BMPs that reduce both volumes and pollutant concentrations will be make up a substantial proportion of future GSI implemented.
- Decentralized BMPs that reduce PCB/Hg concentrations in stormwater do so at 80% efficiency when functioning as designed. While there is some evidence to support this assumption, it is very limited. As such, this should be considered an important source of uncertainty in the outputs.
- Centralized BMPs that reduce PCB/Hg concentrations in treated outflow have characteristic effluent concentrations with correspond with sediment reductions.
- All structural BMPs will perform to their design standard in perpetuity, requiring a proactive commitment to maintenance Permittee's are encouraged to adopt a tracking and accounting system that includes field verification of GSI performance and provide permittees with useful asset management information on GSI.

4 RAA Modeling Results and Compliance Demonstration

This section presents the results of modeling experiments using the structure, methods, inputs and assumptions that have been described in sections 1-3. The results presented include baseline modeling, comparison with the Regional Watershed Spreadsheet Model (RWSM), and GSI reductions modeling.

4.1 Baseline Modeling Results

4.1.1 Baseline conditions

Baseline runoff was calculated for each Solano County Permittee MS4 Areas (Fairfield, Suisun, and Vallejo) according to the methods described in section 2.3, with the results summarized for each city in Figure 4.1. Runoff volumes are much higher in Fairfield (13,268 afy) and Vallejo (13,391) since these cities are much larger than Suisun, which only produced 2,091 afy of runoff. PCB loading is particularly high in the City of Vallejo (477 g) compared to Fairfield (137 g), and Suisun (16 g), owing to the high proportion of source area and old industrial land use in Vallejo.

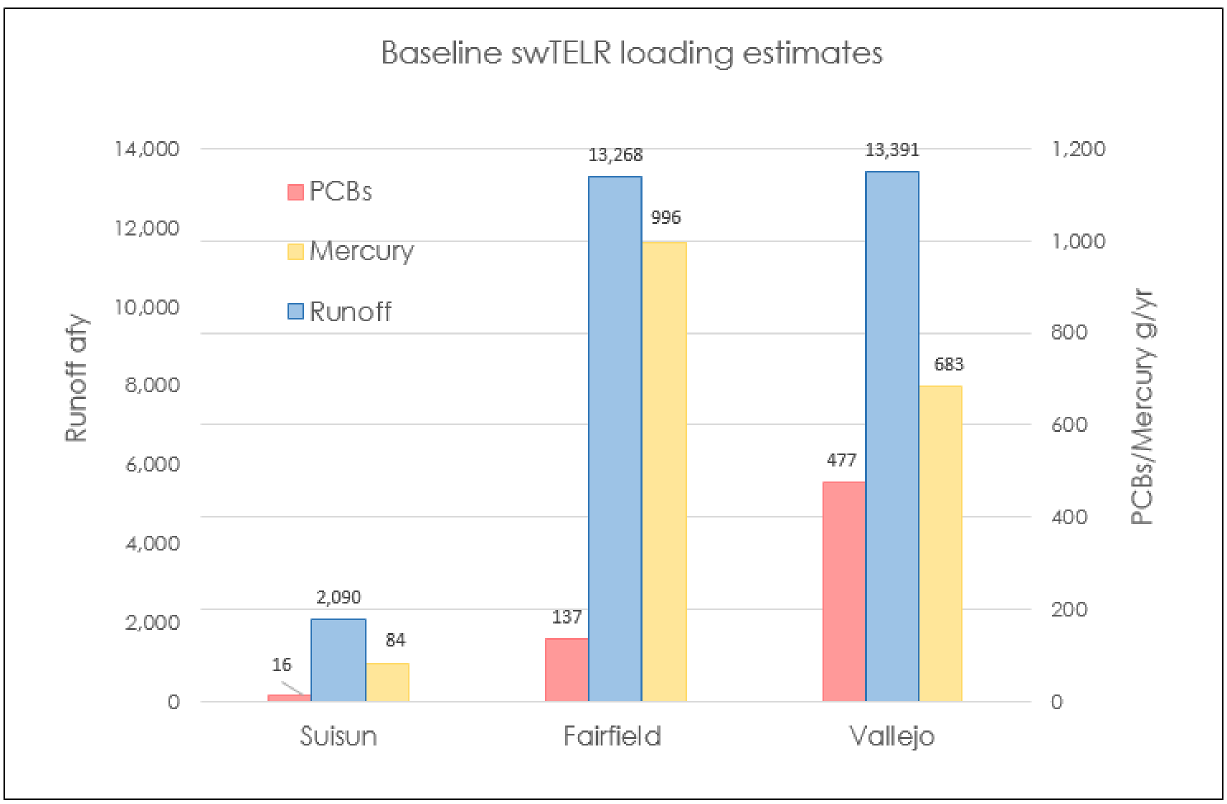

Figure 4.1. Runoff, PCBs, and mercury baseline loading estimates from swTELR.

Baseline runoff estimates were aggregated to the urban catchment scale from calculations performed at the 30-meter grid scale (Figure 4.2). As we would expect, runoff generation is generally highest in areas with high impervious cover and poorly draining soils. These include the urban centers of Vallejo and Suisun City. Baseline runoff is an important driver of spatial patterns of pollutant loading across Solano County; area-normalized runoff ranged from 0.01 ac-ft/ac/yr to 1.2 ac-ft/ac/yr, with an average value of 0.67 ac-ft/ac/yr.

Baseline pollutant loading for PCBs and mercury were calculated using the methods described in sections 2.3 and 3.1and aggregated to the urban catchment scale (Figures 4.3 and 4.4). The runoff estimates shown in Figure 4.2 were used for calculating both PCB and mercury loads. Average baseline loading values for catchments ranged from 0.01 g/ac/year to up to 0.18 g/ac/yr throughout the Solano Permittee MS4 Area (Figure 4.3). High PCB loading catchments are strongly associated with the relative proportion of Source Area or Old Industrial land use coverage within catchments. This is an intuitive result, since runoff concentration values for these land uses are substantially higher than the other land uses (Table 3.1). The greatest concentration of high loading areas is in Vallejo on Mare Island, which is classified almost entirely as Old Industrial land use. Other areas of relatively high PCB loading are the southern part of the Vallejo Waterfront, Vallejo downtown, and Central Fairfield. As we would expect, upland areas on the outskirts of both cities, which are largely undeveloped have very low PCB loading values.

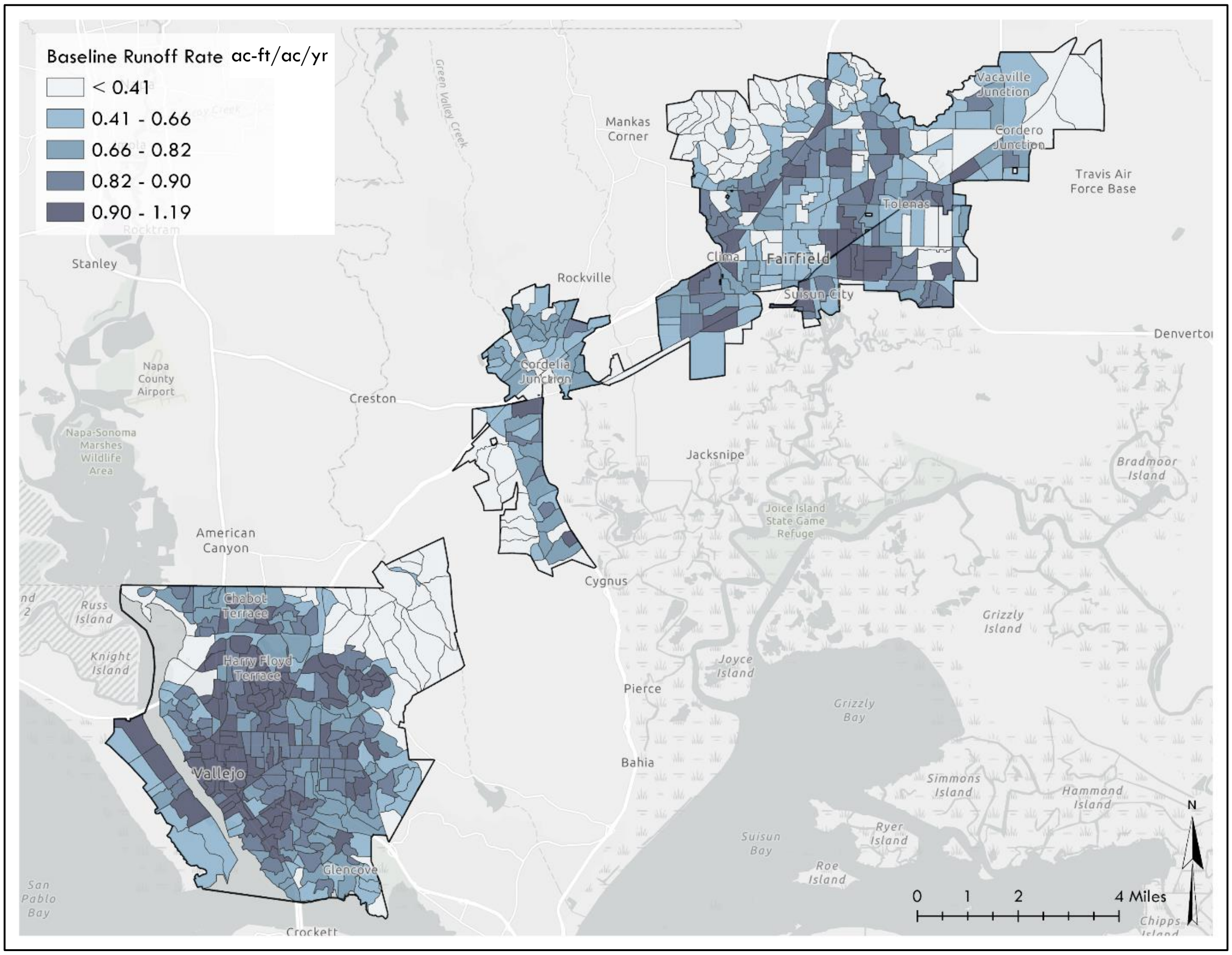

Figure 4.2. Baseline runoff estimates for Solano Permittee MS4 Area

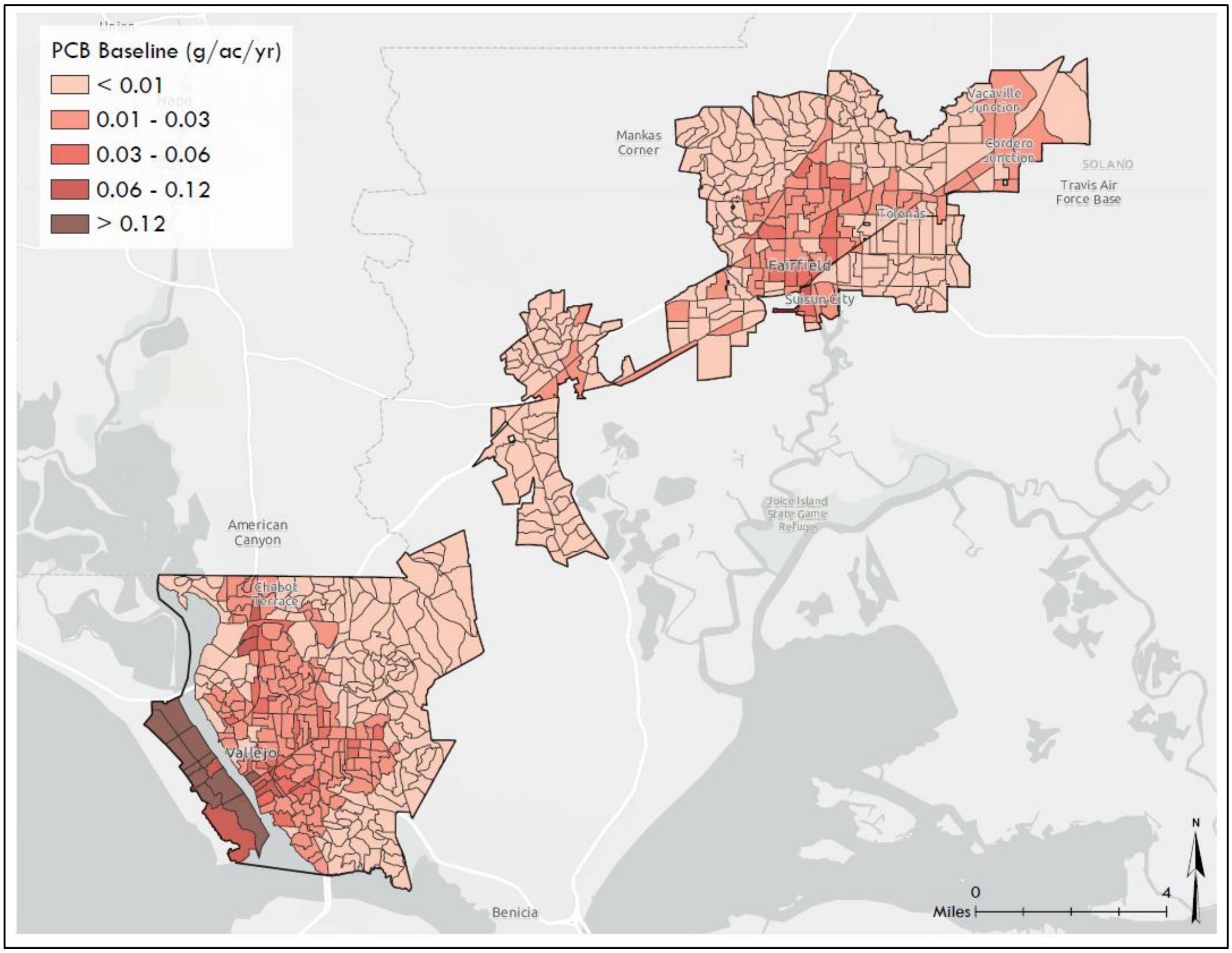

Figure 4.3. Baseline PCB loading estimates for the Solano Permittee MS4 Area

Mercury baseline loading outputs are shown in Figure 4.4. With less difference between land use characteristic runoff concentrations for mercury, loading outputs are more responsive to spatial patterns of runoff compared to PCBs. Loading values range from 0.009 to 0.125 g/acre/year throughout Solano County. Like with PCBs, the most heavily developed areas in downtown Fairfield and Vallejo both show relatively high mercury loading but areas such as Mare Island and the Vallejo waterfront show relatively lower mercury loading values compared to PCBs, primarily due the difference the high characteristic PCB runoff concentrations for Old Industrial and Source Area land uses present in those areas. Industrial areas along Highway 12 also show relatively high mercury loading, which did not show high PCB loading. Undeveloped upland areas in the northern portions of Fairfield and Vallejo show mostly low loading as with PCBs due to low runoff generation in these areas that have substantial open space coverage.

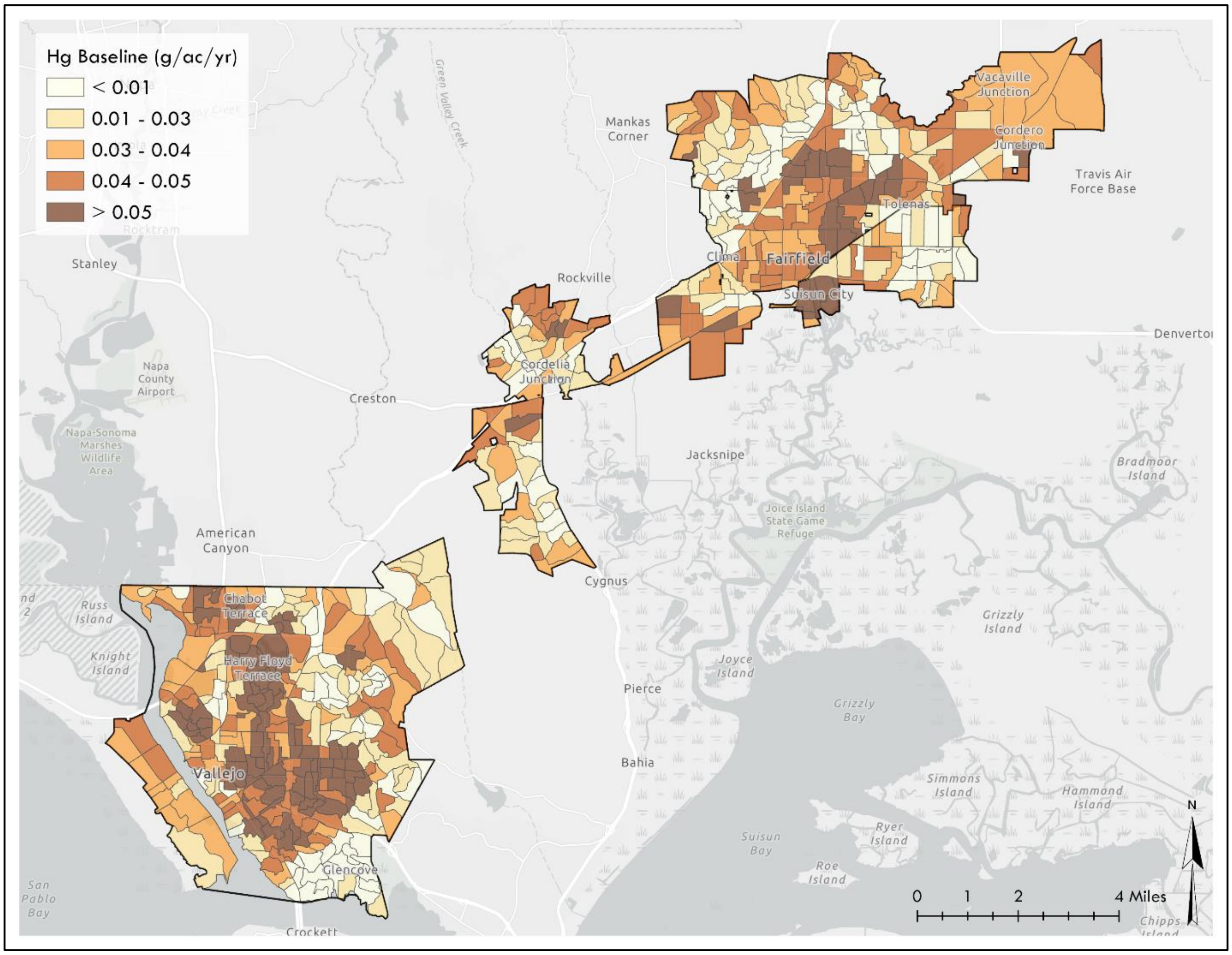

Figure 4.4. Baseline mercury loading estimates for the Solano Permittee MS4 Area

4.1.2 Comparison with Regional Watershed Spreadsheet Model (RWSM)

Comparison between outputs from swTELR and RWSM shows close correspondence between outputs from the two models (Table 4.1). Overall, there was little difference in estimates between swTELR and RWSM runoff estimates (-4%), PCB loads (-16%), or mercury loads (9%), with swTELR providing the lower estimates for runoff and PCBs, and higher estimates for mercury compared to RWSM. Discrepancies between the two models are due almost entirely to the differences in the spatial pattern of runoff estimates, since land use concentrations used in swTELR are identical to those used in RWSM. Even though Solano county is technically part of the North Bay, runoff coefficients used for the RWSM outputs are the same as those used for the East Bay, because rainfall gauges in the East Bay more closely reflect the Solano County rainfall regime. There were no calibration sites for RWSM located in the vicinity of Solano County (McKee et al., 2014); some of the North Bay calibration sites used in RWSM had nearly double the annual rainfall of Fairfield. The decision to use East Bay runoff coefficients was confirmed appropriate by SFEI staff (A. Gilbreath, pers. com., Oct 2018).

Table 4.1. Comparison of average annual loading to SF Bay from RWSM and swTELR.

	RWSM			swTELR			% Difference		
	PCB (g/yr)	Hg (g/yr)	Q (afy)	PCB (g/yr)	Hg (g/yr)	Q (afy)	PCB	Hg	Runoff
Fairfield	131	607	13,244	137	696	12,120	-16%	-12%	-8%
Suisun	15	68	1,655	16	84	2,116	-7%	26%	28%
Vallejo	569	657	13,765	477	683	13,450	-16%	5%	-2%
Totals	**715**	**1,333**	**28,664**	**630**	**1,462**	**27,616**	**-16%**	**9%**	**-4%**

Hydrologic algorithms in swTELR are very sensitive to impervious cover and soil type - runoff generation directly reflects the local impervious cover. Since RWSM outputs are regionally calibrated, they do not appear to reflect the same degree of sensitivity to these factors at more granular scales, which probably accounts for a substantial proportion of the runoff differences between the two models at the individual city level. This is not unexpected, since RWSM was developed as a regional tool and necessarily reflects spatial factors specified at larger spatial scales (McKee et al. 2015) compared to the MS4 and urban catchment-scale estimates provided by swTELR.

To better understand the differences between swTELR and RWSM a multivariate general linear model was constructed at the urban catchment scale for both model outputs using impervious cover as a continuous independent variable and soil type as a categorical independent variable. Soils and impervious cover summarized for each urban catchment delineated in Solano County (n= 596) explained approximately 93% of runoff variance in swTELR (the expected outcome), but only 3.5% in RWSM (an initially surprising outcome). From these findings, we can conclude that: 1) use of TELR baseline estimates will not substantially affect calculations for progress towards overall waste load allocations for Solano Permittees compared to estimates from the RWSM model, 2) RWSM runoff volumes at the catchment scale strongly reflect calibrated parameters, which aligns with its purpose as a tool to estimate loading at the regional or sub-regional scale, 3) spatially explicit estimates from swTELR align more with widely held conceptualizations of how spatial factors such as impervious cover influence urban runoff generation.

4.2 Model Scenario Results

4.2.1 Spatial patterns of pollutant load reductions over time

For each modeling scenario, swTELR and the methods described in Section 3 were applied to generate outputs that incorporated runoff and pollutant loading reductions for different types of GSI. These included land-use redevelopment, decentralized BMPs, and centralized BMPs (regional treatment). These scenarios also included runoff and loading increases projected to result from new development within the Permittee MS4 Area. Overall estimated relative (%) PCB reductions from baseline are greater than those for mercury, which primarily reflects the relatively larger PCB reduction opportunities in Old Industrial and Source Areas that are planned for redevelopment.

Spatial loading outputs for all Solano Permittees are summarized at the urban-catchment level in Figures 4.5 and 4.6, with reductions expressed as grams per acre. The maps illustrate that PCB reductions are focused on Mare Island and within the urban centers of Vallejo and Fairfield for 2020, 2030, and 2040, with less intense clustering of reductions in 2030 and 2040 compared to 2020. Over the course of implementation from the baseline scenarios to 2040, catchments shift from higher to lower loading categories. Outputs from the 2040 scenario show that all catchments that were classified in the highest percentile category in the Baseline Scenario have been eliminated on Mare Island. There are substantially fewer of these relatively high loading catchments on the Vallejo Waterfront, Vallejo and Fairfield downtown areas. Catchments that show the largest relative reductions in the scenarios were usually those which started in the baseline scenario with substantial Source Area or Old Industrial land use. Outlying areas remained virtually unchanged from the baseline scenario due to low redevelopment rates in these catchments, low proportion of high pollutant producing land uses, and new development that generates additional runoff which can create small local pollutant loading increases over time compared to the undeveloped conditions.

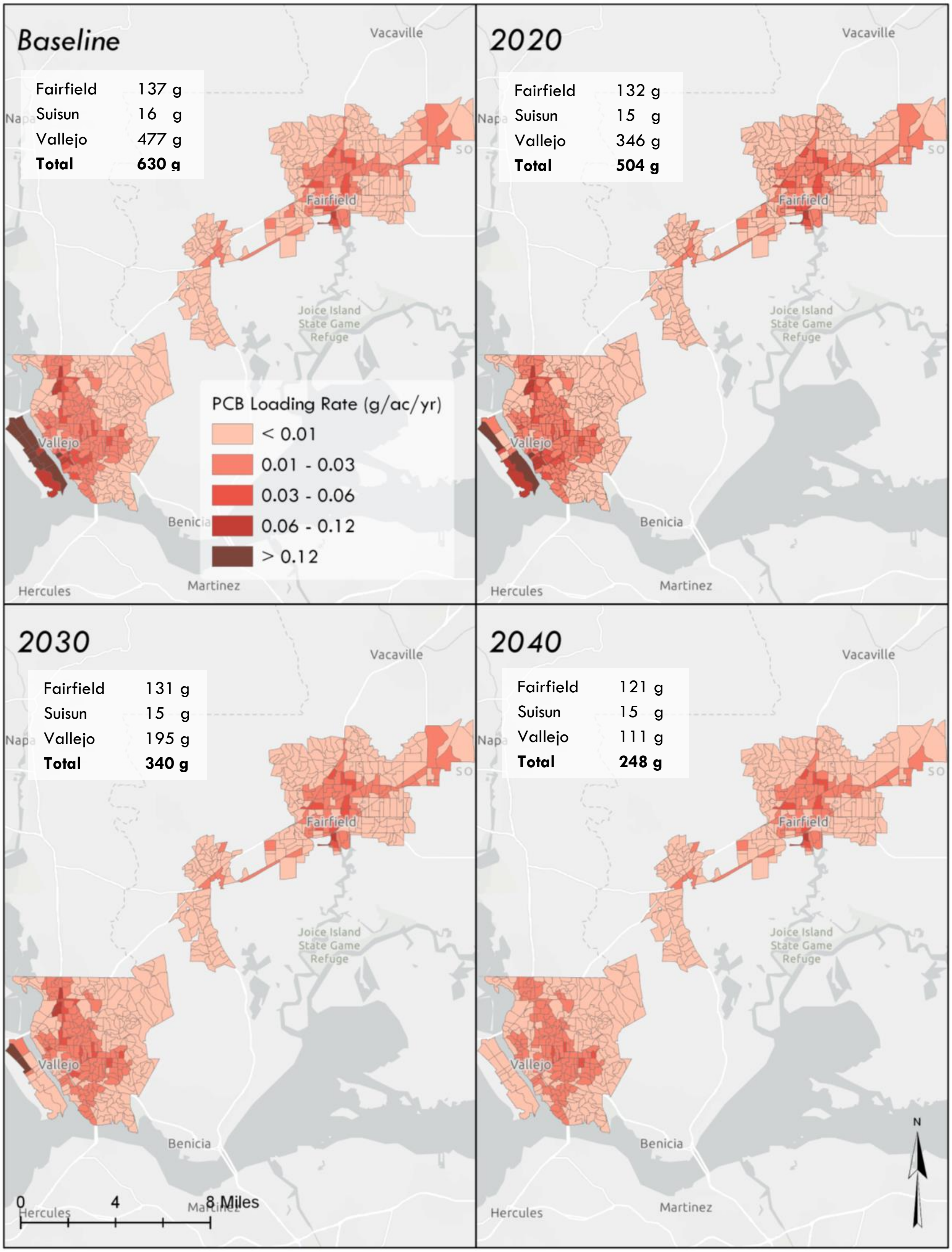

Figure 4.5. Spatial distribution of annual PCB load estimates for baseline and future scenarios

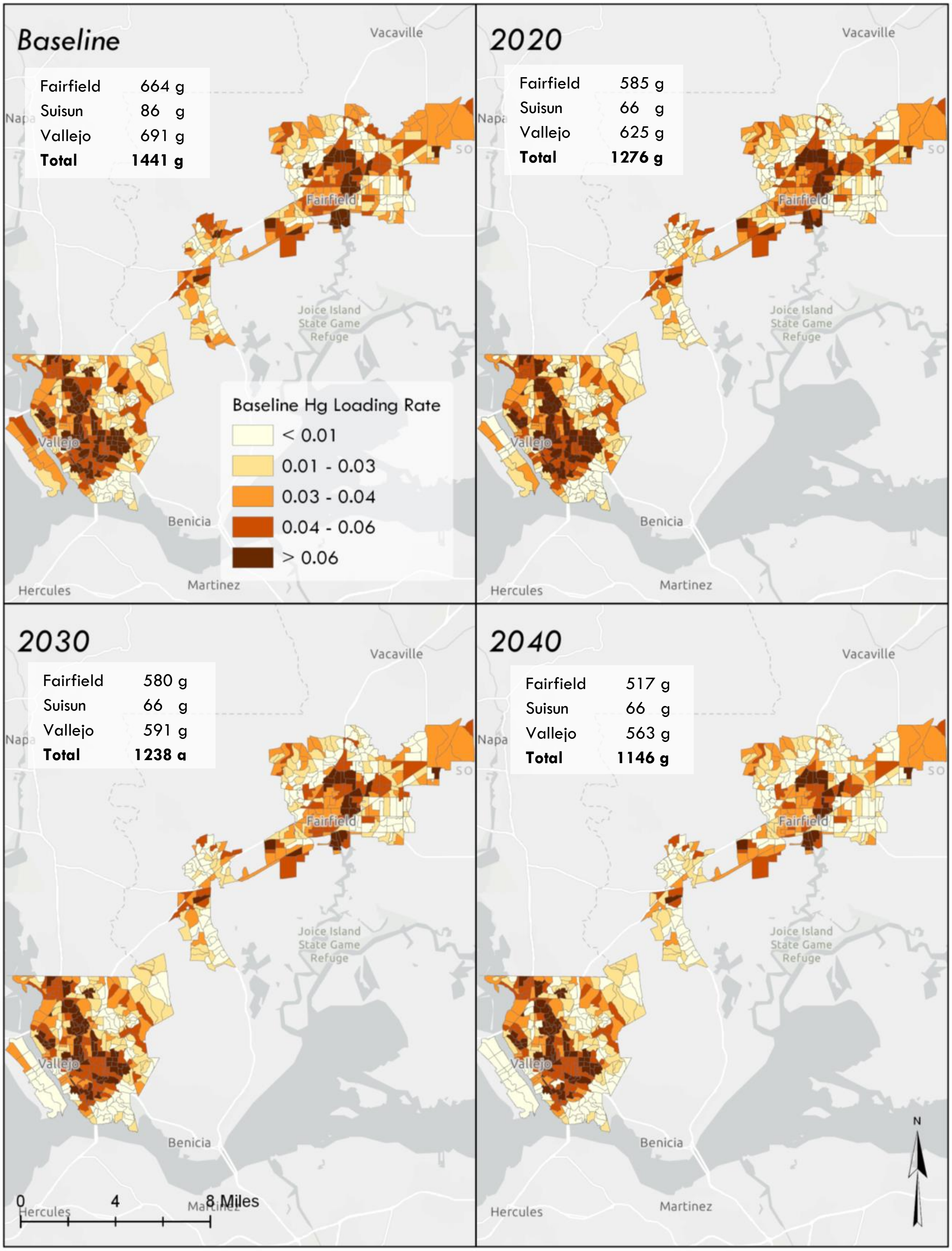

Figure 4.6 Spatial distribution of annual mercury load estimates for baseline and future scenarios

GSI load reductions summary

Total estimated GSI reductions by the year 2040 are 382 grams of PCBs, and 295 grams of Mercury Table 4.2. These reductions constitute a reduction of 61% reduction from baseline for PCBs and a 20% reduction from baseline for mercury. GSI implementation and land use changes can be lumped together compliance demonstration, since they often occur at the same time during redevelopment and both contribute to the GSI reductions targets. However, it is instructive to examine the relative contributions from each component to form a clear picture of expected reductions. For both PCBs and mercury, the primary source of reductions is land use changes that result from redevelopment, making up 98.5% of total PCB reductions and 87% of mercury reductions by 2040 (Figure 4.7). In contrast, reductions from decentralized BMPs and parcel LID make up just 0.5% of PCB load reductions and 9% of mercury load reductions. Routing to centralized BMPs for runoff infiltration and treatment accounts for 1% of PCB load reductions and 9% of mercury load reductions (Figure 4.7). The projected rate of reductions over time for both PCBs and mercury are fairly steady throughout the simulation period (see graphs in Figure 4.7).

Table 4.2. Summary of future scenario loading estimates for PCBs and mercury for the Solano Permittee MS4 Area.

Scenario	Loading		GSI Reductions		% Reduction from Baseline	
	PCB (g)	Hg (g)	PCB (g)	Hg (g)	PCB (g)	Hg (g)
Baseline	630	1,441	-	-		
2020	504	1,276	137	166	22%	12%
2030	340	1,238	289	204	46%	14%
2040	248	1,146	382	295	61%	20%

Most planned GSI implementation is associated with redevelopment, resulting in land use conversion to New Urban, which has the lowest associated pollutant concentration values. Per Table 3.1, PCB concentrations span 3 orders of magnitude from Old Industrial/Source Areas (up to 204 ng/L) to New Urban land uses (3 ng/L); mercury concentrations span one order of magnitude (from 3 to 40 ng/L). Since GSI BMPs can only reduce pollutants that are generated by the associated land use, and since the PCB and mercury loads generated are much smaller after parcels are converted to the New Urban land use, there are simply less pollutants to reduce on redeveloped parcels. Therefore, while GSI implementation will accompany redevelopment land use conversions, the amount of pollutant load reduction that can be attributed directly to BMP capture and treatment of runoff is relatively small. This result corresponds to previous research, which showed that relatively small areas of Old Industrial and Source Area sites have a disproportionate contribution to PCBs loading (McKee et al., 2015).

The disproportionate allocation of reductions to land use conversion is strongly dependent on land use changes actually resulting in dramatic reductions of pollutants in the sediments that they generate, which may not be realistic. Legacy sediments that contain higher levels of pollutants are likely to persist after land-use conversion and GSI installation provides a viable way to mitigate those impacts. While the current inventory of GSI BMPs for Solano Permittees number 185, and their aggregate drainage area is more than 1700 acres, overall this represents only 3% of the Solano Permittee MS4 Area drainage. Specific, planned BMPs will increase total drainage coverage to 4% (2,773 acres) by 2020. With inclusion of redevelopment and new development areas that will be covered under C3 requirements, GSI coverage is projected to increase to 6% (4,414 acres) by 2020 and to 14% (6,503 acres) by 2040.

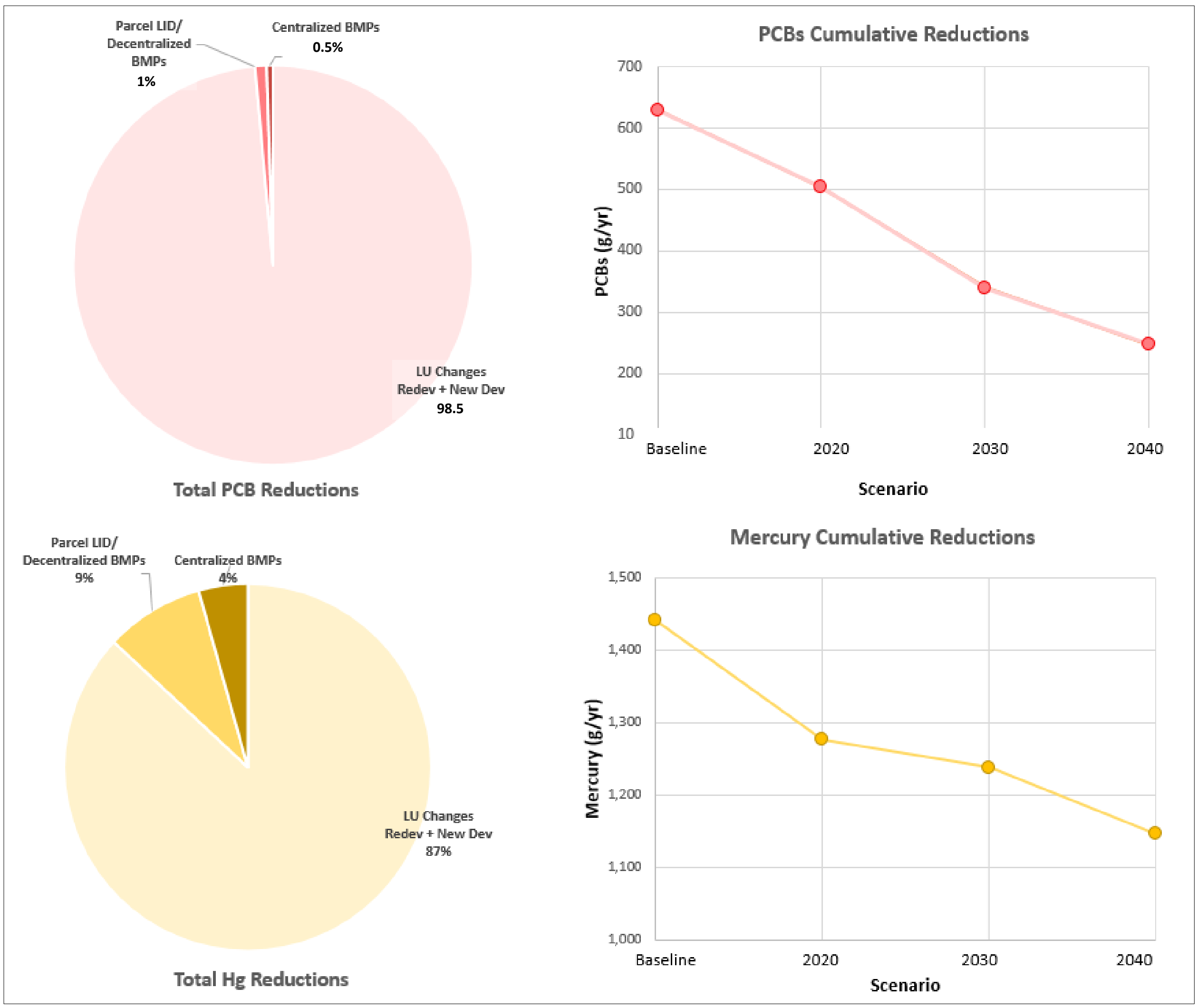

Figure 4.7. Reduction types and trajectory summary for Solano Permittees.

4.2.2 GSI load reductions detail

Examining the modeled reductions by type for each city illustrates pollutant reduction sources in greater detail. Table 4.3 lists the cumulative reductions for each scenario year for each of the Solano Permittee Cities, so that each scenario also includes the reductions from the previous decade scenario. By far, the largest PCB reductions associated with land use changes occurred in Vallejo (377 grams by 2040), compared to the other cities, since Vallejo had the greatest amount of high PCB producing land uses planned for redevelopment. Vallejo and Fairfield had comparable land use change reductions for mercury, at 112 grams and 127 grams respectively by 2040 (Table 4.4). Suisun had the smallest reductions, mostly because the drainage area is very small relative to Vallejo and Fairfield. All cities show comparatively small reductions for GSI relative to the land use changes.

Load reductions resulting from land use changes listed in tables Table 4.3 and 4.4 are the net reductions that include both redevelopment as well as new development. New development results in more pollutant loading due to additional stormwater runoff generation, but in each scenario and for each city, there a there are still net loading reductions. The runoff increases that resulted from the additional impervious coverage are shown as negative values in the reductions column for runoff. These increases are pronounced for Fairfield, where substantial areas of open space have recently been developed as new residential subdivisions. These recent changes were included in the 2020 scenario, and additional new development included in planning documents was allocated to the 2040 scenario. A smaller amount of new development was indicated in the Vallejo 2040 general plan that was allocated to the 2040 scenario and resulted in additional runoff increases. Overall, each city showed net runoff reductions due to implementation of GSU for each scenario year after accounting for new development runoff increases.

Regional treatment via routing of stormwater runoff to centralized BMPs produced similar reductions in Fairfield and Vallejo (Table 4.3). These reductions are due to centralized BMPs that have already been implemented or had detailed specifications available (2020 scenario) or were planned further out into the future (2030 scenario). No additional load reductions were calculated for centralized BMPs for the 2040 scenario, since there is no documentation of planned structures available, although new development areas will likely have adequate space for centralized treatment.

Table 4.3. Future scenarios estimated PCB reductions detail

PCBs		Baseline		Cumulative GSI Reductions by Type						Total Cumulative GI Reductions		Total Cumulative Net Loading	
				LU Changes Redev + New Dev		Decentralized BMPs /Parcel LID		Centralized BMPs					
		Runoff (afy)	Load (g)	Runoff (afy)	Load (g)	Runoff (afy)	Load (g)	Runoff (afy)	Load (g)	Runoff (afy)	Load (g)	Runoff (afy)	Load (g)
Fairfield	**2020**	13,268	137	-178	1.4	831.8	1.3	212.7	1.8	866	5	12,402	132
	2030			-178	1.9	864.1	1.5	419.2	2.9	1,105	6	12,163	131
	2040			-354	13.1	1,522.6	1.7	419.2	1.1	1,588	16	11,681	121
Suisun	**2020**	2,090	16	0	0.0	168.7	0.7	36.4	0.0	205	1	1,885	15
	2030			0	0.0	170.0	0.7	36.4	0.0	206	1	1,884	15
	2040			0	0.1	174.5	0.7	36.4	0.0	211	1	1,879	15
Vallejo	**2020**	13,391	477	0	128.9	642.7	0.6	83.1	2.0	726	131	12,665	346
	2030			0	278.7	1,176.4	1.0	132.8	2.0	1,309	282	12,081	195
	2040			-81	363.5	1,638.8	1.3	132.8	0.8	1,691	366	11,700	111
Solano Permittee Totals			**630**		**377**		**4**		**2**		**382**		**248**

Table 4.4. Future scenarios estimated mercury reductions detail

Mercury		Baseline		Cumulative GSI Reductions by Type						Total Cumulative GI Reductions		Net Loading	
				LU Changes Redev + New Dev		Decentralized BMPs /Parcel LID		Centralized BMPs					
		Runoff (afy)	Load (g)	Runoff (afy)	Load (g)	Runoff (afy)	Load (g)	Runoff (afy)	Load (g)	Runoff (afy)	Load (g)	Runoff (afy)	Load (g)
Fairfield	**2020**	13,268	664	-178	63.7	831.8	9.8	212.7	6.0	866	79	12,402	585
	2030			-178	65.7	864.1	10.6	419.2	7.6	1,105	84	12,163	580
	2040			-354	127.4	1,522.6	13.1	419.2	6.7	1,588	147	11,681	517
Suisun	**2020**	2,090	86	0	16.5	168.7	2.6	36.4	1.1	205	20	1,885	66
	2030			0	16.6	170.0	2.7	36.4	0.0	206	19	1,884	67
	2040			0	17.1	170.0	2.7	36.4	0.0	206	20	1,884	66
Vallejo	**2020**	13,391	691	0	54.8	642.7	4.1	83.1	7.3	726	66	12,665	625
	2030			0	85.8	1,176.4	7.4	132.8	7.4	1,309	101	12,081	591
	2040			-81	112.4	1,638.8	9.9	132.8	6.1	1,691	128	11,700	563
Solano Permittee Totals			**1,441**		**257**		**26**		**13**		**295**		**1,146**

4.2.3 Compliance demonstration

4.2.3.1 *MRP GSI reductions compliance*

Provisions C.11 and C.12 in the MRP require Solano County Permittees to reduce estimated PCBs loading by 8 grams/year and estimated mercury loading by 2 grams/year using green stormwater infrastructure by June 30, 2020. Regionally, Permittees must also project the load reductions achieved via green stormwater infrastructure by 2020, 2030, and 2040, showing that collectively, reductions will amount to 3 kg/year PCBs and 10 kg/year mercury by 2040.

Estimated pollutant load reductions for the Solano Permittees are listed in Table 4.5 illustrate that reductions far exceed the 2020 and 2040 reduction targets. The estimated GSI reductions for each scenario correspond to totals for all cities listed in Tables 4.3 and 4.4. While the 2020 reduction targets listed in Table 4.5 for the Solano Permittees are absolute values listed in the MRP, the 2040 GSI targets have been rescaled based on new calculated baseline values per recommendations in the RAA Guidance (BASMAA, 2017, section 3.5). This calculation uses the proportions of the total estimated reductions for each pollutant to determine GSI targets: 20.8% of the total reductions for PCBs, and 16.1% for mercury. In both cases, GSI reductions are the vast majority of the total reductions. As already discussed, this is because the GSI RAA reductions include those result from redevelopment land-use conversion (BASMAA, 2017).

Table 4.5. Green stormwater infrastructure load reduction estimates and target reductions

	Scenario	Estimated Loading (g)	Estimated GSI Reduction (g)	WLA Reduction Target (g)**	GSI Reduction Target (g)*	Projected GSI % Attainment	% Reduction from Baseline	% Progress to WLA
PCBs	Baseline	630						
	2020	504	126	-	8	100%	20%	-
	2030	340	290	-	58	100%	46%	-
	2040	248	382	530	110	100%	61%	72%
Mercury	Baseline	1441						
	2020	1276	166	-	2	100%	12%	-
	2028	1238	204	0	33	100%	14%	-
	2040	1146	295	-	48	100%	21%	100%

*2020 Reduction targets are fixed values specified in the MRP, 2040 Reduction targets have been rescaled based on new calculated baseline values per RAA Guidance Section 3.5 as a proportion of total estimated reductions (20.8% for PCBs, 16.1% for mercury). Since mercury estimates are already below WLA, they are calculated as a proportion of estimated reductions.

**Based on WLA target of 100g for PCBs, baseline estimate for mercury is below 2028 WLA target for mercury of 1600 g.

4.2.3.2 *Progress towards WLA targets*

The 2040 estimated PCB reductions (382 g) provide Solano Permittees with a 61% reduction below baseline loading estimates, which provides 72% of the reductions that will be required to reach the Solano Permittee's WLA of 100g. It is anticipated that the remainder of the required reductions will be achieved by either source controls or identification of additional GSI opportunities beyond the areas that are already planned for redevelopment. A separate WLA RAA will be performed that includes reductions from source control measures, along with any additional GSI projects that are identified as part of the GSI Workplan that have not already been included in this the current analysis.

Estimated baseline loads for mercury (1441 g) were below the 2028 WLA (1600 g), so this is not a relevant target for tracking progress, since it indicates that there are no mercury reductions required for Solano Permittees to meet the MRP requirement. If instead we appeal to a relative reduction metric, GSI reductions of 295 g are 14% below the baseline estimates, which may be compared with the regional relative mercury reduction target of 50% by 2028. Regardless of the target metric applied, additional GSI projects identified in the GSI Workplan along with source control measures will provide additional mercury reductions.

Modeled baseline estimates from swTELR may present a better alternative for tracking future progress towards mercury reductions compared to those from the TMDL. While the SF Bay regional mercury loading estimates employed extensive data analysis and modeling, allocations to individual communities relied only on population sizes. The close correspondence between swTELR and RWSM mercury load estimates provides a degree of confidence in the swTELR results.

One source of the discrepancy between the two models may be the incongruity between using population as a metric for distributing mercury loads, as in the TMDL, compared to land use, as in the SFEI mercury concentration layer used in this study. Higher populations generally correspond with a greater proportion of urbanized area. The land use layer employed in this study uses a mercury concentration of 80 ng/L for Ag/Open land use, and 3 ng for New Urban land use. So, more populated areas with greater urbanized area can actually result in relatively lower estimated mercury loading in any model using the RWSM land use layer compared to more populous areas. This is the inverse of the logic applied in the TMDL population-based model for estimating load allocations to individual communities.

4.2.4 Spatial prioritization analysis for additional GSI implementation

We explored the potential for additional reductions via GSI throughout the Solano Permittee MS4 Area. A metrics-based spatial prioritization analysis was performed to identify additional parcels and road segments that will be most suitable for GSI implementation, given logistical constraints and additional pollutant load reductions needed to meet future permit requirements. Both parcels and road segments were considered with the spatial metrics adjusted accordingly. The final scoring rubric and metrics were developed collaboratively with Solano Permittees and included and equal weighting of the following factors:

- Soil type

- Slope
- Land ownership
- Land use
- Source parcel status
- Parcel size
- Estimated catchment pollutant loading
- Redevelopment schedule
- Proximity to stormwater structures
- Proximity to Caltrans right of way

The spatial prioritization analysis provides a way to combine implementation feasibility, benefit magnitude, and other logistical factors. A geodatabase was constructed to house all of the GIS data and an automated spreadsheet was created for easy adjustments of metrics and weightings. Outputs from the spatial prioritization analysis serves two purposes: 1) provide some real practical and immediately actionable alternatives for GI implementation and 2) identification of additional means to meet GSI and WLA reduction target requirements. The full process for developing the spatial prioritization analysis is documented in the Green Infrastructure Workplan and here we focus on the outputs and how the outputs can be used to supplement the modeling results already presented to achieve additional future pollutant reductions.

Outputs from the spatial prioritization analysis are presented as maps in Figure 4.8 which shows the scores for each parcel and road segment (approximately 89,000 features total) throughout the Solano County MS4 Permittee Area. Green parcels and road segments indicate that they were in the top 20% of the priority scores and that they were not already treated in one of the modeling scenarios. Most of the parcels or road segments identified in Figure 4.8 are either Old Industrial, Old Transportation or Old Commercial land uses, which corresponds with the highest PCB concentration land uses (see Table 3.1). These parcels indicate the greatest potential for additional GSI implementation to achieve additional pollutant load reductions. GSI Projects identified using this spatial prioritization process can be incorporated for to subsequent modeling efforts to provide updated load reductions. Given that current GSI reductions exceed the GSI reduction requirements, Solano Permittees may also consider identifying synergistic opportunities within areas that have already been slated for redevelopment in the near future.

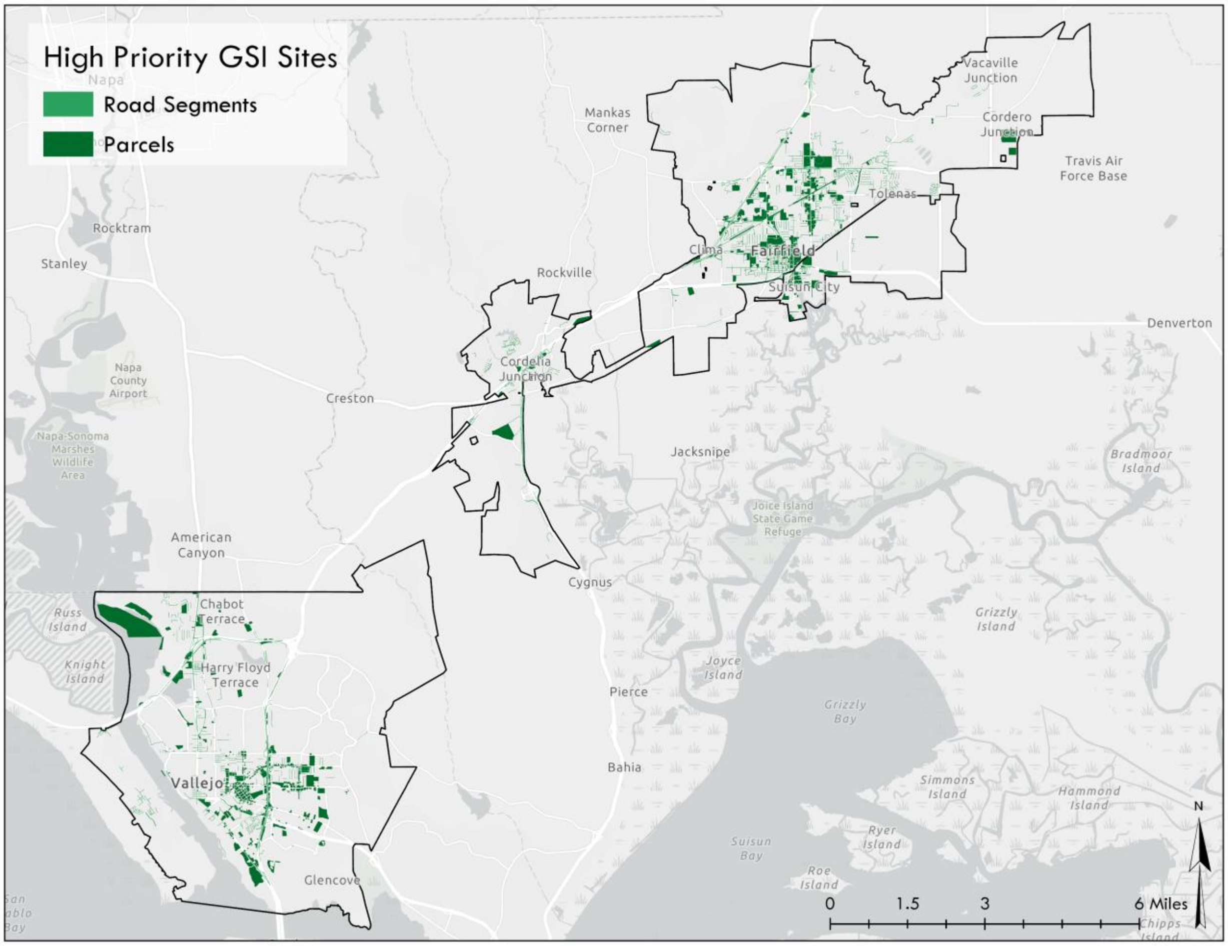

Figure 4.8. High priority parcels and road segments for GSI redevelopment

5 Conclusions

5.1 Results Summary

This data compilation and modeling effort quantifies the water quality benefits of current and planned GSI implementation for Solano County MS4 Permittees. This report satisfies MRP Provisions C.3.j and C.11/C.12.c to demonstrate that GSI implementation will meet specified targets. It also provides information to guide future implementation and development of the GSI Workplan. The modeling results clearly indicate that that if the Solano Permittee redevelopment land use changes proceed along their currently projected trajectory and continue to conform to MRP C3 GSI implementation requirements, they will exceed their GSI reductions targets for PCBs and mercury and make substantial progress towards wasteload allocation targets. Of course, there are limitations to the interpretation the model outputs imposed by various source of uncertainty (discussed in detail below), but the magnitude of exceedance of the GSI reduction targets is strong evidence that the signal of expected changes is probably beyond the boundaries of such uncertainty. Thus, the report provides reasonable assurance that PCB and mercury reduction performance standards established for GSI in MRP 2.0 will be met.

Key findings include:

- Baseline modeling showed that PCB contributions from the City of Vallejo were disproportionately large, primarily due to substantial coverage of Old Industrial land use areas on Mare Island.
- Baseline runoff, PCBs, and mercury estimates corresponded closely with outputs from RWSM at the regional scale.
- Baseline modeling results showed substantial deviations from those estimated for the Solano Permittees in the TMDL wasteload allocations, particularly for mercury. The discrepancy with the TMDL estimates may due to the TMDLs reliance on population to specify load allocations.
- Estimated PCB and mercury reductions meet the GSI reduction targets specified in the MRP for 2020, 2030, and 2040.
- Estimated reductions represent substantial progress towards WLA targets, with the PCB GSI reductions accounting for 72% of reductions required to achieve the 2040 WLA target.
- Reductions are primarily driven by land use conversion, particularly in the case of PCBs, and land use conversions on Mare Island and the Vallejo Waterfront account for most of the PCB reductions.
- A spatial prioritization analysis indicates additional opportunities throughout the Solano Permittees MS4 area for additional GSI implementation that will be further considered in the GSI Workplan.

5.2 RAA Limitations

RAA is a modeling exercise, so it is subject to all of the usual limitations associated with using model outputs to make decisions. Chief among these is the uncertainty associated with the model inputs and the model structure that includes several simplifying assumptions employed for the sake of practicality (see Wijesiri and Liu, 2018, for a recent discussion). We have taken care to communicate those assumptions and identify uncertainties associated with the modeling process throughout this report to support a transparent RAA process. Regardless of the level of rigor employed, the limitations of RAA modeling should be taken into consideration when the outputs are used as the basis for prioritizing action.

Any model is a trade-off for characterizing a system that requires decisions about which elements to simplify and which elements to represent in greater detail. In this RAA we chose to favor spatial granularity above fine scale time resolution. In other words, BMP locations were represented spatially explicitly, but rainfall inputs were represented probabilistically rather than via sequential simulation. As has already been discussed, this choice is based on alignment of the model with the purpose of RAA and the ongoing need to track BMP performance. An important limitation of this approach is that the time-sequencing of events is not preserved, which can produce unique runoff responses. But since continuous simulation model outputs are aggregated to average annual values for RAA, the fine temporal resolution of continuous model outputs are not used any differently than those driven with probabilistic inputs. Moreover, average outputs have previously been judged generally acceptable for stormwater management planning (Lent et al., 2011).

This RAA employed an uncalibrated approach that relied strongly on the input data. Fitting model parameters to observed hydrologic data can improve model performance substantially and most continuous simulation models rely heavily on a calibration of some sort. No relevant long-term hydrologic calibration data were available for the Solano County Permittee MS4 Area. Even if these data were available, the calibration process comes with several limitations related to the ambiguity of identifying optimal parameter sets (see Beven, 2001). Additionally, for several Bay Area communities, the MS4 area may be small relative to the contributing watershed that flows to a gauge. When the MS4 occupies only a small amount of the watershed, fitting a model to the flow response at the bottom of that watershed results in a parameterization that primarily reflects the non-MS4 area. Alternatively, translation of parameterizations from gauged to ungauged basins is a non-trivial task, that has prompted a decade of academic level study via the International Association of Hydrologic Sciences[21].

A key source of modeling uncertainty in this RAA is the characterization of pollutant concentrations on the basis of land-use. Since there is wide variation of PCB and mercury concentrations within

[21] https://iahs.info/pub/index.php

individual land uses it provides an imprecise way to estimate pollutant land surface concentrations. High model sensitivity to pollutant concentration parameters means that model predictions can diverge substantially if these parameters are specified differently (e.g. Park, et al, 2009). Land-use based pollutant concentrations used in this study were based on sampling work conducted by SFEI throughout the SF Bay Area (Wu et al, 2003, McKee et al 2003, McKee, et al, 2015), but this regional dataset may not be representative of the land use pollutant relationships in Solano County, particularly since recent sampling efforts do not include sites in the north side of Suisun Bay (McKee et al. 2015). Representativeness of these data have been acknowledged as a potential source of uncertainty by McKee et al., 2015.

Finally, the structure of the RAA reporting provides some limitations to the interpretation of GSI benefits. Land use changes associated with redevelopment and GSI implementation often happen at the same time. Since land use changes have such a dramatic effect on modeled outputs, and land use changes are lumped in with the GSI reduction estimates, land use changes dominate the calculated GSI reductions. Actual GSI implementation provides a much smaller role in estimated pollutant load reductions once the land use has been changed to one that has characteristically low associated pollutant concentrations. The reality is probably a much less dramatic split between land use change and GSI implementation. An unintended consequence may be that parcels classified as high pollutant concentration land uses may be disproportionately selected for redevelopment even when other factors may weigh in favor of other parcels.

5.3 Recommendations for Ongoing Compliance

Meeting MRP pollutant load reduction targets will require ongoing tracking of BMP implementation and quantification of pollutant load reductions. RAA is a valuable initial step, but it will soon be just another report sitting on a shelf, rather than a tool to direct actions. Implementation will occur over a period of decades and in that time we will learn more than we know now. New BMPs will be created, knowledge of pollutant removal efficiency will grow, and the resources of cities and their priorities will shift. A more dynamic approach to quantifying benefits that can incorporate new information as it becomes available and provide outputs at scales and in formats that are relevant to stormwater managers will be needed. As an alternative to one-off modeling studies, such an approach can provide an iterative verification of progress, reducing risk of failure and tempering expectations of success.

As the capacity of cities grows to provide quantitative estimates of reductions, regulators should consider the value of becoming more flexible on prescriptive requirements to deliver other information that is comparatively less essential. Updatable modeling approaches that focus on the most critical information needs of both stormwater managers and regulators can probably provide more useful information than excessive prescriptive reporting requirements. Such focus will become more important as cities begin to require tracking not hundreds, but thousands of BMPs and GSI projects as implementation proceeds over the coming decades. At the same time, cities will need to move towards a more efficient programs with the capacity to demonstrate compelling evidence of success. To do that, they will need access to the right tools and a strong vision from regulators that helps permittees focus their efforts on the greatest pollutant load reduction opportunities.

The RAA modeling study has clarified a number of recommendations to improve ongoing tracking and verification of pollutant reductions:

1. **Solano permittees should adopt a comprehensive data management approach to track implementation of GSI, such as outlined in the GSI Workplan.** This will help them provide ongoing verification to regulators that the estimates contained in this modeling report are proceeding as planned and avoid accounting errors.

2. **Integrate implementation tracking with a stormwater modeling tool.** This will create efficiencies for ongoing PCB and mercury load reduction quantification as implementation proceeds and also provide ongoing support for heuristic management scenarios to optimize implementation locations and BMP types. It will also serve as a key technical node for integration of GIS datasets relevant to stormwater reporting that are currently stored in disparate manner that makes reporting inefficient.

3. **Use the spatial prioritization approach to identify additional GSI implementation opportunities.** The GIS-based approach developed as part of this study and the GSI Workplan can be used to evaluate high priority areas within privately owned areas already planned for redevelopment or within the public right of way via synergistic implementation opportunities with Caltrans.

4. **Continue to coordinate with BASMAA for quantifying source reduction control measure quantification**. The methods employed should be closely integrated with GSI reduction quantification to ensure that overall WLA accounting is coherent.

5. **Work with regulators to craft requirements for MRP3 that are focused on outcomes and reporting efficiencies.** Negotiations with regional board staff via the BASMAA MRP3 Workgroup should endeavor to reduce reporting requirements for non-essential information that overlaps with performance-based requirements whenever appropriate.

These recommendations are intended to help the Solano Permittees be efficient in demonstrating MRP compliance progress and to help them craft permit requirements and implementation strategies that are conducive to their own community development goals

~~7~~6 References

2NDNATURE, 2006a. Detention Basin Treatment of Hydrocarbon Compounds in Urban Stormwater. Final Report. Prepared for the South Tahoe Public Utility District. March 2006. 143pp.

2NDNATURE, 2006b. Lake Tahoe BMP Monitoring Evaluation Process: Synthesis of Existing Research. Final Report to USFS Lake Tahoe Basin Management Unit, October 2006. 82pp.

2NDNATURE, 2007. Water Quality Evaluations of a Fertilized Turf Surface in the Lake Tahoe Basin (2002-2006). Final Technical Report. Prepared for the Nevada Tahoe Conservation District. May 2007. 89pp.

2NDNATURE, 2008. Water Quality Performance Evaluation of Park Avenue Detention Basins: South Lake Tahoe, CA. Final Technical Report. Prepared for the City of South Lake Tahoe, Engineering Division. August 2008. 117pp.

2NDNATURE, 2010a. PLRM v.1: Focused Stormwater Monitoring to Validate Water Quality Source Control and Treatment Assumptions. Final Phase I Technical Report. March 2010. 118pp.

2NDNATURE, 2010b. Focused stormwater monitoring to validate water quality source control and treatment assumptions. Final Report prepared for U.S. Army Corps of Engineers, June 2010. 118pp.

2NDNATURE, 2010c. Load Reduction Planning Tool v2: A Tool to Estimate the Water Quality Benefits of Parcel Scale Retrofit Projects in the Tahoe Basin. Final Technical and User Guidance Document. Prepared for the Tahoe Regional Planning Agency. November 2010.

2NDNATURE, 2012. Statistical Analysis of Data Obtained from an Incline Village Street Sweeping Effectiveness Study. Final Report to Nevada Division of State Lands, Nevada Tahoe Conservation District and Nevada Division of Environmental Protection, September 2012. 33pp.

2NDNATURE, 2014a. Surrogate Indicators to Monitor Fine Sediment Particles in the Tahoe Basin. Draft Final. March 2014. 27pp.

2NDNATURE, 2014b. Rural Road Rapid Assessment Methodology (Rural Road RAM). Technical Report. Prepared for the Resource Conservation District of Santa Cruz County. September 2014.

2NDNATURE, 2014c. Aligning Stormwater Monitoring Datasets with Priority Management Questions. Final Technical Guidance Document. Prepared for the USFS Pacific Southwest Research Station. December 2014. 68pp.

2NDNATURE, 2015a. Road Operation and Maintenance Practices Effectiveness Testing. Technical Document. November 2015. 88pp.

2NDNATURE, 2015b. Synthesis of Existing Stormwater Models and Potential Applications. Synthesis Report. November 2015.

2NDNATURE, 2016a. Rural Road Rapid Assessment Methodology (Rural Road RAM). Technical Document v2. March 2016. 71pp. (www.ruralroadram.com)

2NDNATURE, 2015c. Road Rapid Assessment Methodology (Road RAM) User Manual v2, Tahoe Basin. Final Document. Prepared for the Nevada Division of Environmental Protection and Lahontan Regional Water Quality Control Board. May 2015

2NDNATURE, 2018a. Parcel Rapid Assessment Method (Parcel RAM) Technical and User Guidance Document v2.1. March 2018. 41pp.

2NDNATURE, 2018b. Best Management Practices Rapid Assessment Methodology (BMP RAM). Technical Document v4.1. March 2018. 54pp.

2NDNATURE, 2018c. MS4 Guidance for Creating Catchment Boundaries and Attributes. Final Document v3.4. April 2018. 55pp.

2NDNATURE and Northwest Hydraulic Consultants, 2011a. Placer County Stormwater TMDL Strategy. Final Technical Report. Prepared for the US Army Corps of Engineers and the County of Placer. July 2011. 90pp.

2NDNATURE and Northwest Hydraulic Consultants, 2011b. Synthesis of Existing Information on Stormwater Infiltration BMPs. Infiltration BMP Design & Maintenance Study. Prepared for the Tahoe Regional Planning Agency. August 2011. 80pp.

2NDNATURE and Northwest Hydraulic Consultants, 2012a. Focused Stormwater Quality Monitoring to Inform Assumptions & Evaluate Predictive Capabilities of Existing Tools. Final Technical Report. Prepared for USFS Pacific Southwest Research Station. June 2012. 149pp.

2NDNATURE and Northwest Hydraulic Consultants, 2012b. Pilot Catchment Validation Study: Lake Tahoe Basin. Final Report to U.S. Army Corps of Engineers, June 2012. 45pp.

2NDNATURE and Northwest Hydraulic Consultants, 2013. Infiltration BMP Design and Maintenance Study. Final Technical Report. Prepared for Tahoe Regional Planning Agency. March 2013. 71pp.

2NDNATURE and Northwest Hydraulic Consultants, 2014. Catchment-Scale Evaluation of Tahoe Stormwater Tools. Final Technical Report. Prepared for USFS Pacific Southwest Research Station. June 2014. 139pp.

2NDNATURE, Northwest Hydraulic Consultants, and Environmental Incentives, 2009. BMP RAM Technical Document, Lake Tahoe Basin. Prepared for the U.S. Army Corps of Engineers, Sacramento District. September 2009.

2NDNATURE, Northwest Hydraulic Consultants, and Environmental Incentives, 2010. Road Rapid Assessment Methodology (Road RAM) Technical Document, Tahoe Basin. Final Report prepared for the California Tahoe Conservancy and Nevada Division of Environmental Protection. November 2010. 74pp. www.tahoeroadram.com

Ackerman, D. and K. Schiff. 2003. Modeling storm water mass emissions to the Southern California Bight. Journal of Environmental Engineering 129:308-317.

Ahiablame, L.M., Engel, B.A. and Chaubey I. 2012. Effectiveness of Low Impact Development Practices: Literature Review and Suggestions for Future Research. Water, Air and Soil Pollution 223 (7): 4253 -4273.

Amato F., X. Querol, C. Johansson, C. Nagl, A. Alastuey, 2010. A review on the effectiveness of street sweeping, washing and dust suppressants as urban PM control methods. Science of the Total Environment 408: 3070–3084.

Arnold Jr., C.L. and C.J. Gibbons, 1996. Impervious surface coverage: the emergence of a key environmental indicator. Journal of the American Planning Association 62(2): 243-258. DOI: 10.1080/01944369608975688

BASMAA, 2017. Bay Area Reasonable Assurance Guidance Document. Prepared by Geosyntec Consultants. June, 2017. 56pp.

Barr Engineering and the Minnesota Pollution Control Agency, 2014. Minimal Impact Design Standards Calculator. Available at http://stormwater.pca.state.mn.us/index.php/MIDS_calculator. Accessed in July to September 2015.

Beaulac, M.N., K.H. Reckhow, 1982. An examination of land use – nutrient export relationships. Water Resources Bulletin, American Water Resources Association 18(6): 1013-1024.

Beck, M.B., ed. 2002. Environmental Foresight and Models: A Manifesto. Amsterdam: Elsevier Science.

Beck, N., L. Kanner, G. Conley, and M. Mathias. 2016. Aligning model specification with management needs: a practical tool to estimate urban stormwater load reductions. Submitted for second round of review, May 2016.

Bedan, E.S. and J.C. Clausen, 2009. Stormwater runoff quality and quantity from traditional and low impact development watersheds. Journal of the American Water Resources Association 45(4): 998-1008. DOI:10.1111/j.1752-1688.2009.00342.x

Beven, K.J., 1989. Changing ideas in hydrology – the case of physically based models. Journal of Hydrology 105, 157-172

Beven, K.J., 1993. Prophecy, reality and uncertainty in distributed hydrological modeling. Advances in Water Resources 16, 41-51

Beven, K.J., 2001. Rainfall-Runoff Modeling the Primer. Wiley, New York, USA. 360 pp.

Beven KJ. The limits of splitting: hydrology. Science of the Total Environment. 1996 Apr 12;183(1-2):89-97. Available from, DOI: 10.1016/0048-9697(95)04964-9

Bhaduri, B., J. Harbor, B. Engel, and M. Grove, 2000. Assessing watershed-scale, long-term hydrologic impacts of land-use change using GIS-NPS model. Environmental Management 26(6): 643-658. DOI:10.1007/s002670010122

Bicknell, B.R., J.C. Imhoff, J.L., Kittle Jr., A.S. Donigian, Jr., and R.C. Johanson, 1997. Hydrological Simulation Program-Fortran. User's manual version 11: U.S. Environmental Protection Agency, National Exposure Research Laboratory, Athens, GA. EPA/600/R-97/080, 755p.

Booth, D.B. 1991. Urbanization and the natural drainage system – impacts, solutions, and prognoses. Northwest Environmental Journal 7:93-118.

Booth, D. B., Karr, J. R., Schauman, S., Konrad, C. P., Morley, S. A., Larson, M. G. and Burges, S. J. 2004. Reviving urban streams: Land use, hydrology, biology and human behavior. JAWRA Journal of the American Water Resources Association, 40: 1351–1364.

Booth, D.B., A.H. Roy, B. Smith, and K.A. Capps. 2016. Global perspectives on the urban stream syndrome. Freshwater Science 34:1169-1175.

Borman H., Diekkruger, B., 2003. Possibilities and limitations of regional hydrological models applied within an environmental change study in Benin (West Africa). Physics and Chemistry of the Earth 28, 1323-1332.

Box, G.E.P, 1976. Science and Statistics. Journal of the American Statistical Association, 71 791-799.

Brander, K.E., K.E. Owen, and K.W. Potter, 2005. Modeled impacts of development type on runoff volume and infiltration performance. Journal of the American Water Resources Association (40)4: 961-970. DOI: 10.1111/j.1752-1688.2003.tb01572.x

Bressy, A., M. Gromaire, C. Lorgeoux, M. Saad, F. Leroy and G. Chebbo. 2012. Towards the determination of an optimal scale for stormwater quality management: Micro-pollutants in a small residential catchment. Water Research. 46: 6799-6810.

Brezonik, P.L., Stadelmann, T.H. (2002) Analysis and predictive models of stormwater runoff volumes, loads, and pollutant concentrations from watersheds in the Twin Cities metropolitan area, Minnesota, USA. 36 (7) 1743-1757.

Butcher, Jonathan, 2003. Buildup, washoff, and event mean concentrations. Journal of the American Water Resources Association, 39(6): 1521-1528. DOI: 10.1111/j.1752-1688.2003.tb04436.x

Butts, M.B., J.T. Payne, M. Kristensen, H. Madsen, 2004. An evaluation of the impact of model structure on hydrological modelling uncertainty for streamflow simulation. Journal of Hydrology 298(1-4): pp 242-266.

California State Water Resources Control Board, 2013. Stormwater discharges from small municipal separate storm sewer systems. Water Quality Order No. 2013-0001-DWQ, General Permit No. CAS000004.

California State Water Resources Control Board, 2016. Strategy to Optimize Resource Management of Storm Water. Storm Water Strategy, STORMS. January 6, 2016. http://www.waterboards.ca.gov/water_issues/programs/stormwater/storms/docs/storms_strategy.pdf

California Regional Water Quality Control Board Lahontan Regional Order No. R6T-2011-101A1 NPDES NO. CAG616001 Updated Waste Discharge Requirements and National Pollutant Discharge Elimination System (NPDES) Permit; Attachment C Monitoring and Reporting Program: http://www.waterboards.ca.gov/rwqcb6/water_issues/programs/tmdl/lake_tahoe/docs/rt620110101/r6t2011_0101a1c.pdf

California Stormwater Quality Association (CASQA), 2003. Stormwater Best Management Practice Handbook, New Development and Redevelopment, January.

Center for Watershed Protection (CWP). 2008. “Deriving Reliable Pollutant Removal Rates for Municipal Street Sweeping and Storm Drain Cleanout Programs in the Chesapeake Bay Basin”. Funded by a U.S. EPA Chesapeake Bay Program grant.

Chandler, R. (1994). Estimating annual urban nonpoint pollutant loads. Journal of Management in Engineering 10(6): 50-59.

Chen, H.J., and H. Chang. 2014. Response of discharge, TSS and E. coli to rainfall events in urban, suburban and rural watersheds. Environmental Science Processes and Impacts. DOI: 10.1039/c4em00327f

Chen, X., W. Zhou, S. Pickett, W. Li, L. Han, 2016. Spatial-Temporal Variations of Water Quality and Its Relationship to Land Use and Land Cover in Beijing, China. International Journal of Environmental Research and Public Health 13(449): 17 pp.

Chui, T.W.D., Mar, B.W., and Horner, R.R., 1981, Highway runoff in Washington State: Model validation and statistical analysis: Washington State Department of Transportation Interim Report No. WA-RD-39.12, 43 p.

Claytor, R. and T. Schueler. 1996. Design of Stormwater Filtering Systems. Center for Watershed Protection. Ellicott City, MD.

Coats, R., M. Larsen, A. Heyvaert, J. Thomas, M. Luck and J. Reuter. 2008. Nutrient and sediment production, watershed characteristics, and land use in the Tahoe basin, California-Nevada. J. Am. Water Res. Assoc., 44(3), 754-770

Conley, G., Beck, N., Riihimaki, C.A. and Hoke, C., 2019. Improving urban trash reduction tracking with spatially distributed Bayesian uncertainty estimates. Computers, Environment and Urban Systems, 77, p.101344.

Conley, G., Beck, N., Riihimaki, C.A. and Tanner, M., 2020. Quantifying clogging patterns of infiltration systems to improve urban stormwater pollution reduction estimates. *Water Research X*, p.100049.

Daum, T., S. Lowe, R. Toia, G. Bartow, R. Fairey, J. Anderson, and J. Jones. 2000. Sediment contamination in San Leandro Bay, CA. San Francisco Estuary Institute, Richmond, CA. 62 pp.

Dotto, C.B.S., G. Mannina, M. Kleidorfer, L. Vezzaro, M. Henrichs, D.T. McCarthy, G. Freni, W. Rauch, and A. Deletic, 2012. Comparison of different uncertainty techniques in urban stormwater quantity and quality modeling. Water Research 46(8): 2545-2558. DOI:10.1016/j.jhydrol.2007.01.023

Dotto, C.B.S., M. Kleidorfer, A. Deletic, W. Rauch, and D.T. McCarthy, 2014. Impacts of measured data uncertainty on urban stormwater models. Journal of Hydrology 508: 28-42. DOI:10.1016/j.jhydrol.2013.10.025

Driscoll, E.D., P.E. Shelley, and E.W. Strecker, 1990. Pollutant loading and impacts from stormwater runoff. Analytical investigation and research report, vol. III. USA: Federal Highway Administration; 1990. FHWA-RD-88-008.

Dwyer, J. F., E.G. McPherson, H.W. Schroeder, and R.A Rowntree. 1992. Assessing the benefits and costs of the urban forest. Journal of Arboriculture, 18, 227-227.

Elliot, A.H. and S.A. Trowsdale. 2007. A review of models for low impact urban stormwater drainage. Environmental Modeling & Software 22(3): 394-405. DOI:10.1016/j.envsoft.2005.12.005

Federal Highway Administration (FHWA). 1984 HEC-19 Model documentation. 303pp. http://www.fhwa.dot.gov/engineering/hydraulics/pubs/hec/hec19.pdf

Federal Highway Administration (FHWA). 2013. Highway Functional Classification Concepts, Criteria and Procedures. 2013 Edition.

Freni, G., G. Mannina, G. Viviani, 2009. Identifiability analysis for receiving water body quality modeling. Environmental Modeling & Software, 24, pp 54-62.

Freni, G., G. Mannina, G. Viviani, 2011. Assessment of integrated urban water quality model complexity through identifiability analysis. Water Research 45:37-50

Gaume, E., J. Villeneuve, M. Desbordes, 1998. Uncertainty assessment and analysis of the calibrated parameter values of an urban storm water quality model. Journal of Hydrology 210, 38 – 50.

Geosyntec Consultants, Inc. and Wright Water Engineers, Inc., 2012. International Stormwater Best Management Practices (BMP) Database: Addendum 1 to Volume Reduction Technical Summary. May 2012.

Geosyntec Consultants, Inc. and Wright Water Engineers, Inc., 2013. International Stormwater Best Management Practices (BMP) Database Advanced Analysis: Influence of Design Parameters on Achievable Effluent Concentrations. September 2013.

Geosyntec Consultants, Inc. and Wright Water Engineers, Inc., 2014. International Stormwater Best Management Practices (BMP) Database Pollutant Category Statistical Summary Report: Solids, Bacteria, Nutrients and Metals. Pollutant Category Statistical Summary Report. December 2014.

Gibb, A., B. Bennett, and A. Birkbeck. 1991. Urban Runoff Quality and Treatment: A Comprehensive Review. British Columbia Research Corporation. Vancover, B.C.

Gilbreath, A., D. Yee and L. McKee. 2012. Concentrations and loads of trace contaminants in a small urban tributary, San Francisco Bay, California. Technical Report of the Sources Pathways and Loading Work Group of the Regional Monitoring Program for Water Quality: Contribution No. 650. San Francisco Estuary Institute. Richmond, CA.

Gilroy, K.L and R.H. McCuen, 2009. Spatio-temporal effects of low impact development practices. Journal of Hydrology 367(3): 228-236. DOI: 10.1016/j.jhydrol.2009.01.008

Greenfield, B.K., Jahn, A., 2010. Mercury in San Francisco Bay forage fish. Environ. Pollut. 158, 2716–2724.

Gobel, P., C. Dierkes, W.G. Coldewey, 2007. Storm water runoff concentration matrix for urban areas. Journal of Contaminant Hydrology 91: 26-42. doi:10.1016/j.jconhyd.2006.08.008

Grove, N.E., R.T. Edwards, and L.L. Conquest, 2001. Effects of scale on land use and water quality relationships: a longitudinal basin-wide perspective. Journal of the American Water Resources Association 37(6): 1721-1734. DOI: 10.1111/j.1752-1688.2001.tb03672.x

Gunter, M.K. 2005. Characterization of nutrient and suspended sediment concentrations in stormwater runoff in the Lake Tahoe Basin. University of Nevada Reno Master of Science in Hydrology Thesis. May 2005.

Gunther, A. J., Salop, P., Bell, D., Feng, A., Wiegel, J., Wood, R., 2001. Initial Characterization of PCB, Mercury, and PAH Contamination in the Drainages of Wester Alameda County, CA. Alameda Countywide Clean Water Program.

Harbor, J., 1994. A practical method for estimating the impact of land use change on surface runoff, groundwater recharge and wetland hydrology. Journal of American Planning Association 60(1), 95-108. DOI:10.1080/01944369408975555.

Harmel, R.D., R.J. Cooper, R.M. Slade, R.L. Haney, and J.G. Arnold, 2006. Cumulative uncertainty in measured streamflow and water quality data for small watersheds. American Society of Agricultural and Biological Engineers 46(3): 689-701.

Harper, H.H. 1998. Stormwater chemistry and water quality. http://www.stormwaterresources.com/Librai-v/045PIChemistry.pdf

Hawkins, R.H., R. Jiang, D.E. Woodward, A.T. Hjelmfelt, and J.A Van Mullem, 2002. Runoff Curve Number Method: Examination of the Initial Abstraction Ratio. In: Proceedings of the Second Federal Interagency Hydrologic Modeling Conference, Las Vegas, Nevada. U.S. Geological Survey, Lakewood, Colorado. CD-ROM.

Herngren L., A. Goonektilleke, G. Ayoko, 2005. Understanding heavy metal and suspended solids relationships in urban stormwater using simulated rainfall. Journal of Environmental Management, 76, pp 149–158.

Herngren L., A. Goonektilleke, G. Ayoko, 2006. Analysis of heavy metals in road-deposited sediments. Analytica Chimica Acta, 571, pp 270–278.

Holman-Dodds, J.K., A.A. Bradley, and K.W. Potter, 2003. Evaluation of hydrologic benefits of infiltration based urban stormwater management. Journal of the American Water Resources Association 39(1): 205-2015. DOI: 10.1111/j.1752-1688.2003.tb01572.x

Hossain, I., M. Imteaz, 2016. Advances in Landscape Runoff Water Quality Modeling: A Review. Springer International Publishing. Chapter 12, pp 225-257.

Houssain, I., A.I. Monzur. “Advances in landscape runoff water quality modeling: a review”, in Landscape Dynamics, Soil and Hydrological Processes in Varied Climates, Vol. 3, eds A. M. Melesse, W. Abtew (Switzerland: Springer International Publishing), 261–277.

Hunt, J.W., B.S. Anderson, B.M. Phillips, J. Newman, R.S. Tjeerdema, K. Taberski, C.J. Wilson, M. Stephenson, H.M. Puckett, R. Fairey, and J. Oakden. 1998. Sediment Quality and Biological Effects in San Francisco Bay: Bay Protection and Toxic Cleanup Program Final Technical Report. California State Water Resources Control Board, Sacramento, CA.

Hunt, W., A. Jarrett, J Smith, L. Sharkey, 2006. "Evaluating Bioretention Hydrology and Nutrient Removal at Three Field Sites in North Carolina." J. Irrig. Drain Eng., 600-608.

Irshad, M., J.A. Faridullah, A.E. Eneji, 2015. Chemical properties of soil and runoff water under different land uses in Abbottabad, Pakistan. Environ Earth Sci 74: 3501-3506.

Jakeman, A.J., G.M. Hornberger, 1993. How much complexity is warranted in a rainfall runoff model? Water Resources Research 29, 2637-2649.

Jamwal, P., A.K. Mittal, J.M. Mouchel, 2008. Effects of urbanisation on the quality of the urban runoff for Delhi watershed. Urban Water Journal 5(3): 247-257.

Järveläinen, J., N. Sillanpää, H. Koivusalo, 2015. Land-use based stormwater pollutant load estimation and monitoring system design, Urban Water Journal, 14:3, 223-236, DOI: 10.1080/1573062X.2015.1086005

Jarvis, N. 2007. A review of non-equilibrium water flow and solute transport in soil macropores: principles, controlling factors and consequences for water quality. European Journal of Soil Science 58:523–546.

Jiang, R. 2001. Investigation of runoff curve number initial abstraction ratio. University of Arizona Master's Thesis. Available at http://arizona.openrepository.com/arizona/handle/10150/191301. Accessed in September 2015.

Jiang, Y, J.R. Frankenberger, L.C. Bowling, and Z. Sun, 2014. Quantification of uncertainty in estimate nitrate-N load in agricultural watersheds. Journal of Hydrology 515: 106-116. DOI:10.1016/j.jhydro.2014.06.027

Karr, J. R. (1999), Defining and measuring river health. Freshwater Biology, 41: 221–234.doi:10.1046/j.1365-2427.1999.00427.

Kayhanian, M., Suverkropp, C., Ruby, A., and Tsay, K., 2007b. Characterization and prediction of 403 highway runoff constituent event mean concentration. Journal of Environmental Management, 404 85(2), 279-295.

Kayhanian, M., B.D. Fruchtman, J.S. Gulliver, C. Montanaro, E. Ranieri, and S. Wuertz. 2012. Review of highway runoff characteristics: Comparative analysis and universal implications. Water Research 46(2012): 6609-6624.

King, K.W., Arnold, J.G., Bingner, R.L., 1999. Comparison of Green-Ampt and Curve Number Methods on Goodwin Creek Watershed Using SWAT. Transactions of the American Society of Agricultural Engineers, 42 (4) 919-925.

KLI and EOA, 2002. Joint stormwater agency project to study urban sources of mercury, PCBs, and organochlorine pesticides. Report prepared by Kinnetic Laboratories, Inc. and Eisenberg, Olivieri and Associates, Inc. for Santa Clara Valley Urban Runoff Pollution Prevention Program, Contra Costa Clean Water Program, San Mateo Countywide Stormwater Pollution Prevention Program, Marin County Stormwater Pollution Prevention Program, Vallejo Flood Control and Sanitation District, Fairfield- Suisun Sewer District. 71pp.

Kokkonen, T.S., and Jakeman, A.J., 2001. A comparison of metric and conceptual approaches in rainfall-runoff modeling and its implications. Water Resources Research 37: doi: 10.1029/2001WR000299.

Ko, F. and J. Baker. 2004. Seasonal and annual loads of hydrophobic organic contaminants from the Susquehanna River basin to the Chesapeake Bay. Marine Pollution Bulletin. 48: 840-851.

Lahontan Regional Water Quality Control Board and Nevada Department of Environmental Protection, 2007. Lake Tahoe TMDL Pollutant Reduction Opportunity Report, September 2007. v1.01

Lahontan Regional Water Quality Control Board and Nevada Department of Environmental Protection. 2010. Final Lake Tahoe Total Maximum Daily Load. November 2010.

Lahontan Regional Water Quality Control Board and Nevada Department of Environmental Protection, 2015. Lake Clarity Crediting Program Handbook for Lake Tahoe TMDL Implementation, December 2015 v2.1.

Langbein, W. B., and S. A. Schumm 1958. Yield of sediment in relation to mean annual precipitation, Eos Trans. AGU, 39(6), 1076–1084, doi:10.1029/TR039i006p01076.

Larsson, M.H. & Jarvis, N.J. 1999. A dual-porosity model to quantify macropore flow effects on nitrate leaching. Journal of Environmental Quality, 28, 1298–1307.

Larsson, M.H. & Jarvis, N.J. 2000. Quantifying interactions between compound properties and macropore flow effects on pesticide leaching. Pest Management Science, 56, 133–141.

Leavesley, G.H., S.L. Markstrom, P.J. Restrepo, R.J. Viger, 2002. A modular approach to addressing model design, scale and parameter estimation issues in distributed hydrologic modeling. Hydrological Processes 16, 173-187

Lee, H.L., K.W. Bang, 2000. Characterization of urban stormwater runoff. Water Resources 34(6) 1773-1780.

Lee, J.G., A. Selvakumar, K. Alvi, J. Riverson, J.X. Zhen, L. Shoemaker, and F. Lai, 2012. A watershed-scale design optimization model for stormwater best management practices. Environmental Modeling & Software 37: 6-18. DOI:10.1016/j.envsoft.2012.04.011

Leigh, M., P. Prouzová, M. Macková, T. Macek, D. Nagle and J. Fletcher. 2006. Polychlorinated biphenyl (PCB)-degrading bacteria associated with trees in a PCB contaminated site. Applied and Environmental Microbiology. 72(4): 2331-2342.

Li, C., W. W. Wang, J. Xiong, P. Chen, 2014. Sensitivity analysis for urban drainage modeling using mutual information. Entropy 16, 5739-5752, doi:10.3390/e16115738

Li D, Wan J, Ma Y, Wang Y, Huang M, et al, 2015. Stormwater Runoff Pollutant Loading Distributions and Their Correlation with Rainfall and Catchment Characteristics in a Rapidly Industrialized City. PLoS ONE 10(3): e0118776. doi: 10.1371/journal.pone.0118776

Lim, K. J., B. A. Engel, S. Muthukrishnan, and J. Harbor, 2006. Effects of initial abstraction and urbanization estimated runoff using CN technology. Journal of the American Water Resources Association 42: 629–643. DOI:10.1111/j.1752-1688.2006.tb04481.x

Lin, J. P. 2004. Review of published export coefficient and event mean concentration (EMC) data, WRAP Technical Notes Collection (ERDC TN-WRAP-04-3), U.S. Army Engineer Research and Development Center, Vicksburg, MS. www.wes.army.mil/el/wrap

Lindenschmidt, K.E., 2006. The effect of complexity on parameter sensitivity and model uncertainty in river water quality modeling. Ecological Modeling 190, 72-86.

Line, D., N. White, D. Osmon, G. Jennings, C. Mojonnier, 2002. Pollutant export from various land uses in the Upper Neuse River Basin. Water Environment Research 74(1): 100-108.

Loganathan, P., S. Vigneswaran, J. Kandasamy, 2013. Road-Deposited Sediment Pollutants: A Critical Review of their Characteristics, Source Apportionment, and Management. Critical Reviews in Environmental Science and Technology 43 (13): 1315-1348.

Los Angeles County Stormwater Monitoring Report: 1998-1999. (1999). http://ladpw.org/wmd/NPDES/9899TC.cfm

Low, T.E. 2008. Light Imprint Handbook: Integrating sustainability and community design. Charlotte: Duany Plater-Zyberk & Company.

Lundy, L., J.B. Ellis, and D.M. Revitt, 2012. Risk prioritization of stormwater pollutant sources. Water Research, 46, pp 6589-6600.

Maheepala, U.K., A.K. Tkyi, B.J.C. Perera, 2001. Hydrological data for urban stormwater drainage systems. Journal of Hydrology 245: 32-47

Mangarella, P., K. Havens, W. Lewis and L. McKee. 2010. Task 3.5.1: Desktop evaluation of controls for polychlorinated biphenyls and mercury load reduction. Technical Report of the Regional Watershed Program: SFEI Contribution 613. San Francisco Estuary Institute, Oakland, CA.

Mannina, G., G. Viviani, 2010. An urban drainage stormwater quality model: Model development and uncertainty quantification. Journal of Hydrology, 381, pp 248-265.

Maryland Department of the Environment NPDES MS4 Permit. 2013. Baltimore City, Maryland. Permit number 11-DP-2215 MD0068292. Available at http://www.mde.state.md.us/programs/Water/StormwaterManagementProgram/Documents/Baltimore%20City%20Final%2012%2019%202013%20Permit.pdf. Accessed in July 2015.

McKee, L.J. Gilbreath, N., Hunt, J.A., Wu, J., and Yee, D., 2015. Sources, Pathways and Loadings: Multi-Year Synthesis with a Focus on PCBs and Hg. A technical report prepared for the Regional Monitoring Program for Water Quality in San Francisco Bay (RMP), Sources, Pathways and

Loadings Workgroup (SPLWG), Small Tributaries Loading Strategy (STLS). SFEI Contribution No. 773. San Francisco Estuary Institute, Richmond, CA.

McKee, L., Mangarella, P., Williamson, B., Hayworth, J., and Austin, L., 2006. Review of methods use to reduce urban stormwater loads: Task 3.4. A Technical Report of the Regional Watershed Program: SFEI Contribution #429. San Francisco Estuary Institute, Oakland, CA.

McKenzie, D.J. and G.A. Irwin. 1983. Water quality assessment of stormwater runoff from a heavily used urban highway bridge in Miami, Florida. FHWA/FL/BMR-84-270. U.S. Geologic Survey. Miami, FL.

Meals, DW. S.A. Dressing, and T.E. Davenport, 2010. Lag time in water quality response to best management practices: A review. Journal of Environmental Quality 39(1): 85-96. DOI:10.2134/jeq2009.0108

Melanen, M. and R. Lauddanen, 1981. Quantity of storm runoff water in urban areas, Publications of the water research institute, 42. National board of waters, Finland.

Mitchell, G, 2005. Mapping hazard from urban non-point pollution: a screening model to support sustainable urban drainage planning. Journal of Environmental Management 74: 1–9. pmid:15572076

Michel, C., V. Andréassian, and C. Perrin, 2005. Soil Conservation Service Curve Number method: How to mend a wrong soil moisture accounting procedure? Water Resources Research 41(2): W02011. DOI:10.1029/2004WR003191

Mouri, G., 2015. Assessment of land cover relocation incorporating the effects of human activity in typical urban and rural catchments for the design of management policies. Environmental Science and Policy 50: 74-87.

Nandakumar, N., R.G. Mein, 1997. Uncertainty in rainfall runoff model simulations and the implications for predicting the hydrologic effects of land-use change. Journal of Hydrology 192 211-232.

National Research Council, 2009. Urban Stormwater Management in the United States. Washington, D.C.: The National Academies Press.

Nordeidet, B., S.O. Astebol, T. Hvitved-Jacobsen 2004. Prioritising and planning of urban stormwater treatment in the Alna watercourse in Oslo. Sci Total Environ, 334-335, 231-8.

Northwest Hydraulic Consultants Inc. (nhc), Geosyntec Consultants, Inc., and 2NDNATURE, LLC. 2010. Pollutant Load Reduction Model. Available at https://www.enviroaccounting.com/TahoeTMDL/Program/Display/ForUrbanJurisdictions. Accessed in May to September 2015.

Pannell, D.J. and F.L. Gibson, 2014. Testing metrics to prioritize environmental projects. Working paper 1401, School of Agricultural and Resource Economics, University of Western Australia, Crawley, Australia.

Perrin, C., Michel, C., and Andreassian, V., 2001. Does a large number of parameters enhance model performance? Comparative assessment of common catchment model structures on 429 catchments, Journal of Hydrology, 242, 275–301.

Petrucci, G., C. Bonhomme, 2014. The dilemma of spatial representation for urban hydrologysemi-distributed modeling: Trade-offs among complexity, calibration, and geographical data. Journal of Hydrology 517, 997-1007.

Polkowska, Z. K. Sharzynska, A. Dubiella-Jackowska, W. Staszek, and J. Namiesnick, 2007. Evaluation of pollutant loading in the runoff waters from a major urban highway (Gdansk beltway, Poland). Global Nest Journal 9(3): 269-275.

Rauch, W., J.-L. Bertrand-Krajewski, P. Krebs, O. Mark, W. Schilling, M. Schütze, and P.A. Vanrolleghem, 2002. Deterministic modeling of integrated urban drainage systems. Water Science & Technology 45(3): 81-94.

Reed, S., V. Koren, M. Smith, Z. Zhang, F. Moreda, D. Seo, 2004. Overall distributed model intercomparison project results. Journal of Hydrology, 298: 27-60.

Restrepo, J.D, Kjerfve, B., Hermelin, M., Restrepo, J.C., Factors controlling sediment yield in amajor South American drainage basin: the Magdalena River, Colombia, Journal of Hydrology, Volume 316, Issues 1–4, 10 January 2006, Pages 213-232, ISSN 0022-1694, http://dx.doi.org/10.1016/j.jhydrol.2005.05.002.

Richards, B.K., Steenhuis, T.S., Peverly, J.H. & McBride, M.B. 1998. Metal mobility at an old, heavily loaded sludge application site. Environmental Pollution, 99, 365–377.

Rode, M. and U. Suhr, 2007. Uncertainties in selected river water quality data. Hydrology and Earth System Sciences Discussions, 11(2): 863-874.

Rossman, L.A., 2008. Storm Water Management Model – User's Manual Version 5.0 National Risk Management Research Laboratory, Office of Research and Development, US Environmental Protection Agency, Cincinnati, Ohio, USA.

Rossman, L.A., 2013. National Stormwater Calculator. Available at Checkhttp://www.epa.gov/nrmrl/wswrd/wq/models/swc. Accessed in May to September 2015.

Roy, D.P., J. Ju, K. Kline, P.L. Scaramuzza, V. Kovalsky, M.Hansen, T.R. Loveland, E. Vermote, and C. Zhang. 2010. Web-enabled Landsat Data (WELD): Landsat ETM+ composited mosaics of the conterminous United States. Remote Sensing of the Environment, 114(1), 35-49. January 15, 2010.

Roy, S., J. Byrne, and C. Pickering. 2012. A systematic quantitative review of urban tree benefits, costs, and assessment methods across cities in different climatic zones. Urban Forestry & Urban Greening, 11(4), 351-363.

Sage, J., C. Bonhomme, S. Ali, M. Gromaire. Performance assessment of a commonly used "accumulation and wash-off" model from long-term continuous road runoff turbidity measurements. Water Research, 78, pp 47-59.

San Francisco Regional Water Quality Control Board. (SFRWQCB) 2006. Proposed Basin Plan Amendment and Staff Report for Revised Total Maximum Daily Load (TMDL) and proposed mercury water quality objectives. August, 2006. 116pp.

San Francisco Regional Water Quality Control Board. (SFRWQCB) 2008. Total Maximum Daily Load for PCBs in San Francisco Bay. Final Staff Report for Proposed Basin Plan Amendment. February 2008. 135pp.

Sartor, J., G. Boyd, F. Agardy, 1972. Water pollutants aspects of street surface contaminants. Journal of Water Pollution Control Fed, 46, pp 458–467.

Schueler, T. 1987. Controlling Urban Runoff: A Practical Manual for Planning and Designing Urban Best Management Practices. MWCOG. Washington, D.C.

Scheuler, T., Youngk, A. Potential Benefits of Nutrient and Sediment Practices to Reduce Toxic Contaminants in the Chesapeake Bay Watershed. Technical report prepared for the Chesapeake Bay Partnership. November 2015. 88pp.

Selbig, W.R., R.T. Bannerman, 2007. Evaluation of Street Sweeping as a Stormwater-Quality-Management Tool in Three Residential Basins in Madison, Wisconsin. U.S. Geological Survey Scientific Investigations Report 2007-5156, 103 pp.

Shi, Z.H., L.D. Chen, N.F. Fang, D.F. Qin, and C.F. Cai, 2009. Research on the SCS-CN initial abstraction ratio using rainfall-runoff event analysis in the Three Gorges Area, China. Catena 77(1): 1-7. DOI:10.1029/2004WR003191.

Shoemaker, L., M. Lahlou, A. Doll, and P. Cazenas. 2002. Stormwater Best Management Practices in an Ultra-Urban Setting: Selection and Monitoring. Federal Highway Administration, U.S. Department of Transportation.

Smullen, J., and K. Cave.1998. "Updating the U.S. Nationwide Urban Runoff Quality Database." 3rd International Conference on Diffuse Pollution: August 31 - September 4, 1998. Scottish Environment Protection Agency. Edinburg, Scotland.

Snowling, S.D., J.R. Kramer, 2001. Evaluating modeling uncertainty for model selection. Ecological Modeling 138, 17-30.

State of Washington Department of Ecology, 2013. NPDES State Waste Discharge General Permit for Large and Medium MS4s. Available at http://www.ecy.wa.gov/programs/wq/stormwater/municipal/phaseIpermit/5YR/2014mod/PhaseI-Permit-2014Final.pdf. Accessed in July 2015.

Strecker, E., E. Driscoll, P. Shelley, D. Gaboury, J. Sartor, 1990. The U.S. Federal Highway Administrations Receiving Water Impact Methodology. The Science of the Total Environment, 93, pp 489-498.

Strecker, E. W., Quigley, M. M.; Urbonas, B. R.; Jones, J. E.; Clary J. K., 2001. Determining Urban Storm Water BMP Effectiveness. Journal Water Resources Planning and Management, 127 (3), pp 144-149.

Stein, E., L. Tiefenthaler, L., Schiff, Kenneth, 2007. Sources, patterns and mechanisms of storm water pollutant loading from watersheds and land uses of the greater Los Angeles are, CA, USA. Southern California Coastal Water Research Project Final report. 103 pp.

Stumm, W., and J. Morgan, 1996. Aquatic Chemistry: Chemical Equilibria and Rates in Natural Waters, Third Edition. New York: John Wiley & Sons, Inc.

Sutherland, R., and S. Jelen. 1997. Contrary to conventional wisdom, street sweeping can be an effective BMP. In: W. James (ed.), Advances in Modeling the Management of Stormwater Impacts, Vol. 5, pp. 179-190. CHI, Guelph, Canada.

Swanson Hydrology and Geomorphology, 2003. Assessment of Seasonal Pollutant Loading and Removal Efficiency of Detention Basins. Prepared for the Tahoe Regional Planning Agency and the US Environmental Protection Agency. February 2003. 59pp.

Tang, A., B.A. Engel, B.C. Pijanowski, and K.J. Lim, 2005. Forecasting land use change and its environmental impact at watershed scale. Journal of Environmental Management 76(1): 35-45. doi:10.1016/j.jenvman.2005.01.006

Tetra Tech, Inc. 2011. Spreadsheet Tool for the Estimation of Pollutant Load (STEPL) Version 4.1. Available at http://it.tetratech-ffx.com/steplweb. Accessed in May to September 2015.

TetraTech, 2014. Urban Land Use Concentration/Loading Rate Literature Review— Summary and Results Memorandum for USGS. 87 pp.

Tomer, M.D. and M.A. Locke, 2011. The challenge of documenting the water quality benefits of conservation practices: a review of USDA-ARS's conservation effects assessment project watershed studies. Water Science & Technology 64(1): 300–310. DOI:10.2166/wst.2011.555

USDA-SCS (U.S. Department of Agriculture-Soil Conservation Service), 1986. Urban hydrology for small watersheds. Technical release 55, NTIS PB87-101580, 2nd edn. USDA SCS, Springfield, Virginia.

USDA SCS (US Department of Agriculture-Soil Conservation Service), 2007. Part 630 Hydrology National Engineering Handbook, Chapter 7 Hydrologic Soil Groups. 210-VI-NEH, Washington, DC.

USDA SCS (US Department of Agriculture-Soil Conservation Service), 2010. Part 630 Hydrology National Engineering Handbook, Chapter 15 Time of Concentration. 210-VI-NEH, Fort Worth, Texas.

USEPA, 1983. Final Report. Results of the Nationwide Urban Runoff Project. Washington, DC.

USEPA, 2008. Final Report. EPA's Report on the Environment. National Center for Environmental Assessment, Washington, DC. May 2008. EPA/600/R-07/045F.

USEPA, 2009. Guidance on the Development, Evaluation, and Application of Environmental Models, Washington, DC. March 2009. 99pp. EPA/100/K-09/003

USEPA, 2013. Our Built and Natural Environments: A technical review of the interactions between land use, transportation, and environmental quality (2nd Edition). EPA 231-K-13-001.

USEPA, 2014. Municipal Separate Stormwater Sewer System (MS4) Main Page. Available at http://water.epa.gov/polwaste/npdes/stormwater/Municipal-Separate-Storm-Sewer-System-MS4-Main-Page.cfm. Accessed in July 2014.

Vallejo Sanitation and Flood District (VSFD) and the City of Vallejo, 2016. Mercury and PCBs Control Measures Implementation Status Report. April, 2016. 19pp.

Voskamp, I.M, and F.H.M Van de Ven, 2015. Planning support system for climate adaptation: Composing effective sets of blue-green measures to reduce urban vulnerability to extreme weather events. Building and Environment 83: 159-167. DOI10.1016/j.buildenv.2015.07.018

Wagener, T., Kollat, J., 2007. Numerical and visual evaluation of hydrological and environmental models using the Monte Carlo analysis toolbox. Environmental Modeling & Software, 22, pp 1021–1033.

Walsh, C.J., D.B Booth, M.J. Burns, T.D. Fletcher, R.L. Hale, L.N. Hoang, G Livingston, M. A. Rippy, A.H. Roy, M. Scoggins, A. W. 2016. Principles for urban stormwater management to protect stream ecosystems. Freshwater Science, 35(1) 398-411.

Wang, L., Wei, J., Huang, Y., Wang, G., Maqsood, I., 2011. Urban nonpoint source pollution buildup and washoff models for simulating storm runoff quality in the Los Angeles County. Environmental Pollution, 159, pp 1932-1940.

Water Environment Federation (WEF) Manual of Practice No. 23 / American Society of Civil Engineers (ASCE) Manual and Report of Engineering Practice No. 87, 1998. Urban Runoff Quality Management.

Weiss, P. T., J.S. Gulliver, and A.J. Erickson. (2007). Cost and Pollutant Removal of Storm-Water Treatment Practices. Journal Of Water Resources Planning & Management, 133(3), 218-229.

Wijesiri, B., Liu, A., Egodawatta, P., McGree, J. and Goonetilleke, A., 2019. Understanding Uncertainty Associated with Stormwater Quality Modelling. In Decision Making with Uncertainty in Stormwater Pollutant Processes (pp. 1-13). Springer, Singapore.

Whalen, P., and M. Cullum. 1989. An Assessment of Urban Land Use/Stormwater Runoff Quality Relationships and Treatment Efficiencies of Selected Stormwater Management Systems. South Florida Management District Resource Planning Department, Water Quality Division. Technical Publication 88-9.

Woodward, D.E., R.H. Hawkins, R. Jiang, A.T. Hjelmfelt, Jr., J.A. Van Mullem, and Q.D. Quan, 2003. Runoff Curve Number Method: Examination of the Initial Abstraction Ratio. In Conference Proceeding Paper, World Water and Environmental Resources Congress 2003: pp.1-10.

Wu, J.; Gilbreath, A.; McKee, L. J. 2017. Regional Watershed Spreadsheet Model (RWSM): Year 6 Progress Report. SFEI Contribution No. 811. San Francisco Estuary Institute: Richmond, CA. http://www.sfei.org/documents/regional-watershed-spreadsheet-model-rwsm-year-6-final-report

Yee, D. and L.J. McKee. 2010. Task 3.5: Concentrations of PCBs and Hg in soils, sediments and water in the urbanized Bay Area: implications for best management. A technical report of the Watershed Program. SFEI Contribution 608. San Francisco Estuary Institute, Oakland CA 94621. 36

Yang, H., G. Wang, L. Wang, B. Zheng, 2015. Impact of land use changes on water quality in headwaters of the Three Gorges Reservoir. Environ Sci Pollut Res 23(1): 11448-11460.

Yuan, Y., Hall, K., & Oldham, C., 2001. A preliminary model for predicting heavy metal contaminant loading from an urban catchment. Science of the Total Environment, 266(1-3), 299-307.

Yuan, Y., W. Wenming, S.C. McCutcheon, E.V. Taguas, 2012. Initial abstraction and curve numbers for semiarid watersheds in Southeastern Arizona. Hydrological Processes, 28 (3) 774-783.

Zoppou, C., 2001 Review of urban storm water models. Environmental Modeling & Software 16(3): 195-231. DOI:10.1016/j.envsoft.2011.09.01

Appendix A

Beck, N. G., Conley, G., Kanner, L., & Mathias, M. (2017). An urban runoff model designed to inform stormwater management decisions. *Journal of environmental management*, *193*, 257-269.

Appendix B

BMP type definitions used in swTELR

CENTRALIZED BMPS – TYPICALLY PUBLICLY OWNED & MAINTAINED BMPS, TREATING A LARGE (>20 ACRES) URBAN DRAINAGE WITH MULTIPLE LAND USES AND OWNERSHIP			
STRUCTURAL BMP TYPE	**OTHER NAMES**	**DESCRIPTION**	**TREATMENT PROCESSES**
Bed Filter	*Underground Sand Filter* *Surface Sand Filter* *Perimeter Sand Filter* *Organic Media Filter*	A flow-through structure that uses granular media (e.g. sand or activated alumina) to actively filter stormwater to remove stormwater pollutants. Filtration is controlled by the flow rate through the media and discharge via an underdrain or outlet. Little to no volume loss occurs. May be confined space but not always. If treating a smaller area (<20 impervious acres), it is likely a **filtration device**.	MEDIA FILTRATION
Detention Basin	*Detention Pond (impervious)* *Dry Pond*	A flow-through basin with discrete inlets and outlets designed to detain stormwater runoff for some minimum time to reduce peak flows. Design treatment capacity and draw down time will vary across specific BMPs. One or more outflow offices may exist but there is at least one at base of basin to allow complete draining between storms. Increased draw down times can increase particle capture via settling within the basin, though generally these BMPs do not allow for adequate settling. Little to no volume loss via infiltration due to impervious or highly impermeable base. Vegetation may or may not be present. If treating a smaller area (<20 impervious acres), it is likely a **settling basin**.	PARTICLE CAPTURE

Structural BMP Type	Other Names	Description	Treatment Processes
Dry Basin	*Extended Detention Basin* *Dry Pond* *Pervious Detention Pond*	A flow-through basin with discrete inlets and outlets designed to detain stormwater runoff for some minimum time to reduce peak flows. Design treatment capacity and draw down time will vary across specific BMPs. One or more outflow offices may exist but there is at least one at base of basin to allow complete draining between storms. Increased draw down times can increase particle capture via settling within the basin. Footprint is pervious and infiltration capacity of base maintained to consistently infiltrate some fraction of volumes detained to unsaturated zone. Wetland and riparian vegetation species distribution is minimal to absent. Moderate distribution of grass and/or tree species likely and acceptable. If treating a smaller area (<20 impervious acres), it is likely a **bioretention**.	INFILTRATION PARTICLE CAPTURE
Infiltration Basin	*Large-Scale Infiltration Feature*	A flow-through BMP with highly permeable substrate (aggregate or rock) designed to store and infiltrate significant volumes of stormwater into unsaturated zone. Little to no surface detainment storage. Vegetation distribution should be minimal and preferably absent. May be confined space but not usually. If treating a smaller area (<20 impervious acres), it is likely an **infiltration feature**.	INFILTRATION
Media Filter	*Proprietary Subsurface Filtration Systems:* *Stormfilter®* *Perk Filter™* *Jellyfish®*	A proprietary subsurface flow-through structure that uses a membrane or other media to actively filter stormwater to remove stormwater pollutants. Proprietary models include media or membranes that may be selected to target the specific removal of the pollutants of concern, resulting in downgradient stormwater concentration reductions. Filtration is controlled by the flow rate through the media and discharge via an underdrain or outlet. Little to no volume loss occurs.	MEDIA FILTRATION

		May be confined space but not always. If treating a smaller area (<20 impervious acres), it is likely a **filtration device**.	

STRUCTURAL BMP TYPE	OTHER NAMES	DESCRIPTION	TREATMENT PROCESSES
Treatment Vault	*Hydrodynamic Separator (e.g. Vortechs, CDS®, DVS)* *Wet Vault* *Detention Vault* *Flow Separation Vault* *Gross Solids Retention Devices* *Large Scale Settling Basins*	A subsurface flow-through structure that physically separates sediment, trash, leaf litter, debris and other particulate pollutants from stormwater via various separation or settling techniques. No volume reduction occurs due to impervious base. May be confined space but not always. Accumulation of material at base of BMP can be observed and measured via manhole access. If no access points exist, the BMP can be inventoried as Confined Space and assessed based on a set maintenance interval. If treating a smaller area (<20 impervious acres), it is likely a **sediment trap**.	PARTICLE CAPTURE

Wet Basin	*Wet Pond* *Retention Pond* *Wetland Swale* *Wet Extended Retention Pond* *Stormwater Wetlands* *Constructed Wetlands*	A flow-through basin with discrete inlets and outlets designed to retain some volume stormwater runoff in a persistent pool of surface water. Designs may include additional detainment storage of stormwater for some minimum time to reduce peak flows. Wet pool capacity, treatment capacity and draw down time of treated volumes will vary across specific BMPs. One or more outflow offices may exist at different elevations. Lowest outlet elevation sets wet pool capacity. Dense vegetation is common. Dominant vegetation is wetland species and can be supplemented with riparian species with very high densities. Substrate is typically fine organic matter and silt, making volume reductions via infiltration negligible. Volume reductions, if any, occur primarily by evapotranspiration. If treating a smaller area (<20 impervious acres), it is likely a **biofiltration**.	BIO-GEOCHEMICAL CYCLING PARTICLE CAPTURE

DECENTRALIZED BMPS – TYPICALLY TREATING < 1 ACRE OF IMPERVIOUS AREA BUT UP TO 20 ACRES,
TYPICALLY ACCEPTS RUNOFF FROM A SINGLE LAND USE DRAINAGE AREA,
ASSOCIATED WITH NEW / RE-DEVELOPMENT AND ROADSIDE PROJECTS,

STRUCTURAL BMP TYPE	OTHER NAMES	DESCRIPTION	TREATMENT PROCESSES
Bio-filtration	*Lined rain garden with no infiltration* *Urban Biofilter* *Tree Box Biofilter (TreePod, Filterra)*	A vegetated BMP where stormwater is filtered through a specialized soil media and discharged via an underdrain. BMP may be lined with membrane or concrete. Outlet design requires surface ponding prior to surface outflow typically with a max ponding depth of 6”. Site designed biofiltration systems use specialized soil media ideally 18-24 inches in depth to enhance biogeochemical processes to retain and transform pollutants. Proprietary designs vary and may or may be confined space and difficult to access for inspection.	BIO-GEOCHEMICAL CYCLING PARTICLE CAPTURE

		If treating a larger area (>20 impervious acres), it is likely a **wet basin**.	
Bio-retention	*Biofilter* *Rain garden with infiltration* *Self-Retaining Areas*	A vegetated retention structure where the base of the BMP is not lined and must infiltrate volumes and allow infiltration to unsaturated zone. Designs may or may not include an underdrain. Outlet design requires surface ponding prior to surface outflow typically with a max ponding depth of 6”. Outlet design either passive surface outlet (e.g., curb cut) or piped overflow (e.g., overflow inlet and underdrain) used to allow retention and ponding. Constructed with specialized soil media ideally 18-24 inches in depth to enhance biogeochemical processes to retain and transform pollutants. Typically includes rock or aggregate subsurface reservoir under the soil media to enhance storage/infiltration. Designs may include settling forebay at inlet(s) to remove sediment. Vegetation types include species that can tolerate stormwater ponding and drought conditions. If treating a larger area (>20 impervious acres), it is likely a **dry basin**.	INFILTRATION BIO-GEOCHEMICAL CYCLING PARTICLE CAPTURE

Structural BMP Type	Other Names	Description	Treatment Processes
Bioswale	*Grass Swale* *Grass Filter Strips* *Vegetated Buffer Strips* *Bioslopes*	A flow-through area with dense vegetation coverage (>80%). Flow surface topography allows inundation of adjacent vegetated areas during storm runoff. Design includes gentle sloped flow paths and dense vegetation to promote primary stormwater surface filtration, adsorption to vegetation and settling. Biological processes include geochemical transformation and plant uptake. Infiltration performance and volume reductions may vary. These are not highly engineered systems. Size and application of bioswales can vary.	BIO-GEOCHEMICAL CYCLING INFILTRATION
Filtration Device	*Filtration Device* *Proprietary Inserts* *Catch Basin Inserts* *Drain inserts* *Inlet filters* *Decentralized Media Filter*	A proprietary flow-through structure that uses a membrane or other media to actively filter stormwater to target the specific removal of stormwater pollutants of concern, resulting in downgradient stormwater concentration reductions. Design may include the installation of an insert within the sediment trap or drop inlet structure to treat various pollutants. Examples include REM Triton Filter, CULTEC StormFilter, FlexStorm Inlet Filters, Kristar FloGard, etc. Filtration is controlled by the flow rate through the media and discharge via an underdrain or outlet. Little to no volume loss occurs. May be confined space but not always. If treating a larger area (>20 impervious acres), it is likely a **media filter**.	MEDIA FILTRATION
Infiltration Feature	*Infiltration Trench* *Dry Well* *Exfiltration Trench* *Percolation Trench* *French Drain* *Roof Drip-Line*	A small-scale structure designed to retain stormwater from small impervious drainage area and infiltrate into unsaturated zone. Land surface modified to sustain maximum infiltration rates, typically consisting of vertical excavation of native soils and filling with coarse drain rock or other highly permeable material. Vegetation is absent. May be confined space but not usually. If treating a larger area (>20 impervious acres), it is likely an **infiltration basin**.	INFILTRATION

STRUCTURAL BMP TYPE	OTHER NAMES	DESCRIPTION	TREATMENT PROCESSES
Pervious Pavement	*Permeable Pavement* *Porous Asphalt* *Pervious Concrete* *Porous Aggregate* *Pervious Pavers* *Permeable Pavers*	Use of sustainable materials to create a durable, pervious surface overlaying a crushed stone base that allow stormwater to percolate and infiltrate into the underlying soil. Porous pavement can include an underlying reservoir to increase infiltration rates. Footprint of structural BMP type can vary greatly, typically used for parking lots, sidewalks, driveways or other hardscaped surfaces. When stormwater is routed to pervious pavement for treatment through infiltration, the pervious pavement is considered a structural BMP and should be inventoried in BMP RAM. When pervious pavement is solely treating the precipitation falling on the pavement, it is considered part of LID design and should be included in Parcel RAM condition observations.	INFILTRATION
Sediment Trap	*Catch Basin with sump,* *Sediment Chamber,* *Vertical CMP,* *Small Hydrodynamic Separators,* *Bubble Up*	A small decentralized BMP designed to capture and retain sediment, leaf litter, trash, coarse particles and/or other stormwater pollutants. Capture of material may occur through variable flow modifications or passive settling, but result is vertical accumulation of material at base of BMP reservoir with regular material cleanout required. Minimal to no stormwater volume reduction occurs. Water quality improvement downgradient expected as result of concentration reduction due to material capture within BMP. May be confined space but not always. Typically accepts runoff from road or a parking lot. If treating a larger area (>20 impervious acres), it is likely a **treatment vault**.	PARTICLE CAPTURE
Settling Basin	*Settling Pond,* *Sediment Basin* *Decant Pond* *Concrete Forebay* *Forebay*	Open flow-through structures used to detain stormwater volumes and settle particulate pollutants prior to outflow. Pollutant load reductions are realized by concentration reductions with no volume reduction via infiltration due to impervious or highly impermeable base. May be confined space but not usually. Size and application of settling basins can vary: • Large scale settling basin draining a mixed land use area can be classified and assessed as a **treatment vault.** • Smaller sized settling basins draining a single land use area can be classified and assessed as a **sediment trap**. • If treating a larger area (>20 impervious acres), it is likely a **detention basin**.	PARTICLE CAPTURE

Appendix C

Catchment attributes and routing.

Catchment ID	Area (acres)	Discharge Point Type	Receiving Water	Terminal Catchment	Connectivity (%)	Impervious (%)	Primary Soil Group	Average Slope
Vallejo								
DT5	62.6	Discrete	Mare Island Strait	DT6	100	76.9	D	5.2
LC13	70.7	Distributed	Blue Rock Springs Creek		100	42.1	D	4.4
GC8	104.4	Distributed	Carquinez Strait		100	28.1	C	19.7
LC43	59.6	Discrete	Napa River	LC44	100	47.2	D	6.3
SA41	35.8	Distributed	Mare Island Strait	SA55	100	66.8	C	1
SP9	30.6	Distributed	White Slough		100	57.5	D	0.9
WC4	31	Discrete	American Canyon Creek	WC7	100	13.4	D	22.1
LC15B	34.7	Distributed	Rindler Creek		100	64	C	3.6
MI24	41	Distributed	Mare Island Strait		100	59.8	C	1.5
DT4	39.4	Distributed	Mare Island Strait		100	73.1	D	4.2
LC17	67.7	Discrete	Rindler Creek	LC19B	100	33.6	D	31.5
MI11	22.7	Distributed	Napa River		100	58.9	D	15.5
SA19	50.4	Discrete	Mare Island Strait	SA55	100	60.6	C	6.2
SA51	57.8	Discrete	Mare Island Strait	SA55	100	65.6	C	2.1
LC59	130.9	Distributed	Sulphur Springs Creek		100	0.1	A	24.8
SP14	30.2	Distributed	Napa River		100	54.1	C	1.5
CP13	51.1	Distributed	Southhampton Bay		100	0	D	26.5
MI23	206.3	Distributed	Napa River		100	60.8	D	0.4
LC19B	41.1	Discrete	Rindler Creek	LC19B	100	73.7	D	19.1
AC27B	10.6	Distributed	Napa River	AC5	100	56.9	C	6.1
SP5B	102.1	Distributed	San Pablo Bay		100	48	C	4.2
AC14	55.8	Distributed	Napa River	AC5	100	71.3	C	1.3
AC15	23.1	Discrete	Napa River	AC5	100	72.3	C	0.5
AC16	48	Distributed	Napa River	AC5	100	52.7	D	7.2
AC17	29.5	Discrete	Napa River	AC5	100	52.1	D	9.1
AC18	65.4	Discrete	Napa River	AC5	100	55.3	C	5.4
AC20	54.6	Discrete	Napa River	AC5	100	71	C	1.1
AC31	31.2	Discrete	White Slough	AC31	100	70.7	C	1.7
AC21	51.4	Discrete	White Slough	AC31	100	62.7	D	9.6
DT3	37	Discrete	Mare Island Strait		100	68.9	D	4.9
CP11	97.4	Distributed	Southhampton Bay	CP12	100	3.2	C	17.2
LS18	25.6	Distributed	Lake Dalwigk	LS31	100	71.7	C	4.6
SA3	25.8	Distributed	Mare Island Strait	SA55	100	51.5	C	3.5
SA56	24.1	Discrete	Mare Island Strait	SA55	100	71.2	D	6.1
AC10B	47.6	Discrete	Napa River		100	68.5	D	6.4
DT6	16.2	Discrete	Mare Island Strait	DT6	100	59.1	D	1.5
DT7	42.1	Discrete	Mare Island Strait		100	60.1	D	9.6
SA25	20.4	Distributed	Mare Island Strait		100	60.8	C	0.8
GC1A	99.7	Discrete	Carquinez Strait		100	40.6	D	25.7
GC10	79.5	Distributed	Carquinez Strait		100	28.3	D	16.8
GC11	48.9	Discrete	Carquinez Strait	GC4A	100	46.4	D	14.9
GC12	47.7	Distributed	Carquinez Strait		100	54.9	D	20.9
LC58	17.2	Discrete	Rindler Creek	LC20B	100	76.2	D	17.3
AC41	52.9	Discrete	Napa River	AC5	100	71.1	D	0.3
LC4B	61.3	Distributed	Blue Rock Springs Creek		100	54.2	D	12.6
LC37B	54	Distributed	Lake Chabot		100	72.9	D	8.6

GC1B	77.8	Discrete	Carquinez Strait	GC1C	100	48.8	D	17.1
GC1C	51	Discrete	Carquinez Strait	GC1C	100	58.4	D	19.3
LC20B	102.7	Discrete	Rindler Creek	LC20B	100	57.8	D	13.9
CP4B	94.1	Discrete	Southhampton Bay	CP5	100	25.1	D	21.8
SA14	31.2	Discrete	Mare Island Strait	SA55	100	66.5	C	1.3
SA16	42.9	Discrete	Mare Island Strait	SA55	100	63.7	D	16.4
LS7	34.6	Distributed	Mare Island Strait		100	56	D	16.2
LS8	66.5	Distributed	Mare Island Strait		100	55.4	D	13
MI10	35.7	Distributed	Mare Island Strait		100	28	D	26.8
SA50	45.9	Discrete	Mare Island Strait	SA55	100	68.6	C	1.5
SA52	25.5	Discrete	Mare Island Strait	SA55	100	72.5	C	1.9
SA53	27.7	Distributed	Mare Island Strait		100	69.5	D	6.2
SA54	31.5	Distributed	Mare Island Strait		100	71.7	D	5.3
SA55	42.3	Discrete	Mare Island Strait	SA55	100	72.2	C	1.8
SA59	30.2	Discrete	Mare Island Strait	SA55	100	77.9	C	1.3
SA62	33.9	Discrete	Mare Island Strait	SA55	100	55.6	D	16.1
SA63	28.4	Distributed	Mare Island Strait		100	71.5	C	1
SA64	21.3	Discrete	Mare Island Strait		100	73.7	C	0.8
SA7	36	Distributed	Mare Island Strait		100	62.1	D	14.5
SA8	45.8	Discrete	Mare Island Strait	SA55	100	57.5	D	10.5
AC53	51.6	Distributed	White Slough		100	79.9	D	0.4
AC36	27.8	Distributed	Napa River		100	57.9	D	12.6
AC37	24	Distributed	Napa River	AC5	100	71.9	C	2.6
AC38	28.2	Distributed	Napa River	AC5	100	57.7	C	1.9
AC39	35.5	Discrete	Napa River	AC5	100	53.1	D	14
AC5	42.9	Discrete	Napa River	AC5	100	34.3	D	0.9
AC55	23.3	Discrete	Napa River	AC5	100	67.4	C	0.7
AC7	61.4	Discrete	Napa River	AC5	100	69.2	C	1.2
MI20	51.4	Distributed	Mare Island Strait		100	44.6	C	3.7
DT11	26.6	Discrete	Mare Island Strait	DT11	100	62.9	D	6.9
AC50	70.9	Distributed	White Slough	AC51	100	78.6	D	0.4
AC51	15.6	Discrete	White Slough	AC51	100	86.2	D	0.5
AC52	21.1	Distributed	Napa River	AC5	100	67.6	D	0.5
DT2	23	Discrete	Mare Island Strait	DT2	100	74.8	D	1.6
AC13	46.2	Distributed	Napa River	AC5	100	61.3	C	2
AC1	26.7	Discrete	Mare Island Strait	SA55	100	67.8	C	1
AC10A	70.3	Discrete	Napa River	AC5	100	66.9	C	4
AC12	53.7	Distributed	Napa River	AC5	100	75.5	D	4.5
AC22	75.9	Discrete	White Slough	AC31	100	63.1	D	9.3
AC23	27.6	Distributed	White Slough	AC31	100	58.1	D	9.3
AC24	47.6	Distributed	Napa River		100	61.9	D	5.4
AC25	45.9	Distributed	Napa River		100	55.1	D	8.6
AC26	85	Discrete	Napa River		100	61.8	D	8.6
AC27A	56.8	Discrete	Napa River	AC5	100	67.6	C	2.7
AC28	63.3	Discrete	White Slough	AC31	100	60.7	D	11.2
AC29	72.7	Discrete	White Slough	AC31	100	64.8	D	11.6
AC3	47.8	Discrete	Mare Island Strait	SA55	100	64.2	C	1.3
AC30	63	Discrete	White Slough	AC31	100	59.1	C	4.9
AC32	60.8	Discrete	White Slough	AC31	100	67.8	C	2.7
AC34	59.7	Distributed	White Slough	AC31	100	70.4	C	4.7
AC35	52.8	Distributed	Napa River	AC5	100	80.6	C	0.4
AC40	66.6	Distributed	Napa River	AC5	100	39.4	D	9.7
AC42	45.9	Distributed	Napa River		100	50.4	D	9.9
AC44	42	Distributed	Napa River	AC5	100	36	D	3.6
AC8	78.7	Distributed	Napa River	AC5	100	59.7	C	1.7

AC45	48	Discrete	Napa River	AC5	100	57.5	D	2.5
AC46	49	Distributed	White Slough		100	79.2	D	1
AC47	38.8	Discrete	White Slough	AC31	100	58.4	C	0.8
AC48A	148.3	Distributed	White Slough		100	15.9	D	0.4
CP1	124.4	Discrete	Southhampton Bay		100	38.2	D	20.2
CP10	85.8	Discrete	Southhampton Bay	CP12	100	42.8	D	13.2
CP12	125.7	Discrete	Southhampton Bay	CP12	100	43.6	D	11.2
CP2	41.3	Distributed	Southhampton Bay		100	56.1	D	11.8
CP3	65.3	Distributed	Southhampton Bay	CP12	100	45.6	D	17.1
CP4A	70.4	Discrete	Southhampton Bay	CP5	100	41	D	20.6
DT12	67.8	Discrete	Mare Island Strait	DT11	100	69.3	D	4.8
CP5	76	Discrete	Southhampton Bay	CP5	100	55	D	15
CP7	64.6	Distributed	Southhampton Bay	CP5	100	15.3	D	16.9
CP8	66.7	Discrete	Southhampton Bay	CP5	100	18.3	D	15.9
CP9	63.4	Discrete	Southhampton Bay	CP12	100	57	D	12.6
DT1	46	Discrete	Mare Island Strait	DT2	100	74.6	D	9.5
GC2A	84	Discrete	Carquinez Strait		100	57.7	D	13.5
GC3	87.2	Discrete	Carquinez Strait	GC1C	100	35.2	D	24.1
GC4A	95.3	Discrete	Carquinez Strait	GC4A	100	42.2	D	17.5
GC6	55.8	Discrete	Carquinez Strait		100	36.6	C	18
GC7	36.5	Distributed	Carquinez Strait	GC4A	100	2.5	C	26.8
LC12A	81	Discrete	Rindler Creek		100	61.9	D	10.4
LC1A	199.9	Distributed	Blue Rock Springs Creek		100	8.7	D	18.2
LC10	25.4	Distributed	Rindler Creek		100	62.5	D	5.5
LC11	23.7	Distributed	Rindler Creek		100	70.2	C	7.2
LC18	200.8	Distributed	Rindler Creek		100	1.7	A	27.4
LC19A	121.3	Distributed	Rindler Creek		100	3.5	D	26.9
LC20A	105.8	Distributed	Rindler Creek		100	4.7	D	22.9
LC21	249.9	Distributed	Rindler Creek		100	11.2	D	20.7
LC22	98.9	Distributed	American Canyon Creek		100	1.3	D	22.3
LC24	113.7	Distributed	American Canyon Creek		100	35.7	D	16.7
LC26A	108.4	Discrete	Blue Rock Springs Creek	LC34A	100	49.6	D	18.8
LC35	19.8	Discrete	Lake Chabot	LC34	100	63.6	D	4.6
LC36	62.3	Discrete	Rindler Creek		100	63.1	D	17.1
LC27	144.7	Distributed	Lake Chabot		100	47.8	C	2.1
LC3A	61.8	Discrete	Blue Rock Springs Creek	LC34A	100	57.5	D	16
LC31	85.8	Discrete	Lake Chabot	LC34	100	59.7	D	12.3
LC32	46.9	Discrete	Lake Chabot	LC34	100	66.5	C	10.7
LC33	29.3	Discrete	Lake Chabot	LC34	100	60.8	C	4.4
LC34	54.2	Discrete	Lake Chabot	LC34	100	60.3	C	3.2
LC44	90.2	Distributed	Napa River	LC44	100	57.5	C	3
LC45	53.4	Discrete	Napa River	LC44	100	65.9	D	5.8
LC56	38.3	Discrete	Blue Rock Springs Creek	LC50	100	80.9	D	16.1
LC46	83.3	Distributed	White Slough	LC38	100	60.2	D	14
LC47	54	Discrete	White Slough	LC38	100	73.9	C	1.2
LC48	33	Discrete	Rindler Creek	LC19B	100	75.5	D	20.3
LC49	31.7	Discrete	Rindler Creek	LC19B	100	71.4	D	14.7
LC5	50.5	Distributed	Blue Rock Springs Creek		100	57.6	D	14.2
LC50	53.5	Discrete	Blue Rock Springs Creek	LC50	100	77.2	D	19.3
LC51	38.9	Discrete	Blue Rock Springs Creek	LC51	100	82	D	20.5
LC52	34.3	Discrete	Blue Rock Springs Creek	LC51	100	74.1	D	20.1
LC6	86.1	Distributed	Blue Rock Springs Creek		100	42.4	D	17.5
LC8	32.4	Distributed	Blue Rock Springs Creek		100	76.8	C	3.6
LS1	66.6	Discrete	Mare Island Strait		100	55.2	D	14.4
LS10	57.5	Discrete	Mare Island Strait		100	66.6	D	6.5

LS11	30.6	Discrete	Lake Dalwigk		100	51	D	9.1
LS12	24.2	Discrete	Lake Dalwigk		100	47.4	D	12.9
LS13	41.1	Discrete	Lake Dalwigk	LS31	100	51.8	D	11.2
LS14	52.1	Discrete	Lake Dalwigk	LS31	100	44	D	10
LS15	35.3	Discrete	Lake Dalwigk	LS31	100	44.6	D	12.2
LS16	39.1	Discrete	Lake Dalwigk	LS31	100	59.1	D	7
LS23	97.5	Distributed	Lake Dalwigk	LS31	100	44.1	D	5.6
MI12	23.5	Discrete	Mare Island Strait	DT11	100	63.3	D	11
LS19	70.6	Distributed	Carquinez Strait		100	56.9	D	11.7
LS20	55.6	Distributed	Lake Dalwigk	LS31	100	38.8	D	8.4
LS21	50.6	Discrete	Lake Dalwigk	LS31	100	53.3	D	8.1
LS22	85.8	Discrete	Lake Dalwigk	LS31	100	49	D	8
LS24	42.4	Distributed	Lake Dalwigk	LS31	100	55	D	6.7
LS25	34.2	Discrete	Lake Dalwigk	LS31	100	61.4	D	6.6
LS26	53.8	Discrete	Lake Dalwigk	LS31	100	57.1	D	5.8
LS27	38.8	Distributed	Lake Dalwigk	LS31	100	58.3	D	6
LS29	34.7	Distributed	Lake Dalwigk	LS31	100	70	C	3.8
LS3	37.7	Discrete	Mare Island Strait		100	61.4	D	9.8
LS4	45.4	Distributed	Mare Island Strait		100	55.3	D	6.2
LS30	64.7	Distributed	Lake Dalwigk	LS31	100	71.7	C	1.7
LS31	24.5	Discrete	Lake Dalwigk	LS31	100	72.1	C	2.6
LS32	18.5	Distributed	Lake Dalwigk	LS31	100	52.4	D	9.2
LS33	79.4	Discrete	Lake Dalwigk		100	65.2	C	2.9
LS34	21.7	Distributed	Mare Island Strait		100	70.1	D	5
LS36	59.4	Distributed	Lake Dalwigk		100	40.5	C	3.3
LS37	35.5	Distributed	Mare Island Strait		100	66.6	C	1.2
SA13	29.5	Discrete	Mare Island Strait	SA55	100	64.9	C	1.9
MI4	26.7	Discrete	Mare Island Strait	MI4	100	45.8	D	18.6
MI17	50.5	Distributed	Napa River		100	52.1	D	14.6
MI13	20.5	Distributed	Napa River		100	49.4	D	16.8
MI15	47.6	Distributed	Napa River		100	57.2	D	7.7
MI16	47.1	Distributed	Napa River		100	49.7	D	4
MI18	37.9	Discrete	Mare Island Strait	MI18	100	31	D	4.7
MI2	29.5	Distributed	Mare Island Strait		100	32.9	D	24.1
MI3	75.3	Discrete	Mare Island Strait	MI4	100	44.4	D	22.3
SA18	20.5	Discrete	Mare Island Strait	SA55	100	68.4	C	6.4
MI6	76.9	Discrete	Mare Island Strait		100	52.3	D	12.7
MI7	76.7	Discrete	Mare Island Strait	MI18	100	60.6	D	8.5
MI8	68.2	Discrete	Mare Island Strait		100	68.4	C	2.7
SA10	67.2	Discrete	Mare Island Strait	SA55	100	39.3	D	15
SA11	26.2	Discrete	Mare Island Strait	SA55	100	53.5	D	12.3
SA12	46.6	Discrete	Mare Island Strait	SA55	100	61.4	C	3.8
SA17	68.7	Discrete	Mare Island Strait	SA55	100	57.1	D	17.5
SA2	53.4	Discrete	Mare Island Strait	SA55	100	41.8	D	12.1
SA21	52.2	Discrete	Mare Island Strait	SA55	100	55.4	D	11.9
SA22	90.9	Discrete	Mare Island Strait	SA55	100	48.4	D	12.5
SA23	31	Distributed	Mare Island Strait	SA55	100	53.1	C	2.5
SA24	37	Distributed	Mare Island Strait	SA55	100	52.9	C	5.3
SA26	56.8	Distributed	Mare Island Strait	SA55	100	54.1	C	4.9
SA27	47	Discrete	Mare Island Strait	SA55	100	51.9	D	5.6
SA29	58.7	Discrete	Mare Island Strait	SA55	100	61.2	C	1.1
SA31	48.4	Discrete	Mare Island Strait	SA55	100	70.5	C	1
SA32	41.9	Discrete	Mare Island Strait	SA55	100	63.7	C	3.5
SA37	59.1	Discrete	Mare Island Strait	SA55	100	56.6	D	11.7
SA38	30.3	Discrete	Mare Island Strait	SA55	100	58.2	C	5.7

SA39	70.1	Distributed	Mare Island Strait	SA55	100	60.2	D	13.2
SA4	22.9	Distributed	Mare Island Strait	SA55	100	59.1	C	2.3
SA40	34.4	Distributed	Mare Island Strait	SA55	100	71.7	C	6.5
SA42	65.1	Distributed	Mare Island Strait	SA55	100	57	C	1.4
SA43	36.6	Discrete	Mare Island Strait	SA55	100	57.6	D	6
SA44	43.4	Discrete	Mare Island Strait	SA55	100	45.4	D	4.4
SA6	29.6	Discrete	Mare Island Strait	SA55	100	64	C	2.2
SA45	37.1	Distributed	Mare Island Strait	SA55	100	47.7	D	4.5
SA46	50.3	Distributed	Mare Island Strait	SA55	100	59.3	D	4.4
SA48	14.6	Discrete	Mare Island Strait	SA55	100	70.8	C	0.8
SA49	51.9	Discrete	Mare Island Strait	SA55	100	51.7	C	1.2
SA5	62.1	Distributed	Mare Island Strait	SA55	100	61.1	C	5.1
SA9	73.6	Discrete	Mare Island Strait	SA55	100	55.8	D	8
SP1A	54.8	Discrete	Napa River		100	37.1	D	7
SP11	48.1	Distributed	Napa River		100	71.7	C	1.5
SP12	53.6	Distributed	Napa River		100	71.6	C	0.6
SP13	84.8	Distributed	Napa River		100	63.8	C	0.9
SP2A	73.8	Distributed	Napa River	SP7	100	33.4	D	1.4
SP3A	29.5	Discrete	Napa River	SP7	100	42.4	C	0.6
SP5A	78.2	Discrete	Napa River	SP7	100	48	C	0.6
SP6A	78.1	Discrete	Napa River	SP7	100	20.8	D	1.2
SP7	58.7	Discrete	Napa River	SP7	100	63.6	C	0.7
SV1A	247.6	Distributed	Sulphur Springs Creek		100	11.6	A	19
SWANZY	20.4	Distributed	Mare Island Strait		100	53.4	D	13.5
WC1	49.3	Discrete	American Canyon Creek	WC7	100	61.6	D	7.4
GC13	79.5	Distributed	Carquinez Strait		100	4.1	C	20.1
WC2	29.1	Discrete	American Canyon Creek	WC7	100	60.6	D	4.5
WC3	50.9	Discrete	American Canyon Creek	WC7	100	36.2	D	14.2
WC5	52.4	Distributed	American Canyon Creek		100	1.3	D	21
SV4	142.1	Distributed	Sulphur Springs Creek		100	0	A	26.1
WC6	101.1	Distributed	American Canyon Creek	WC7	100	54.6	C	7.4
WC8	51.2	Distributed	American Canyon Creek	WC7	100	0.7	D	26.4
SV3	310.4	Distributed	Sulphur Springs Creek		100	0	A	26.6
SP6B	395.8	Distributed	San Pablo Bay		100	20.8	D	10.6
AC56	213.2	Distributed	White Slough		100	6.7	D	0.3
SP15	93.5	Distributed	Napa River		100	12.9	D	0.6
MI22	105.5	Distributed	Napa River		100	39	C	1.2
LC63	163.5	Distributed	Rindler Creek		100	1.4	D	20.4
SP16	140.4	Distributed	Napa River		100	7.8	D	0.7
LC60	273.7	Distributed	Sulphur Springs Creek		100	0	A	23
MI25	51.3	Distributed	Mare Island Strait		100	61	C	2.1
MI26	195.7	Distributed	Mare Island Strait		100	70.1	D	2.3
SV2C	271.7	Distributed	Sulphur Springs Creek		100	1.9	A	25.5
SV2A	75	Discrete	Sulphur Springs Creek		100	24.3	C	14.6
SV2D	50.4	Distributed	Sulphur Springs Creek		100	17.1	C	19.2
SV1B	255.7	Distributed	Sulphur Springs Creek		100	11.5	A	20.2
SV1C	83.9	Distributed	Sulphur Springs Creek		100	16.9	A	19.7
LC1B	135.9	Distributed	Blue Rock Springs Creek		100	9.7	D	16.6
LC1C	119.4	Distributed	Blue Rock Springs Creek		100	19	D	10.4
LC61	66	Distributed	American Canyon Creek		100	2.4	C	27.5
LC62	109.1	Distributed	American Canyon Creek		100	0	A	23.1
AC48B	137.9	Distributed	White Slough		100	6.1	D	0.3
CP4C	31.9	Distributed	Southhampton Bay	CP5	100	47.8	D	21.1
GC4B	79.6	Distributed	Carquinez Strait		100	48.6	D	14.5
LC26B	63	Discrete	Blue Rock Springs Creek	LC34A	100	65.4	D	13.8

LC12B	79.5	Discrete	Rindler Creek		100	51.7	D	7.2
LC3B	35.8	Discrete	Blue Rock Springs Creek	LC34A	100	54.6	D	17.3
LC4C	52	Distributed	Blue Rock Springs Creek		100	45.3	D	20.8
GC2B	48.5	Discrete	Carquinez Strait		100	46.5	D	13.8
LC4D	48.4	Distributed	Blue Rock Springs Creek		100	47.4	D	16.9
SP1B	161	Distributed	San Pablo Bay		100	37.1	D	0.3
M121	275.7	Distributed	Mare Island Strait		100	30.4	D	11.7
SP3B	35.5	Distributed	San Pablo Bay		100	42.4	C	1.3
LC16	58.3	Discrete	Rindler Creek		100	76.8	D	13.3
LC14	46.7	Distributed	Rindler Creek		100	37	C	2
LC15A	109.5	Discrete	Rindler Creek		100	71.6	D	8
LC23	62	Distributed	American Canyon Creek		100	25.6	D	21.8
LC37A	189.6	Distributed	Lake Chabot		100	37	D	8.1
LC39	44.9	Distributed	Lake Chabot		100	71.2	D	12.2
LC4A	82	Distributed	Blue Rock Springs Creek		100	44.6	D	17.3
LC38	72.3	Discrete	White Slough	LC38	100	49.9	C	9.3
LC40	53	Distributed	Napa River	LC44	100	64.1	D	10.5
LC42	47.1	Distributed	Napa River	LC44	100	69	D	7.3
LC7	33.4	Distributed	Blue Rock Springs Creek		100	68.1	D	8.2
LS35	54.4	Distributed	Mare Island Strait		100	57.7	C	3.1
LC55	25	Discrete	Blue Rock Springs Creek		100	64.7	D	17.5
LC9	28.6	Distributed	Rindler Creek		100	69.4	D	13.7
MI5	35.4	Discrete	Mare Island Strait		100	47.2	D	20.5
SA1	20.1	Distributed	Mare Island Strait		100	47	D	9.7
SA35	56.4	Discrete	Mare Island Strait	SA55	100	60.7	C	1.6
SP10	21.1	Distributed	Napa River		100	56.8	C	1.1
MI27	166.8	Distributed	Napa River		100	79.3	D	1.1
LC3C	57.9	Discrete	Blue Rock Springs Creek	LC34A	100	42.6	D	22.7
DT10	23.9	Discrete	Mare Island Strait	DT11	100	63.1	D	6.6
GC5	55.5	Discrete	Carquinez Strait		100	41.4	C	14.9
SA15	30.6	Distributed	Mare Island Strait	SA55	100	65.7	C	1.5
SV2B	239.6	Distributed	Sulphur Springs Creek		100	15.5	A	18.7
WC7	56.5	Discrete	American Canyon Creek	WC7	100	43.9	C	7
SV2E	26.1	Distributed	Sulphur Springs Creek		100	5.6	D	10.9
SP4	73.2	Discrete	San Pablo Bay		100	36.6	D	1.1
SP2B	128	Distributed	San Pablo Bay		100	33.4	D	0.5
Fairfield								
JAM-1	50.8	distributed	Jameson Creek		100	28	C	5.1
AMER-1	107.6	discrete	American Canyon Creek		100	38.1	D	3.3
DAN-1	76.2	distributed	Dan Wilson Creek		100	45.2	D	1.3
ALZ-1	54.5	distributed	Alonzo Creek	ALZ-1	100	58.7	A	0.4
FREE-2	63.5	discrete	Freeborn Creek		100	55.6	A	2.3
AMER-3	81.9	discrete	American Canyon Creek		100	39.2	D	1.2
GRN-25	46.3	discrete	Green Valley Creek	GRN-11	100	47.4	D	9.6
GRN-26	51.4	distributed	Green Valley Creek		100	10	D	1
ALZ-4	31.5	distributed	Alonzo Creek		100	5.9	D	0.3
LED-7	45.7	discrete	Ledgewood Creek	LED-5	100	58.3	A	0.6
LED-4	47.8	discrete	Ledgewood Creek	LED-4	100	72.5	D	1
GRN-20	27.1	discrete	Green Valley Creek	GRN-21	100	33.4	D	13.3
AMER-5	122.2	distributed	American Canyon Creek		100	0.1	D	17.3
COY-22	94.5	distributed	McCoy Creek		100	69.2	A	0.6
ALZ-18	124.5	discrete	Alonzo Creek		100	43.5	D	13.1
COY-8	29.3	discrete	McCoy Creek	COY-3	100	54.8	D	1.2
COY-12	93.6	distributed	McCoy Creek		100	60.7	D	0.3
MAR-16	83.8	distributed	Marsh 1		100	0.4	D	0.5

LED-19	86.3	discrete	Ledgewood Creek	LED-22	100	11.8	A	20
COY-21	97.6	distributed	McCoy Creek		100	14.9	D	0.9
ALZ-29	39.7	distributed	Alonzo Creek		100	9.4	D	13.4
DAN-9	61	distributed	Dan Wilson Creek		100	18.4	C	4.6
COY-29	159.6	distributed	McCoy Creek		100	0.8	D	12.7
GRN-27	29.7	distributed	Green Valley Creek		100	51.5	A	1
JAM-6	76	distributed	Jameson Creek		100	1.2	C	17.3
SODA-34	54.3	distributed	Soda Springs Creek		100	59.7	C	3.2
UNI-5	354.9	distributed	Union Creek		100	1.6	D	4.4
COY-2	104.8	distributed	McCoy Creek		100	51.3	D	0.7
LED-1	80	discrete	Ledgewood Creek	LED-5	100	63.5	A	0.6
SODA-1	92.6	distributed	Soda Springs Creek		100	72.5	A	0.4
LAU-25	49.5	distributed	Laurel Creek	LED-23	100	51.9	D	5.8
AMER-4	37.6	distributed	American Canyon Creek		100	29.3	D	3.8
COY-3	46.4	discrete	McCoy Creek	COY-3	100	55.4	D	1.4
LED-2	103	discrete	Ledgewood Creek	LED-4	100	65.6	D	0.5
LAU-19	43.4	discrete	Laurel Creek		100	52.3	D	2.2
LAU-1	93.9	discrete	Laurel Creek	LED-23	100	54.9	D	0.8
SODA-2	80.1	discrete	Soda Springs Creek	SODA-25	100	55.7	A	0.8
COY-1	68.2	discrete	McCoy Creek	COY-3	100	56.1	D	1.2
LED-3	56.6	distributed	Ledgewood Creek	LED-22	100	28.2	A	16.6
LAU-2	75.4	discrete	Laurel Creek		100	24.9	C	5.6
COY-4	36	distributed	McCoy Creek		100	27.9	D	1.3
LAU-3	80.1	distributed	Laurel Creek		100	44.2	D	0.7
LAU-4	94.5	discrete	Laurel Creek		100	61.6	D	0.6
LAU-35	52.7	discrete	Laurel Creek	LED-23	100	57.8	A	0.7
ALZ-2	89.5	discrete	Alonzo Creek	ALZ-8	100	58.7	A	2.8
COY-20	72.8	distributed	McCoy Creek		100	18.8	C	2.1
LAU-5	108.5	discrete	Laurel Creek	LED-23	100	61.4	D	1
SODA-3	75.6	discrete	Soda Springs Creek	SODA-25	100	63.8	D	5.3
COY-5	125.4	distributed	McCoy Creek		100	1.2	D	0.7
LAU-6	106.7	distributed	Laurel Creek		100	60.1	D	1.2
SODA-4	88.7	distributed	Soda Springs Creek	LED-23	100	37.2	D	8.4
LAU-7	58.8	discrete	Laurel Creek		100	47.9	B	9.2
ALZ-3	111.5	discrete	Alonzo Creek		100	6.8	C	25.1
SODA-5	64.5	discrete	Soda Springs Creek		100	26.9	D	18.6
ALZ-23	42.3	discrete	Alonzo Creek		100	12	C	21.2
LAU-8	58.4	discrete	Laurel Creek		100	41.2	D	6
LAU-9	66.7	discrete	Laurel Creek		100	13.7	D	7.3
AMER-2	237.5	distributed	American Canyon Creek		100	0	D	25
GRN-1	110.7	distributed	Green Valley Creek		100	12.9	D	15.2
GRN-13	76.1	discrete	Green Valley Creek	GRN-11	100	57.8	A	1
GRN-2	70.3	distributed	Green Valley Creek		100	40.6	C	1.5
SODA-6	130	distributed	Soda Springs Creek		100	18.5	C	18.6
GRN-18	97.8	distributed	Green Valley Creek		100	0.2	D	32.5
GRN-6	46.6	discrete	Green Valley Creek	GRN-6	100	47	D	0.9
MAR-3	126.7	distributed	Marsh 1		100	39.2	D	0.6
SODA-7	50.8	distributed	Soda Springs Creek		100	34.2	A	3.5
FREE-1	128.3	discrete	Freeborn Creek		100	24	D	3.5
FREE-3	58.4	discrete	Freeborn Creek		100	36.7	D	6.8
FREE-4	43.2	discrete	Freeborn Creek		100	20.6	D	5.2
GRN-14	23.8	distributed	Green Valley Creek		100	13.5	D	13.7
ALZ-6	59	discrete	Alonzo Creek	ALZ-1	100	70.6	A	0.6
JAM-2	82.5	distributed	Jameson Creek	JAM-3	100	19.6	D	1.1
UNI-2	76.4	distributed	Union Creek		100	24.9	D	0.7

JAM-3	93.9	discrete	Jameson Creek	JAM-3	100	44.9	D	1.9
DAN-2	71.9	distributed	Dan Wilson Creek		100	53.2	C	1
GRN-3	90.8	distributed	Green Valley Creek		100	61.7	A	0.9
GRN-4	129.3	distributed	Green Valley Creek		100	53.9	D	1.2
GRN-5	49.4	discrete	Green Valley Creek	GRN-6	100	60	C	1.1
GRN-7	52.4	discrete	Green Valley Creek	GRN-6	100	57.5	A	2
GRN-8	29.3	discrete	Green Valley Creek	GRN-6	100	62.4	A	2.5
GRN-19	41.3	distributed	Green Valley Creek		100	34	D	16.6
GRN-9	53	distributed	Green Valley Creek		100	52	A	0.8
GRN-10	52.3	distributed	Green Valley Creek		100	46.3	A	0.6
GRN-11	28.9	discrete	Green Valley Creek	GRN-11	100	45.8	C	0.7
GRN-12	30.8	distributed	Green Valley Creek		100	39.4	A	0.1
GRN-15	54.1	discrete	Green Valley Creek		100	34.7	D	12.1
GRN-16	23.8	discrete	Green Valley Creek		100	33	D	11.6
GRN-17	35.6	distributed	Green Valley Creek		100	5.1	D	27.8
GRN-21	34.5	discrete	Green Valley Creek	GRN-21	100	22.2	D	20
DAN-3	61	discrete	Dan Wilson Creek		100	41.4	D	10.8
DAN-4	69.3	distributed	Dan Wilson Creek		100	53.6	D	0.9
GRN-22	36.7	distributed	Green Valley Creek		100	46.1	D	3.3
DAN-5	51.2	distributed	Dan Wilson Creek		100	26.5	C	1.2
GRN-23	50.8	discrete	Green Valley Creek		100	48.6	D	5.1
GRN-24	34	discrete	Green Valley Creek		100	46.5	D	9.5
LED-5	94.7	discrete	Ledgewood Creek	LED-5	100	40.2	D	0.5
LED-6	39.4	distributed	Ledgewood Creek		100	64.2	A	0.6
COY-17	83.5	discrete	McCoy Creek		100	52.1	D	0.5
ALZ-5	90.3	distributed	Alonzo Creek		100	55.2	A	0.5
ALZ-10	72.6	distributed	Alonzo Creek	ALZ-8	100	65.4	A	2.4
LED-8	66.6	distributed	Ledgewood Creek	LED-5	100	65.4	A	0.5
ALZ-7	101	distributed	Alonzo Creek	ALZ-8	100	66.4	D	2.8
ALZ-8	99.9	discrete	Alonzo Creek	ALZ-8	100	85	A	0.9
ALZ-9	25.5	discrete	Alonzo Creek	ALZ-8	100	73.2	A	0.8
ALZ-11	48.4	discrete	Alonzo Creek	ALZ-8	100	78.5	A	1
ALZ-12	68.8	discrete	Alonzo Creek	ALZ-8	100	62.8	A	2.6
ALZ-16	102.8	distributed	Alonzo Creek		100	0.6	C	25.8
LED-9	69.2	discrete	Ledgewood Creek		100	44.8	D	0.8
LAU-20	67	discrete	Laurel Creek	LED-23	100	61.3	A	0.6
ALZ-13	69.1	distributed	Alonzo Creek		100	7.6	A	13.4
LED-10	107.3	distributed	Ledgewood Creek		100	7	D	25
COY-6	85.6	distributed	McCoy Creek		100	1.6	A	3
SODA-8	89.9	distributed	Soda Springs Creek		100	0	C	27.2
SODA-9	109.5	discrete	Soda Springs Creek		100	33.3	D	13.5
SODA-10	74.8	discrete	Soda Springs Creek		100	45.3	D	7.5
LAU-13	66.9	distributed	Laurel Creek		100	55	D	1.4
LAU-10	76.4	discrete	Laurel Creek		100	33	A	8.7
SODA-14	117.5	distributed	Soda Springs Creek		100	56.4	A	0.6
COY-7	69.3	discrete	McCoy Creek	COY-3	100	62.1	B	0.5
LAU-11	94.8	discrete	Laurel Creek	LAU-14	100	46.1	B	4.3
LAU-12	73.3	distributed	Laurel Creek		100	5.6	B	7.4
LAU-18	104	distributed	Laurel Creek		100	39	D	1.1
LAU-14	38.6	discrete	Laurel Creek	LAU-14	100	34.9	B	1.8
LED-14	35.5	distributed	Ledgewood Creek		100	0.9	D	33.3
LAU-15	76.9	distributed	Laurel Creek		100	54	A	2.9
LAU-16	31	distributed	Laurel Creek		100	44.8	B	7.7
LAU-17	76.1	distributed	Laurel Creek		100	49.4	A	1.1
LAU-21	56.9	distributed	Laurel Creek		100	60.2	D	0.9

LAU-22	84.8	distributed	Laurel Creek		100	61.3	D	0.6
LAU-23	85	discrete	Laurel Creek	LED-23	100	66.3	D	0.6
LED-12	100.3	discrete	Ledgewood Creek		100	5.9	C	24.1
SODA-11	111.2	discrete	Soda Springs Creek	SODA-11	100	66.6	D	0.7
SODA-12	66.7	discrete	Soda Springs Creek	SODA-11	100	58.2	A	0.6
UNI-1	89.7	distributed	Union Creek		100	31.9	D	0.4
SODA-13	107.6	discrete	Soda Springs Creek	SODA-11	100	72.1	A	0.9
ALZ-14	36.5	distributed	Alonzo Creek		100	35	D	0.3
MAR-14	92.6	discrete	Marsh 1	MAR-14	100	70.7	D	0.6
SODA-15	96.3	discrete	Soda Springs Creek	SODA-25	100	66.4	A	1.3
FREE-5	119	distributed	Freeborn Creek		100	0	B	18.9
AMER-6	199.7	distributed	American Canyon Creek		100	0.1	D	15.7
ALZ-15	110.9	distributed	Alonzo Creek		100	12.5	C	22.4
ALZ-17	113.9	discrete	Alonzo Creek		100	23.2	A	16.8
LED-11	124.6	discrete	Ledgewood Creek		100	7.8	A	27.1
LED-13	106.9	distributed	Ledgewood Creek		100	5.7	D	23.7
ALZ-19	77	discrete	Alonzo Creek		100	35.6	D	8.5
ALZ-20	48.3	distributed	Alonzo Creek	ALZ-8	100	23.9	A	1
SODA-20	39.5	discrete	Soda Springs Creek	SODA-25	100	39.9	A	11.7
COY-9	31	distributed	McCoy Creek		100	64.2	D	3.4
COY-10	72	distributed	McCoy Creek		100	54.7	D	0.9
COY-11	31.8	distributed	McCoy Creek		100	58.9	D	2.5
SODA-16	122.8	distributed	Soda Springs Creek		100	0.1	C	26.4
SODA-18	97.7	distributed	Soda Springs Creek	SODA-25	100	62.1	D	5.6
LED-15	71.5	distributed	Ledgewood Creek		100	24.2	D	0.6
ALZ-21	80.6	discrete	Alonzo Creek	ALZ-28	100	39.5	A	10.4
SODA-17	89.9	distributed	Soda Springs Creek		100	4.5	C	21.8
LAU-24	52.3	distributed	Laurel Creek		100	57.9	A	1
SODA-19	72.7	distributed	Soda Springs Creek	SODA-25	100	49.6	D	6.3
LED-16	73.1	discrete	Ledgewood Creek	LED-16	100	54.2	D	0.6
SODA-22	89	distributed	Soda Springs Creek	SODA-25	100	53	D	2.5
LED-17	34.3	distributed	Ledgewood Creek		100	53.9	D	0.8
LED-18	41.7	discrete	Ledgewood Creek	LED-16	100	49.9	D	0.7
COY-13	84.9	distributed	McCoy Creek		100	8.1	D	1
SODA-21	60.6	discrete	Soda Springs Creek	SODA-25	100	50.1	D	5
SODA-23	111.3	distributed	Soda Springs Creek		100	0	C	28.6
ALZ-22	64.1	distributed	Alonzo Creek		100	10.3	C	19.9
ALZ-24	54.7	distributed	Alonzo Creek		100	3.1	D	26.5
DAN-7	40.1	distributed	Dan Wilson Creek		100	45.5	C	7.8
LAU-27	93.6	distributed	Laurel Creek		100	26.1	C	2.3
LAU-28	47	distributed	Laurel Creek		100	9.7	C	2.9
ALZ-37	50.4	discrete	Alonzo Creek		100	55.9	A	0.9
DAN-8	113	distributed	Dan Wilson Creek		100	53.2	C	0.5
LAU-26	92.2	distributed	Laurel Creek		100	7.8	B	3
FREE-7	41.3	distributed	Freeborn Creek		100	64.6	D	2.2
DAN-6	86.6	distributed	Dan Wilson Creek		100	49.1	D	2
COY-14	60.9	distributed	McCoy Creek		100	48.4	B	0.5
FREE-6	118	distributed	Freeborn Creek		100	7.2	D	12.3
SODA-24	103.8	discrete	Soda Springs Creek	SODA-25	100	61.9	A	1.4
SODA-25	32.7	discrete	Soda Springs Creek	SODA-25	100	72.6	A	0.6
ALZ-35	43.3	distributed	Alonzo Creek		100	37.4	D	10.9
SODA-26	84.9	discrete	Soda Springs Creek		100	39.5	C	12
SODA-27	69.8	distributed	Soda Springs Creek		100	35.4	C	8.3
SODA-28	45.8	distributed	Soda Springs Creek		100	1.2	D	28.1
COY-15	72.5	discrete	McCoy Creek	COY-3	100	64.1	B	0.5

COY-16	48	discrete	McCoy Creek	COY-3	100	50.8	B	0.4
SODA-29	54.1	distributed	Soda Springs Creek	SODA-25	100	76.2	A	1
LAU-29	89.3	discrete	Laurel Creek	LED-23	100	53.7	D	0.9
COY-18	67.5	distributed	McCoy Creek		100	31.9	D	0.7
COY-19	99.4	distributed	McCoy Creek		100	1.4	D	1.9
LAU-30	85.1	distributed	Laurel Creek		100	36.9	D	2.5
LED-20	56.5	discrete	Ledgewood Creek	LED-22	100	25.6	D	16.2
ALZ-25	33.4	distributed	Alonzo Creek		100	0.6	A	15.5
ALZ-27	76.9	distributed	Alonzo Creek	ALZ-8	100	54.6	D	1.3
UNI-6	338.1	distributed	Union Creek		100	2.2	D	3.1
LED-21	78.7	distributed	Ledgewood Creek		100	39.5	D	0.9
SODA-31	35.8	discrete	Soda Springs Creek	SODA-25	100	54.2	A	3.3
JAM-4	93.5	distributed	Jameson Creek		100	20.9	D	5.4
ALZ-26	42.4	distributed	Alonzo Creek		100	39	D	6.2
ALZ-28	41.4	discrete	Alonzo Creek	ALZ-28	100	59.1	C	2.4
SODA-35	61.5	discrete	Soda Springs Creek	SODA-25	100	57.1	D	3.4
LED-22	39.9	discrete	Ledgewood Creek	LED-22	100	37.9	D	5.6
LED-23	55	distributed	Ledgewood Creek		100	9.4	A	20.8
SODA-30	69.5	discrete	Soda Springs Creek	SODA-25	100	62	A	1.1
ALZ-30	95.9	discrete	Alonzo Creek		100	17.1	C	18.8
SODA-32	74.9	discrete	Soda Springs Creek		100	60.3	D	0.6
ALZ-31	98.7	distributed	Alonzo Creek		100	70.8	A	0.4
LAU-31	87.8	discrete	Laurel Creek	LED-23	100	56.7	D	0.7
ALZ-32	46.4	discrete	Alonzo Creek		100	24.5	A	16.8
SODA-33	79.7	distributed	Soda Springs Creek		100	0	C	23
LAU-33	47.6	discrete	Laurel Creek		100	29.9	D	8.8
MAR-22	39.9	distributed	Marsh 1		100	2.4	D	0.2
JAM-5	73.5	discrete	Jameson Creek	JAM-3	100	45.3	D	1.3
LAU-32	40.7	discrete	Laurel Creek		100	21.7	B	17.8
LED-24	50	distributed	Ledgewood Creek		100	14.7	A	18.7
GRN-28	63.9	distributed	Green Valley Creek		100	38	D	0.5
ALZ-33	63.2	discrete	Alonzo Creek		100	37.1	A	11.9
ALZ-34	64.3	discrete	Alonzo Creek		100	52.8	D	3.4
SODA-36	55.7	discrete	Soda Springs Creek	SODA-25	100	49.7	A	0.5
LAU-34	14.4	discrete	Laurel Creek	LED-23	100	53.1	D	1.5
COY-23	63.2	discrete	McCoy Creek	COY-3	100	58.3	B	1
ALZ-36	55.7	discrete	Alonzo Creek		100	41.5	C	9.4
JAM-7	113.6	distributed	Jameson Creek		100	65.9	D	1.2
LED-25	38.3	discrete	Ledgewood Creek	LED-5	100	65.5	A	0.5
MAR-10	109.4	distributed	Marsh 1		100	0.3	B	19.5
ALZ-38	37.2	distributed	Alonzo Creek		100	52	C	5.2
AMER-7	146.8	distributed	American Canyon Creek		100	3.1	D	11.7
UNI-3	722.4	distributed	Union Creek		100	0.2	D	3.4
COY-24	98.3	distributed	McCoy Creek		100	50.2	D	1.7
COY-25	318.6	distributed	McCoy Creek		100	2.4	D	1
COY-26	186.7	discrete	McCoy Creek		100	42.4	D	1.3
COY-27	658.9	distributed	McCoy Creek		100	11.1	D	3.1
COY-28	157.9	discrete	McCoy Creek		100	18.9	D	1.4
COY-30	90.3	distributed	McCoy Creek		100	0.1	C	8.6
COY-31	106.2	distributed	McCoy Creek		100	1.7	D	4.3
UNI-4	109.7	distributed	Union Creek		100	0.1	D	2.6
MAR-7	131.5	distributed	Marsh 1		100	0.7	D	2.8
GRN-29	35	distributed	Green Valley Creek		100	61.6	A	0.8
MAR-1	94.5	discrete	Marsh 1	MAR-14	100	41.5	D	0.5
MAR-17	36.7	distributed	Marsh 1		100	44.9	D	0.5

MAR-8	116.6	discrete	Marsh 1		100	51.6	D	0.5
MAR-9	79.6	distributed	Marsh 1		100	67.5	D	0.6
MAR-2	90.7	discrete	Marsh 1		100	37.7	B	3.5
MAR-4	94.8	discrete	Marsh 1		100	57.8	C	3.2
MAR-5	120.6	distributed	Marsh 1		100	47.4	D	2.4
MAR-6	392.5	distributed	Marsh 1		100	7.7	D	0.6
MAR-20	81.5	discrete	Marsh 1	MAR-14	100	65.2	D	0.5
MAR-11	125.6	discrete	Marsh 1	MAR-11	100	53.2	D	0.5
MAR-12	65.1	discrete	Marsh 1	MAR-11	100	39.6	D	0.8
MAR-13	113.8	distributed	Marsh 1		100	1.3	D	0.4
MAR-15	96.7	distributed	Marsh 1		100	57.4	D	0.7
MAR-18	69.2	distributed	Marsh 1		100	45.2	D	0.8
MAR-21	77.9	distributed	Marsh 1		100	0	B	19.8
MAR-25	127.7	distributed	Marsh 1		100	0	C	16.6
MAR-19	85.4	discrete	Marsh 1	MAR-14	100	16.4	D	0.5
MAR-23	46.8	discrete	Marsh 1		100	60.7	C	2.7
MAR-24	30.1	distributed	Marsh 1		100	49.4	D	1.2
Suisun								
MAR-26	81.9	distributed	Marsh #1		100	43.5	D	1.2
MAR-27	125.8	distributed	Marsh #1		100	47.9	A	3.2
COY-40	70.4	distributed	McCoy Creek		100	12.5	B	1.9
COY-32	143.4	distributed	McCoy Creek		100	11	A	2.6
MAR-28	78.3	discrete	Marsh #1	COY-35	100	57.6	D	1.1
SODA-37	92.4	distributed	Soda Springs Creek		100	41.1	D	1.7
LAU-43	117.5	discrete	Laurel Creek	LAU-43	100	62.1	D	1
LAU-42	96.6	discrete	Laurel Creek	LAU-43	100	59.1	D	2.1
MAR-29	31.9	distributed	Marsh #1		100	55.5	D	0.5
MAR-30	88.9	distributed	Marsh #1		100	28.5	D	2.5
LAU-41	96.7	discrete	Laurel Creek		100	61.8	D	1.7
MAR-42	29.4	distributed	Marsh #1		100	63.3	A	5.3
LAU-40	48	discrete	Laurel Creek	LAU-43	100	72.5	D	1.7
COY-33	67.6	distributed	McCoy Creek		100	53.7	D	2.4
COY-34	50.6	distributed	McCoy Creek		100	59.4	D	3.1
COY-35	74.7	discrete	McCoy Creek	COY-35	100	58.9	D	2.1
MAR-31	122	discrete	Marsh #1	COY-35	100	56.5	A	1.3
LAU-39	76	distributed	Laurel Creek		100	67.7	D	1.4
MAR-32	71.4	distributed	Marsh #1		100	50.6	D	1.5
MAR-33	49.8	distributed	Marsh #1		100	22.9	D	1.4
MAR-37	127.2	distributed	Marsh #1		100	10.9	A	2
COY-36	59.3	discrete	McCoy Creek		100	46.1	A	3
COY-37	37	distributed	McCoy Creek		100	47	D	2.7
MAR-39	51.9	discrete	Marsh #1		100	71	D	0.5
COY-38	137.7	distributed	McCoy Creek		100	10.6	D	3.1
COY-39	99.2	distributed	McCoy Creek		100	53.7	B	2
MAR-34	80.1	distributed	Marsh #1		100	51.4	D	1
MAR-35	56.1	distributed	Marsh #1		100	50.2	D	0.9
MAR-36	32.6	distributed	Marsh #1		100	55.2	D	1
MAR-38	60.7	distributed	Marsh #1		100	32.4	D	5.1
SODA-38	20.7	distributed	Soda Springs Creek		100	47.2	D	0.2
MAR-40	29.8	distributed	Marsh #1		100	3.9	D	0.9
MAR-41	95.8	discrete	Marsh #1		100	60.2	D	0.5
LAU-38	34.4	distributed	Laurel Creek		100	8.5	D	1.5
MAR-43	61.5	discrete	Marsh #1	MAR-44	100	60.9	A	3.9
MAR-44	67.3	discrete	Marsh #1	MAR-44	100	50.5	D	2
COY-41	94.1	distributed	McCoy Creek		100	42.4	D	2.2

LAU-37	30.6	distributed	Laurel Creek		100	13	D	4.8
MAR-45	51.9	discrete	Marsh #1	COY-35	100	57.5	A	1
COY-42	60	distributed	McCoy Creek		100	39.5	D	1.2
MAR-46	47.2	discrete	Marsh #1		100	66.1	D	0.6
COY-43	28.7	discrete	McCoy Creek		100	42.6	D	2.6
LAU-36	19.2	distributed	Laurel Creek		100	35.9	D	2.1
MAR-47	64.7	distributed	Marsh #1		100	43.6	D	6.9

Appendix D

Solano Permittee decentralized BMPs.

City	BMP ID	Status	Scenario	BMP Type	Drainage Area (ac)	Receiving Water	Catchment	Latitude	Longitude
Fairfield	2455 Huntington	Installed	2020	Biofiltration	11.247	McCoy Creek	COY-2	38.27765067	-121.97435
Fairfield	1200 B Gale Wilson B	Installed	2020	Bioretention	0.241	Alonzo Creek	ALZ-10	38.26109353	-122.0475298
Fairfield	Denny's Restaurant	Planned	2030	Bioretention	0.77	Dan Wilson Creek	DAN-2	38.21955338	-122.127658
Fairfield	3950 Business Center	Installed	2020	Bioretention	2.296	Dan Wilson Creek	DAN-4	38.22868832	-122.1258213
Fairfield	Jayo Subdivision	Planned	2030	Bioretention	4.05	Dan Wilson Creek	DAN-4	38.22868832	-122.1258213
Fairfield	3900 Business Center	Installed	2020	Bioretention	8.533	Dan Wilson Creek	DAN-5	38.23116717	-122.1182872
Fairfield	4475 Central	Installed	2020	Bioretention	0.509	Dan Wilson Creek	DAN-8	38.22014694	-122.1300926
Fairfield	4500 Business Center	Installed	2020	Bioretention	2.551	Green Valley Creek	GRN-26	38.22604915	-122.1326145
Fairfield	4625 Mangels	Installed	2020	Bioretention	3.688	Green Valley Creek	GRN-26	38.2251654	-122.1358266
Fairfield	Partnership Health 2	Planned	2030	Bioretention	4.43	Green Valley Creek	GRN-28	38.22411267	-122.1326464
Fairfield	3630 Ritchie	Installed	2020	Bioretention	3.295	Green Valley Creek	GRN-29	38.21379883	-122.1362455
Fairfield	2600 Estates	Installed	2020	Bioretention	0.406	Laurel Creek	LAU-27	38.30664231	-122.029309
Fairfield	3201 Hartford	Installed	2020	Bioretention	0.326	Ledgewood Creek	LED-2	38.25466074	-122.0670856
Fairfield	Caliber Collision	Planned	2030	Bioretention	1.46	Marsh 1	MAR-8	38.24675285	-122.0743114
Fairfield	2600 Maxwell	Installed	2020	Bioretention	1.737	Marsh 1	MAR-11	38.23099408	-122.0799684
Fairfield	770 Chadbourne	Installed	2020	Bioretention	4.635	Marsh 1	MAR-11	38.23034689	-122.0835006
Fairfield	800 Chadbourne	Installed	2020	Bioretention	6.313	Marsh 1	MAR-11	38.22897736	-122.0819342
Fairfield	Innova Maxwell	Planned	2030	Bioretention	2.63	Marsh 1	MAR-11	38.23087887	-122.0800178
Fairfield	2487 Courage	Installed	2020	Bioretention	1	Marsh 1	MAR-12	38.23405747	-122.081283
Fairfield	2901 Cordelia	Installed	2020	Bioretention	8.189	Marsh 1	MAR-13	38.2279119	-122.0874744
Fairfield	Solano Logistics D	Planned	2030	Bioretention	3.5	Marsh 1	MAR-13	38.22789676	-122.0903076
Fairfield	Jelly Belly Warehouse Expansion	Planned	2030	Bioretention	4.09	Marsh 1	MAR-15	38.23809914	-122.0746228
Fairfield	360 Beck A	Installed	2020	Bioretention	1.5	Marsh 1	MAR-19	38.2333092	-122.066136
Fairfield	360 Beck B	Installed	2020	Bioretention	1.5	Marsh 1	MAR-19	38.23279513	-122.0661494
Fairfield	E&P Properties	Planned	2030	Bioretention	9.92	Marsh 1	MAR-20	38.23590326	-122.0706416
Fairfield	2051 Walters	Installed	2020	Bioretention	0.981	McCoy Creek	COY-10	38.26628535	-121.9880675

City	BMP ID	Status	Scenario	BMP Type	Drainage Area (ac)	Receiving Water	Catchment	Latitude	Longitude
Fairfield	2400 Huntington	Installed	2020	Bioretention	1	McCoy Creek	COY-2	38.27764825	-121.9745453
Fairfield	Fairfield/Vacaville Train Station	Planned	2030	Bioretention	1	McCoy Creek	COY-27	38.28614529	-121.9680942
Fairfield	1800 North Texas	Installed	2020	Bioretention	0.065	Soda Springs Creek	SODA-13	38.26235658	-122.0341855
Fairfield	3329 North Texas	Installed	2020	Bioretention	0.358	Soda Springs Creek	SODA-18	38.289267	-122.0341714
Fairfield	3345 North Texas	Installed	2020	Bioretention	0.988	Soda Springs Creek	SODA-18	38.2905095	-122.0341275
Fairfield	2525 North Texas	Installed	2020	Bioretention	0.475	Soda Springs Creek	SODA-29	38.27556882	-122.0342614
Fairfield	2590 North Texas	Installed	2020	Bioretention	0.76	Soda Springs Creek	SODA-29	38.27600953	-122.0340355
Fairfield	2700 North Texas	Installed	2020	Bioretention	0.289	Soda Springs Creek	SODA-29	38.27675262	-122.0340485
Fairfield	2470 Hilborn	Installed	2020	Bioswale	0.381	Alonzo Creek	ALZ-18	38.27532514	-122.0522109
Fairfield	600 Gregory	Installed	2020	Bioswale	0.448	Alonzo Creek	ALZ-6	38.24820883	-122.0560475
Fairfield	201 Pittman	Installed	2020	Bioswale	1.071	Dan Wilson Creek	DAN-2	38.22012023	-122.1272167
Fairfield	200 Business Center	Installed	2020	Bioswale	4.295	Dan Wilson Creek	DAN-4	38.22868832	-122.1258213
Fairfield	4755 Business Center	Installed	2020	Bioswale	1.846	Green Valley Creek	GRN-12	38.22096842	-122.1373021
Fairfield	4775 Business Center	Installed	2020	Bioswale	2.46	Green Valley Creek	GRN-12	38.22060358	-122.1382177
Fairfield	4650 Business Center	Installed	2020	Bioswale	1.693	Green Valley Creek	GRN-26	38.22225683	-122.1340899
Fairfield	167 Grobric	Installed	2020	Bioswale	1.162	Green Valley Creek	GRN-29	38.21607168	-122.1343305
Fairfield	4856 Auto Plaza	Installed	2020	Bioswale	2.298	Green Valley Creek	GRN-3	38.21258775	-122.1396229
Fairfield	4865 Auto Plaza	Installed	2020	Bioswale	4.591	Green Valley Creek	GRN-3	38.21244225	-122.1397805
Fairfield	5001 Fermi	Installed	2020	Bioswale	5.818	Jameson Creek	JAM-3	38.2037402	-122.139484
Fairfield	5133 Fulton	Installed	2020	Bioswale	4.053	Jameson Creek	JAM-7	38.20708849	-122.144373
Fairfield	5160 Fulton	Installed	2020	Bioswale	2.388	Jameson Creek	JAM-7	38.20714647	-122.145164
Fairfield	1057 Horizon	Installed	2020	Bioswale	3.452	Laurel Creek	LAU-22	38.27342649	-122.0147834
Fairfield	2001 Meyer	Installed	2020	Bioswale	1.426	Ledgewood Creek	LED-15	38.2379282	-122.0635347
Fairfield	1200 Oliver	Installed	2020	Bioswale	2.345	Ledgewood Creek	LED-2	38.25516097	-122.0671784
Fairfield	1717 Clift	Installed	2020	Bioswale	1.033	Ledgewood Creek	LED-5	38.24272299	-122.0593736
Fairfield	Courage Dr Beck Ave	Installed	2020	Bioswale	1.5	Marsh 1	MAR-1	38.23765765	-122.0676488
Fairfield	2950 Auto Mall	Installed	2020	Bioswale	2.909	Marsh 1	MAR-9	38.24153261	-122.0839885
Fairfield	2955 Automall	Installed	2020	Bioswale	2.296	Marsh 1	MAR-9	38.24164932	-122.0836312
Fairfield	801 Chadbourne	Installed	2020	Bioswale	7.92	Marsh 1	MAR-11	38.22874137	-122.0832968
Fairfield	2700 Low	Installed	2020	Bioswale	5.016	Marsh 1	MAR-12	38.23676132	-122.0847769
Fairfield	2525 N Watney	Installed	2020	Bioswale	2.5	Marsh 1	MAR-15	38.23624603	-122.0791156
Fairfield	Sheldon Oil Company	Planned	2030	Bioswale	1	Marsh 1	MAR-19	38.23528702	-122.0607524
Fairfield	2510 Clay Bank	Installed	2020	Bioswale	0.982	McCoy Creek	COY-15	38.2752175	-122.0064988
Fairfield	Clorox	Planned	2030	Bioswale	1	McCoy Creek	COY-2	38.27960416	-121.9710685

City	BMP ID	Status	Scenario	BMP Type	Drainage Area (ac)	Receiving Water	Catchment	Latitude	Longitude
Fairfield	Peabody Road	Installed	2020	Bioswale	16.368	McCoy Creek	COY-27	38.29709076	-121.9675707
Fairfield	Texas Corners	Planned	2030	Bioswale	0.72	Soda Springs Creek	SODA-11	38.24997707	-122.0341621
Fairfield	1833 N Texas	Installed	2020	Bioswale	2.778	Soda Springs Creek	SODA-13	38.26356253	-122.0342475
Fairfield	3333 North Texas	Installed	2020	Bioswale	1.832	Soda Springs Creek	SODA-18	38.28960861	-122.0341365
Fairfield	3400 North Texas	Installed	2020	Bioswale	9.507	Soda Springs Creek	SODA-18	38.2927325	-122.0326218
Fairfield	824 Washington	Installed	2020	Bioswale	2.17	Soda Springs Creek	SODA-25	38.25055608	-122.0390686
Fairfield	Senior Manor Parking Lot	Planned	2030	Bioswale	1	Soda Springs Creek	SODA-36	38.2535156	-122.0404984
Fairfield	2910 Industrial	Installed	2020	Bioswale	0.696	Union Creek	UNI-2	38.27338698	-121.9633523
Fairfield	Jepson Parkway 2A	Planned	2030	Bioswale	1	Union Creek	UNI-5	38.2938595	-121.9554919
Fairfield	1200 B Gale Wilson A	Installed	2020	Filtration Device	3.656	Alonzo Creek	ALZ-10	38.26109353	-122.0475298
Fairfield	3650 Nelson	Installed	2020	Filtration Device	1	Laurel Creek	LAU-10	38.29454858	-122.0317184
Fairfield	3500 Nelson	Installed	2020	Filtration Device	2.025	Laurel Creek	LAU-7	38.29380211	-122.0316656
Fairfield	2263 N Texas	Installed	2020	Filtration Device	0.013	Soda Springs Creek	SODA-15	38.26986308	-122.034208
Fairfield	3340 N Texas	Installed	2020	Filtration Device	2.941	Soda Springs Creek	SODA-18	38.29215565	-122.0332795
Fairfield	4350 Central	Installed	2020	Sediment Trap	3.194	Dan Wilson Creek	DAN-2	38.22350691	-122.1251014
Fairfield	4610 West America	Installed	2020	Sediment Trap	1	Green Valley Creek	GRN-22	38.23045612	-122.1309696
Fairfield	3330 Dover	Installed	2020	Sediment Trap	0.028	Laurel Creek	LAU-15	38.28939339	-122.024848
Fairfield	3355 North Texas	Installed	2020	Sediment Trap	1.015	Soda Springs Creek	SODA-18	38.28987196	-122.0341651
Suisun	Cottonwood_DB	Installed	2020	Bioretention	3.2	Laurel Creek	LAU-36	38.253919	-122.021465
Suisun	Summerwood_DB	Installed	2020	Bioretention	2.5	Laurel Creek	LAU-36	38.253905	-122.022136
Suisun	Walmart_BR_1	Installed	2020	Bioretention	2.6	Marsh #1	MAR-33	38.24175304	-121.9886363
Suisun	Walmart_BR_2	Installed	2020	Bioretention	2.6	Marsh #1	MAR-33	38.24255777	-121.9884485
Suisun	Walmart_BR_3	Installed	2020	Bioretention	2.6	Marsh #1	MAR-33	38.24332878	-121.9892102
Suisun	Walmart_BR_4	Installed	2020	Bioretention	2.6	Marsh #1	MAR-33	38.24332035	-121.9911978
Suisun	Walmart_BR_5	Installed	2020	Bioretention	2.6	Marsh #1	MAR-33	38.24329929	-121.9920561
Suisun	Walmart_BR_6	Installed	2020	Bioretention	2.6	Marsh #1	MAR-33	38.24142651	-121.9898674
Suisun	Walmart_DB	Installed	2020	Bioretention	15.8	Marsh #1	MAR-33	38.240915	-121.989429
Suisun	Holiday Inn Express	Installed	2020	Bioretention	1.6	Marsh #1	MAR-38	38.24209415	-122.0383736
Suisun	Crystal Middle School Site	Installed	2020	Bioretention	7.1	Marsh #1	MAR-39	38.23657066	-122.0436108
Suisun	Railroad Avenue Extension	Planned	2030	Bioretention	1.7	Marsh #1	MAR-41	38.24420303	-122.0330427
Suisun	Jubilee Commercial	Installed	2020	Bioretention	1.2	Marsh #1	MAR-43	38.26456217	-121.9873755
Suisun	ZE_BT_01	Installed	2020	Bioretention	1.6	Marsh #1	MAR-43	38.263235	-121.9877
Suisun	ZE_BT_03	Installed	2020	Bioretention	2.5	Marsh #1	MAR-43	38.264415	-121.986915
Suisun	ZE_BT_04	Installed	2020	Bioretention	0.7	Marsh #1	MAR-43	38.264101	-121.985862

City	BMP ID	Status	Scenario	BMP Type	Drainage Area (ac)	Receiving Water	Catchment	Latitude	Longitude
Suisun	ZE_BT02	Installed	2020	Bioretention	0.4	Marsh #1	MAR-43	38.264158	-121.987761
Suisun	McCoy Creek Trail	Installed	2020	Bioretention	1	McCoy Creek	COY-41	38.25395217	-122.0113701
Suisun	Caterpillar Club House	Installed	2020	Bioretention	0.5	McCoy Creek	COY-42	38.24250196	-122.0191968
Suisun	Summerwood_GS 01	Installed	2020	Bioswale	0.5	Laurel Creek	LAU-36	38.254922	-122.023184
Suisun	Summerwood_GS 02	Installed	2020	Bioswale	0.2	Laurel Creek	LAU-36	38.254427	-122.022624
Suisun	HSC_FI	Installed	2020	Filtration Device	12.8	Laurel Creek	LAU-39	38.244877	-122.021441
Suisun	RR_Storage_Filters	Installed	2020	Filtration Device	1.1	McCoy Creek	COY-39	38.260923	-122.011153
Suisun	Summerwood_CDS	Installed	2020	Sediment Trap	2.5	Laurel Creek	LAU-36	38.254196	-122.024351
Suisun	Walmart_City CDS	Installed	2020	Sediment Trap	7.5	Marsh #1	MAR-33	38.243349	-121.989895
Suisun	Hampton_CDS	Installed	2020	Sediment Trap	0.9	Marsh #1	MAR-38	38.242237	-122.039346
Suisun	Andrews_N_SC	Installed	2020	Sediment Trap	1.5	Marsh #1	MAR-42	38.254194	-121.985953
Suisun	Andrews_S_SC	Installed	2020	Sediment Trap	2.8	Marsh #1	MAR-42	38.253443	-121.985822
Suisun	Beale_N_SC	Installed	2020	Sediment Trap	2.5	Marsh #1	MAR-42	38.255578	-121.986025
Suisun	Beale_S_SC	Installed	2020	Sediment Trap	2.5	Marsh #1	MAR-42	38.254878	-121.986035
Suisun	Hickam_N_SC	Installed	2020	Sediment Trap	3	Marsh #1	MAR-42	38.254255	-121.985453
Suisun	Hickam_S_SC	Installed	2020	Sediment Trap	3.7	Marsh #1	MAR-42	38.253438	-121.985359
Suisun	Vandenberg_N_SC	Installed	2020	Sediment Trap	1.5	Marsh #1	MAR-42	38.255659	-121.985495
Suisun	Vandenberg_S_SC	Installed	2020	Sediment Trap	2.9	Marsh #1	MAR-42	38.254884	-121.985516
Suisun	Carswell Ct_SC	Installed	2020	Sediment Trap	7	Marsh #1	MAR-43	38.262615	-121.987286
Suisun	Dover_N_SC	Installed	2020	Sediment Trap	2.6	Marsh #1	MAR-43	38.257337	-121.985992
Suisun	Dover_S_SC	Installed	2020	Sediment Trap	2.6	Marsh #1	MAR-43	38.25671	-121.985995
Suisun	Ford Ord_SC	Installed	2020	Sediment Trap	1.6	Marsh #1	MAR-43	38.259527	-121.985967
Suisun	Keesler_N_SC	Installed	2020	Sediment Trap	2.6	Marsh #1	MAR-43	38.258861	-121.985965
Suisun	Keesler_S_SC	Installed	2020	Sediment Trap	2.8	Marsh #1	MAR-43	38.258068	-121.985987
Suisun	Neward_N_SC	Installed	2020	Sediment Trap	5.1	Marsh #1	MAR-43	38.261022	-121.986269
Suisun	Newark_S_SC	Installed	2020	Sediment Trap	2.5	Marsh #1	MAR-43	38.260269	-121.986128
Suisun	Four Seasons_CDS	Installed	2020	Sediment Trap	4.3	Marsh #1	MAR-44	38.243597	-121.985876
Suisun	Breezewood_CDS	Installed	2020	Sediment Trap	3.9	McCoy Creek	COY-39	38.260753	-122.009642
Suisun	Amberwood_CDS	Installed	2020	Sediment Trap	3.5	McCoy Creek	COY-41	38.257989	-122.012995
Suisun	McCoy_CDS	Installed	2020	Sediment Trap	3.3	McCoy Creek	COY-42	38.241326	-122.01897
Vallejo	Sonoma_Blvd_BR	Installed	2020	Bioretention	3.5	Mare Island Strait	SA55	38.0937663	-122.2497144
Vallejo	850_Redwood_BR3	Installed	2020	Bioretention	0.25	Napa River	AC35	38.1228762	-122.2543064
Vallejo	Automall_Basin	Installed	2020	Bioretention	2.7	Rindler Creek	LC21	38.13728229	-122.2143281
Vallejo	Couch_St_BR1	Installed	2020	Bioretention	0.75	White Slough	AC34	38.12397765	-122.2503421

City	BMP ID	Status	Scenario	BMP Type	Drainage Area (ac)	Receiving Water	Catchment	Latitude	Longitude
Vallejo	Couch_St_BR2	Installed	2020	Bioretention	0.75	White Slough	AC34	38.1236316	-122.2502697
Vallejo	850_Redwood_BR1	Installed	2020	Bioretention	0.25	White Slough	AC53	38.12342271	-122.2542527
Vallejo	850_Redwood_BR2	Installed	2020	Bioretention	0.25	White Slough	AC53	38.12313152	-122.2540945
Vallejo	AdmiralCallaghan_Bioswale	Installed	2020	Bioswale	1	Blue Rock Springs Creek	LC8	38.12364848	-122.2277015
Vallejo	9832_Vallejo_Streetscape	Installed	2020	Bioswale	0.05	Mare Island Strait	DT5	38.10213344	-122.2583216
Vallejo	AustinCk_Bioswale	Installed	2020	Bioswale	1	Napa River	AC41	38.11837319	-122.2568035
Vallejo	Kaiser_Broadway_2	Installed	2020	Bioswale	0.24	White Slough	AC34	38.12756672	-122.2471529
Vallejo	Kaiser_Broadway_3	Installed	2020	Bioswale	0.24	White Slough	AC34	38.12754984	-122.2474506
Vallejo	Kaiser_Broadway_4	Installed	2020	Bioswale	0.24	White Slough	AC34	38.12737894	-122.2474158
Vallejo	Kaiser_Broadway_5	Installed	2020	Bioswale	0.24	White Slough	AC34	38.1273916	-122.2471368
Vallejo	HiddenbrookPark	Installed	2020	Infiltration Feature	1	Sulphur Springs Creek	SV4	38.1366937	-122.1687949
Vallejo	Kaiser_Broadway_1	Installed	2020	Infiltration Feature	0.24	White Slough	AC34	38.12769121	-122.2477591
Vallejo	9810_Curtola_Pkwy	Installed	2020	Pervious Pavement	1	Lake Dalwigk	LS33	38.09378108	-122.2396427
Vallejo	Chase_St_PP	Installed	2020	Pervious Pavement	0.4	Mare Island Strait	LS35	38.09659274	-122.2399378
Vallejo	SP14101B	Installed	2020	Settling Basin	3.2	Napa River	SP14	38.15244205	-122.2838573
Vallejo	SP14201B	Installed	2020	Settling Basin	3.2	Napa River	SP14	38.15302772	-122.2806181
Vallejo	SP14401B	Installed	2020	Settling Basin	3.2	Napa River	SP14	38.1546249	-122.2792984
Vallejo	SP14501B	Installed	2020	Settling Basin	3.2	Napa River	SP14	38.1551305	-122.2807271
Vallejo	SP14601B	Installed	2020	Settling Basin	3.2	Napa River	SP14	38.15512579	-122.2820948